RADC-TR-76-297
Final Technical Report
October 1976

DEVELOPMENT OF A COMPUTER MODEL FOR SCATTERING OF ELECTROMAGNETIC WAVES BY A TURBULENT WAKE

General Electric Company
Re-entry & Environmental Systems Division

ROME AIR DEVELOPMENT CENTER
AIR FORCE SYSTEMS COMMAND
GRIFFISS AIR FORCE BASE, NEW YORK 13441

Paul E. Bisbing is the Principal Investigator for this contract. Ronald L. Fante is the RADC Project Engineer (Contract Monitor).

This report has been reviewed by the RADC Information Office (OI) and is releasable to the National Technical Information Service (NTIS). At NTIS it will be releasable to the general public, including foreign nations.

This technical report has been reviewed and approved for publication.

APPROVED: Ronald L. Fante
RONALD L. FANTE
Project Engineer

APPROVED: Allan C. Schell
ALLAN C. SCHELL
Acting Chief
Electromagnetic Sciences Division

FOR THE COMMANDER: John P. Kluss

Plans Office

UNCLASSIFIED

SECURITY CLASSIFICATION OF THIS PAGE (When Data Entered)

REPORT DOCUMENTATION PAGE

READ INSTRUCTIONS BEFORE COMPLETING FORM

1. REPORT NUMBER: RADC-TR-76-297	2. GOVT ACCESSION NO.
3. RECIPIENT'S CATALOG NUMBER	
4. TITLE (and Subtitle): DEVELOPMENT OF A COMPUTER MODEL FOR SCATTERING OF ELECTROMAGNETIC WAVES BY A TURBULENT WAKE	5. TYPE OF REPORT & PERIOD COVERED: Final technical rept. 1 JUL 75 - 30 JUN 76
	6. PERFORMING ORG. REPORT NUMBER
7. AUTHOR(s): PAUL E. BISBING	8. CONTRACT OR GRANT NUMBER(s): F19628-76-C-0011
9. PERFORMING ORGANIZATION NAME AND ADDRESS: GENERAL ELECTRIC COMPANY, RE-ENTRY & ENVIRONMENTAL SYSTEMS DIVISION, PHILADELPHIA, PA. 19101	10. PROGRAM ELEMENT, PROJECT, TASK AREA & WORK UNIT NUMBERS: 61102F 21530201 02
11. CONTROLLING OFFICE NAME AND ADDRESS: DEPUTY FOR ELECTRONIC TECHNOLOGY (RADC), ETEP, HANSCOM AIR FORCE BASE, MA 01731, MONITOR/RONALD FANTE/	12. REPORT DATE: OCTOBER 1976
	13. NUMBER OF PAGES: 116 (12) 119 pp.
14. MONITORING AGENCY NAME & ADDRESS (if different from Controlling Office)	15. SECURITY CLASS. (of this report): UNCLASSIFIED
	15a. DECLASSIFICATION/DOWNGRADING SCHEDULE

16. DISTRIBUTION STATEMENT (of this Report)

APPROVED FOR PUBLIC RELEASE; DISTRIBUTION UNLIMITED.

17. DISTRIBUTION STATEMENT (of the abstract entered in Block 20, if different from Report)

18. SUPPLEMENTARY NOTES

19. KEY WORDS (Continue on reverse side if necessary and identify by block number)

ELECTROMAGNETIC SCATTERING
RANDOM MEDIA
IONIZED WAKES
RE-ENTRY PHYSICS
RADAR SCATTERING
COMPUTER MODELS

20. ABSTRACT (Continue on reverse side if necessary and identify by block number)

THIS REPORT DESCRIBES A THEORETICAL MODEL FOR THE RADAR SCATTERING BY A TURBULENT, RE-ENTRY INDUCED IONIZED WAKE. THE EQUATIONS USED, THEIR DERIVATIONS, AND THE FORTRAN LISTING OF THE COMPUTER CODE ARE GIVEN AND EXPLAINED IN DETAIL. THE OUTPUT FROM A SAMPLE RUN OF THE PROGRAM IS GIVEN AND EXPLAINED. COMPARISONS ARE MADE BETWEEN THE RESULTS OF THIS MODEL AND PUBLISHED DATA FROM LABORATORY EXPERIMENTS ON MICROWAVE SCATTERING FROM TURBULENT PLASMA. THE RESULTS OF SOME PARAMETRIC CALCULATIONS ARE GIVEN ALSO. →OVER

DD FORM 1 JAN 73 1473 EDITION OF 1 NOV 65 IS OBSOLETE

UNCLASSIFIED

SECURITY CLASSIFICATION OF THIS PAGE (When Data Entered)

404 884

20. (CONTINUED)

THIS THEORETICAL MODEL ASSUMES THAT THE ELECTRICAL PROPERTIES OF THE WAKE PLASMA ARE KNOWN IN TERMS OF CERTAIN STATISTICAL AND SPATIAL DISTRIBUTIONS. THE TECHNIQUE USED BY THE MODEL IS A DISTORTED WAVE BORN APPROXIMATION IN WHICH THE PROPAGATION IN THE BACKGROUND MEDIUM IS CALCULATED RIGOROUSLY FOR A LAYERED CYLINDER OF MEAN WAKE PLASMA. THE MODEL PROVIDES PREDICTIONS OF THE BACKSCATTERING AMPLITUDE AND THE FIRST AND SECOND MOMENTS OF THE DOPPLER SPECTRUM, BOTH AT EACH INPUT WAKE AXIAL STATION AND AS A FUNCTION OF APPARENT AXIAL STATION IN THE BACKSCATTERED PULSE. DIRECT AND CROSS POLARIZED SCATTERING ARE INCLUDED FOR BOTH LINEAR AND CIRCULAR POLARIZATION RADARS.

EVALUATION

1. This report is the Final Report on the contract. It covers research done on the radar cross section of turbulent wakes during the twelve month period 1 Jul 75 to 30 Jun 76. The objective of this work is the generation of a computer code which can accurately predict the radar cross section of turbulent reentry wakes of arbitrary diameter, electron density and strength of turbulence.

2. The above work is of value since it provides a method for computing the radar cross section of ballistic missiles and decoys, including the doppler spectrum of the return. It will be used by the USAF to evaluate the possibility of discriminating between the reentry wakes of large and small vehicles.

Ronald L. Fante

RONALD L. FANTE
Project Engineer
Microwave Detection Techniques Br.
Electromagnetic Sciences Division

P R E F A C E

The research reported on in this document was conducted by Paul E. Bisbing. It is related to work done under subcontract No. A00621-DT-A-E to TRW Systems, TRW Inc. for prime contract No. DAHC 60-72-C-0096, sponsored by the U. S. Army Ballistic Missile Defense Advanced Technology Center.

CONTENTS

CONTENTS (Continued)

I. INTRODUCTION

The subject of this report is a computer model for the radar backscattering from a re-entry induced ionized wake. The report gives both the theoretical derivations and the FORTRAN coding for the model, and thus it serves as both a final report and a user's manual.

The model is based on a previously existing model[1], which applied the same basic technique but in a simpler way. Improvements in both theory and method of application have been made during this study.

The basic technique of this model is to use a distorted wave Born approximation in which the nonrandom background medium is represented as a radially nonuniform cylindrical plasma. The propagation of electromagnetic (em) waves in this background medium is formulated rigorously and solved numerically to a high degree of accuracy. The results of these calculations are used to "distort", or weight, the Born approximation for the scattering by the turbulent fluctuations. Section II gives a more detailed general description of the model and Section III gives the full details in a manner which relates directly to the computer code. Section IV discusses the results of some calculations intended to demonstrate the model's agreement with published data and to show the significance of certain phenomena included in the model. Section V, which concludes the report, gives recommendations for future development.

1. P.E. Bisbing, "Final Report: The EM Scattering Model for Re-entry Wakes. Volume I. The Wake Field Penetration Model of Radar Scattering, "General Electric Company, RESD, Report No. 75SDR2386-I, December 1975.

II. GENERAL DESCRIPTION OF THE MODEL

A. Background

This section is intended to give the theoretical basis for this model. This theory fits within the general topic of the interaction of waves with random media. In particular it relates to em wave scattering by turbulent plasma. Inasmuch as this report is not intended as a survey, we refer the reader to the review of this topic by Granatstein and Feinstein[2]. Also, the closely related topic of em wave propagation through random media has been surveyed recently by Fante[3]. Thus we will refer only to works which have established those points which are pertinent to the approach used herein.

The most basic part of the model is the Born approximation, which appears to have been originally applied by Pekeris[4] to acoustic scattering in turbulent media. Its first application to radio waves was by Booker and Gordon[5] and to ionized media, by Booker[6]. Tatarski[7] gave it a generalized form in terms of the turbulence spectrum function. The name "Born approximation" is borrowed from quantum theory to denote single scattering; i.e., it is assumed that waves propagate undistorted in the medium. Improvements to this approximation have accounted for various aspects of the medium which tend to distort the wave before (and after) it reaches the scatterer in question. Thus the name "distorted wave Born approximation".

Refraction in the mean wake plasma is a very significant source of distortion for em waves in ionized media because it tends to bend the path of propagation away from the interior of the medium. In fact when the line of incidence makes a low angle to the wake axis this effect is important at electron densities which are sufficiently low that the undistorted Born approximation would apply at normal incidence. Thus propagation in the background medium is the main source of distortion used in this model. Other distorting effects are included in ways which are similar to previous theories.

B. A Green's Theorem

In mathematical terms the Born approximation is the first term in a perturbation-iteration series called the Neumann series. A survey by Keller[8] gives

---

2. V.L. Granatstein and D.L. Feinstein, "Multiple Scattering and Transport of Microwaves in Turbulent Plasmas", Advances in Electronics and Electron Physics, Vol. 32, pp. 311-381, Academic Press, N. Y., 1973.
3. R.L. Fante, "Electromagnetic Beam Propagation in Turbulent Media", Proc. IEEE, Vol. 63, No. 12, pp 1669-1692, Dec. 1975.
4. C.L. Pekeris, "Note on the Scattering of Radiation in an Inhomogeneous Medium", Physical Review, Vol. 71, No. 4, pp. 268-269, 15 February 1947.
5. H.G. Booker and W.E. Gordon, "A Theory of Radio Scattering in the Troposphere", Proc. IRE, Vol. 38, pp 401-412, April 1950.
6. H.G. Booker, "Radio Scattering in the Lower Ionosphere", J. Geophysical Research, Vol. 64, No. 12, 2164-2177, December 1959.
7. V.I. Tatarski, Wave Propagation in a Turbulent Medium, translated by R.A. Silverman, McGraw-Hill, N.Y., 1961 (especially Chapter 4).
8. J.B. Keller, "A Survey of the Theory of Wave Propagation in Continuous Random Media", Proceedings of the Symposium on Turbulence of Fluids and Plasmas, New York-1968, Polytechnic Press, Brooklyn, 1969 (pp. 131-142).

the derivation of this series in very simple terms. Letting M and V represent the nonrandom and purely random differential operators, respectively, μ the unknown wave function and g the known source function, the equation to be solved is

$$(M + V)\mu = g \ . \tag{1}$$

Operate on both sides by the inverse of M.

$$(1 + M^{-1}V)\mu = M^{-1}g \tag{2}$$

This equation can be written as follows:

$$\mu = -M^{-1}V\mu + M^{-1}g \tag{3}$$

Returning to (2), multiply both sides by the inverse of the binomial, using the binomial theorem on this inverse, giving

$$\mu = \sum_{n=0}^{\infty} (-M^{-1}V)^n M^{-1}g \tag{4}$$

which is the Neumann series. This result can be written more explicitly as follows:

$$\mu = \sum_{n=0}^{\infty} \mu_n \tag{5}$$

$$\mu_o = M^{-1}g \tag{6}$$

$$\mu_n = -M^{-1}V\mu_{n-1}, \quad n>o \tag{7}$$

where μ_n represents the n^{th} order contribution to μ.

Now let us specify the above system of equations for em waves. Assume all quantities have the time dependence, $\exp(-i\omega t)$, where i is the imaginary number, ω is the radian frequency and t is the time. Then the vector electric field E obeys the differential equation

$$\nabla\times\nabla\times E = k^2(K+K')E + ikJ \tag{8}$$

where k is the free-space wave number (2π divided by the wavelength), K and K' respectively are the mean and random components of the complex dielectric constant of the plasma and J is the source (transmitter) current density distribution. This equation is the analog of (1), where μ is E, M is $k^2K-\nabla\times\nabla\times$, V is k^2K' and g is $-ikJ$. The inverse of M is customarily expressed in terms of a dyadic Green's function G, which satisfies Maxwell's equations for the electric field of a unit point vector source in the mean medium only.

$$\nabla\times\nabla\times G = k^2KG + 4\pi I\delta(r-r') \tag{9}$$

In this equation I is the identity dyadic, δ is the Dirac delta function and r and r' respectively are the radius vectors of the field and source points. Apply the divergence theorem of Gauss to the combination $[G\times(\nabla\times E)-E\times(\nabla\times G)]$. Use of certain vector identities gives

$$\int[G\cdot(\nabla\times\nabla\times E) - E\cdot(\nabla\times\nabla\times G)]dV = \int(\nabla\times E)\cdot(G\times dS)$$

$$-\int(\nabla\times G)\cdot(E\times dS) \qquad (10)$$

where dV is the element of volume enclosed within the surface having outward normal element dS. Let this surface be an infinitely large sphere containing both the source and the scatterer relatively near its origin. Then both E and G are outgoing radiation on the surface and the curl is proportioned to the vector product with the normal, so the right hand side of (10) vanishes. Substitution of (8) and (9) in (10) gives

$$4\pi E = k^2\int K'E\cdot G dV + ik\int J\cdot G dV \qquad (11)$$

which is the analog of (3), so M^{-1} is an integral over a scalar product with G. The analog of the Neumann series is the following:

$$E = \sum_{n=0}^{\infty} E_n \qquad (12)$$

$$4\pi E_0 = ik\int J\cdot G dV \qquad (13)$$

$$4\pi E_n = k^2\int K'E_{n-1}\cdot G dV, \quad n>0 \qquad (14)$$

In summary, (11) is a Green's theorem, in which G represents propagation in the background medium (the mean or nonrandom component of the total medium). It leads to the perturbation - iteration solution represented by (12) through (14), provided this series converges.

C. Representation of the Background Medium

Almost all previous theories ignore the background medium; i.e., K is assumed to be unity everywhere. Then G is the free-space Green's function and the usual Born series comes about. Accounting for the background medium obviously is not easy, but in the present problem we can at least represent it such that G can be calculated. Thus let the mean wake be an infinitely long cylinder of plasma in which the electron density and collision frequency depend only on the radial distance from the axis. (The effect of axial gradients will be evaluated later.)

Consider (13), the equation for the zero-order approximation. If the background medium were free space, E_0 would be the field radiated by the transmitter because G is the free-space Green's function. The effect on G of adding the inhomogeneous background medium is to add a scattered wave, which also couples to J in the integral. But if the transmitter is in the far field, the coupling of the scattered part of G to J can be neglected. Thus the significance of the right hand side of (13) is that E_0 is the vector field induced in the background medium by the transmitter. Note, however, that it is the total induced field, incident plus scattered, even though the latter component is assumed not to couple to the transmitter.

The dyadic nature of G is more essential in (14), since, when the perturbation-iteration scheme is carried out, E_n must be evaluated locally, at all points in the medium. The dyadic qualities of G can be obviated, however, when the n^{th} order far scattered field is evaluated. Simply take the dot product of

both sides of (14) with the unit vector representing the receiver polarization. This means that E_n on the left represents this approximation to the field which couples to the receiver and that G in the integral is the total (incident plus scattered) vector electric field induced in the background medium by the receiver if it were operated as a transmitter. This last result comes about because of reciprocity; i.e., the coupling between the receiver and a small test antenna in the background medium is independent of which antenna is used to transmit. Therefore the effect of the background medium is quite simple in the first-order approximation of the far field since one needs only to calculate the vector fields induced by incident plane waves.

In order to lead up to the radar cross section calculation let us put (14) in the form of the first-order approximation to the fields scattered by an incident, unit amplitude, plane wave. Then E_0 in the integrand is the total vector electric field induced in the mean medium by this incident plane wave. The fact that G is the fields induced by radiation from the receiver implies that

$$4\pi r E_1 = k^2 e^{ikr} \int K' E_0 \cdot G_0 dV \tag{15}$$

In this equation r is the distance from the receiver to the origin of the scatterer and G_0 is the total electric field induced in the mean medium by a unit amplitude plane wave propagating away from the receiver and having its phase reference at the origin of the scatterer. The incident waves for E_0 and G_0 have the polarization of the transmitter and the receiver, respectively.

We now give the problem of calculating E_0 and G_0 precise definition. The incident wave E_i propagates at an angle α to the wake axis, as shown in Figure 1. The axis is also the z-axis of a right handed cylindrical coordinate system (ρ, ϕ, z), where the direction $\phi = o$ lies in the plane of incidence and points in the forward direction. The complex amplitude of the incident wave has the following form: (The time variation will be suppressed in all quantities.)

$$E_i = \exp\left[ik(\rho \sin\alpha \cos\phi + z \cos\alpha)\right] \tag{16}$$

Arbitrary polarization of the receiver or transmitter is represented by superposition of two principal plane polarizations. The electric field of the incident wave for perpendicular (often called transverse below) polarization is taken, by arbitrary choice, to point into the plane of Figure 1 when the wave is at the origin. Thus

$$E_{i_t} = E_i(\hat{\rho} \sin\phi + \hat{\phi} \cos\phi) \tag{17}$$

where E_{i_t} denotes the vector incident field for transverse polarization and $\hat{}$ denotes a unit vector. Let the direction of parallel polarization be such that at normal incidence the electric vector at the origin would be aligned with the positive z-axis.

$$E_{i_p} = E_i[\hat{z} \sin\alpha - (\hat{\rho} \cos\phi - \hat{\phi} \sin\phi)\cos\alpha] \tag{18}$$

With the assumption that the electron density and collision frequency depend only on ρ, the problem of the background medium is completely specified. Its solution is worked out in detail below.

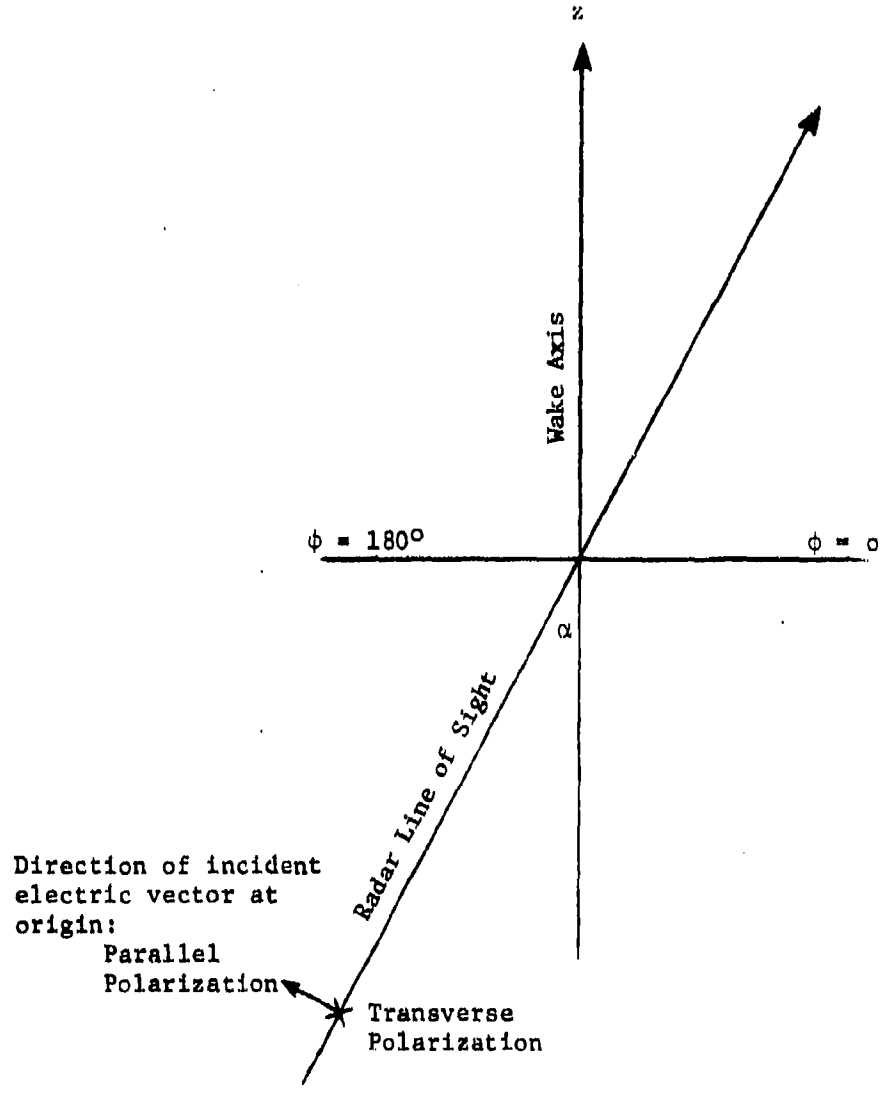

FIGURE 1. PROBLEM DEFINITION

D. Representation of Turbulence Effects

Once we have calculated the complex vectors E_0 and G_0 at all points in the wake, the first-order approximation to the turbulence scattering is given by (15). However, a number of difficulties are encountered at this point.

Perhaps the greatest difficulty with (15) is the statistics since K' is a random variable. The most direct approach, if the statistical distribution of K' were known, would be a Monte Carlo analysis in which the fixed distribution of $E_0 \cdot G_0$ would be multiplied by each realization of K'. Perhaps such an approach would be feasible, but it has not been attempted in this study. Instead we have relied on the correspondence between (15) and the Born approximation, which occurs when the background medium vanishes. Thus we assume that the statistics can be handled in a manner similar to the Born approximation. Except for a spreading owing to the finite volume, the Born solution is proportional to the three-dimensional Fourier transform of the turbulence autocorrelation function at a wavenumber which belongs to the vector resultant of the product $E_0 \cdot G_0$, each member of which is a unit amplitude plane wave. This wavenumber is in fact equal to the gradient of the argument* of the dot product of the two plane waves. Therefore we approximate the statistical effect of turbulence by taking the spectrum function at the wavenumber which is equal to the gradient of the argument of $E_0 \cdot G_0$.

The Born result is proportional also to the volume integral of the mean square fluctuation of the dielectric constant. It is obvious, however, that if either the incident wave or the scattered wave were attenuated in the medium, this volume integral would have to be appropriately weighted. Suppose, for a moment, that E_0 and G_0 have the same phase as the incident wave but different amplitudes at various points in the medium. Then the expectation of the radar cross section, which is proportional to the mean square of (15), would be equal to the Born result with the volume integral weighted by $|E_0 \cdot G_0|^2$. Therefore we include this weighting in our model. Of course the phase of $E_0 \cdot G_0$ varies throughout the medium, so the spectrum function at the appropriate wavenumber weights the volume integral also, rather than factoring out as in the Born approximation for homogeneous turbulence. The result to this point may be written in terms of radar cross section σ as follows:

$$\sigma = 4\pi r_e^2 \int \frac{\overline{N'^2} |E_0 \cdot G_0|^2 \, S(k_e) dV}{1 + (\nu/\omega)^2} \tag{19}$$

$$S(k) \equiv \int D(r) e^{ik \cdot r} dV \tag{20}$$

where r_e is the classical electron radius (2.81777×10^{-15}m), N' is the electron density fluctuation (overbar denotes mean), and ν is the electron collison frequency. In the definition (20) for the spectrum function S(k), k is a vector wavenumber, r is the radius vector and D(r) is the autocorrelation function of the electron density fluctuations. The effective vector wavenumber k_e is the gradient of the argument (phase) of $E_0 \cdot G_0$.

Application of (19) is not done without difficulty in certain instances

* The term "argument" denotes the mathematical term for a component of a complex variable; i.e., it is the angle in radians between the real axis and the complex vector.

owing to the plasma resonance effect, in which the electric field tends to infinity at the surface where K tends to zero. Thus the term $|E_0 \cdot G_0|^2$ causes the integral to diverge when the mean wake is overdense (electron density greater than $\pi/(\lambda^2 r_e)$, where λ is the free-space wavelength) and sufficiently collisionless. In the prior study (see Ref. 1) we did not account for k_e, using instead the argument that at low aspect angle the wavenumber was not greatly perturbed from that for free space so the Born spectrum function factors out. Unfortunately many of the numerical results were several orders of magnitude greater than the Born approximation. This was especially true in cases for which the diffraction effect allows the electric field to penetrate where refraction would otherwise stop it. One avenue of investigation was followed in that study in great detail. This was based on the fact that the magnetic field and the product of the dielectric constant and the electric field are not resonant even when the electric field is. Going back to the derivation of a Green's theorem (see Section IIA), the analogs of (8) and (9) can be written for magnetic fields and (10) can be written to include electric and/or magnetic fields. Also, (10) can include K explicitly by applying the divergence theorem to K^n times the type of combination originally used above to derive (10), where n is an arbitrary numerical power to which K is raised. One can derive an unlimited number of Green's theorems which have various combinations of K and either electric or magnetic field quantities in place of E and G in (11). Although all but the purely electric field theorem (11) have additional terms involving K and sometimes $\nabla K'$, the term in K' is always similar to the first term on the right hand side of (11). In addition to the result of (11) we studied the results of theorems using $H \cdot F$, $KE \cdot F$, and $KE \cdot KG$, where H and F are the magnetic field and its Green's function, respectively. The above-mentioned additional terms were neglected and radar cross section was calculated parametrically for each of the four theorems. The conclusion was reached that negligible benefit could be obtained from these alternatives. In all cases where the resonance effect was absent for any reason, all four theorems gave essentially the same results.* In other cases even most of the nonresonant theorems tended to diverge because of other effects, and none of the theorems agreed on the answer.

The resonance effect has been used by Ruquist[9] to derive a surface scattering effect. But we find a few difficulties in that approach also. In the diffraction regime the resonance is diffuse in that the electric field is high at not only the critical surface but also over a large fraction of the volume. In the geometric optics regime the critical surface is inside the surface where refraction causes ray turning, so one would not normally associate surface scattering with the critical surface except at normal incidence.

The approach which we have adopted to avoid the resonance effect is to neglect the contribution of the critical surface to the integral in (19) at all points where $|E_0 \cdot G_0|^2$ is greater than unity on that surface. The rationale for this is based on the fact that the electric field has a phase reversal at the resonant point; i.e., the phase varies infinitely rapidly through the

---

* The exception to this conclusion is in the cross polarized backscattering, which was generally considerably smaller when the magnetic field was used.

9. R.D. Ruquist, "Resonant Scattering from Weak Fluctuations in Plane Stratified Dielectric Media", Proc. IEEE, Vol. 63, No. 1, pp. 205-206, Jan. 1975.

critical surface. As a result the wavenumber goes to infinity, where the spectrum function vanishes exponentially. This argument is admittedly a bit weak since the phase of $E_0 \cdot G_0$ does not have a discontinuity at the critical surface, because the product of two functions which change sign at a point does not itself change sign. On the other hand it is found in numerical studies that the effective wavenumber, defined as the gradient of the phase of $E_0 \cdot G_0$, does increase rapidly in the neighborhood of the critical surface. An example of this result is given below.* It is interesting to note that in some theoretical studies appearing in the literature the effective wavenumber is taken as the free-space wavenumber times the square root of the dielectric constant of the background medium. In that approximation one would have zero wavenumber at the critical surface, which would not help cancel the resonance effect. Of course the literature which uses that approximation also uses geometric optics, which is bothered not by resonance but by caustics.

It goes without saying that the second and higher order approximations for the turbulence scattering are very complicated. Thus at this time we have not developed the technique for rigorously applying the model to the multiple scattering problem. However, in order to include the main effects of higher order terms, we have opted for an approximate representation within the framework of the first-order theory. Two phenomena, attenuation owing to random scattering and depolarization from multiple random scattering, are included in this representation. The equations for both of these effects are taken directly from the literature, especially in the case of depolarization. A small exception is the fact that scattering attenuation is not integrated along ray paths, since rays are not used in this model. The local scattering attenuation is used instead to define a plasma having equivalent attenuation owing to absorption. This plasma is then linearly added to the original mean plasma distribution in order to simulate the effect of scattering attenuation on the coherent wave.

The doppler frequency spectrum of the scattering is implicitly represented by (15) when the theories of Lane[10] and Schapker[11] are invoked. These authors showed that the spectrum of the electron velocity fluctuations in the wake is Gaussian, which implies that the first and second moments are sufficient to describe it. Also in the Born approximation the doppler spectrum is a linear combination of the electron velocity spectra in the wake, so each of the doppler moments is the same linear combination of the corresponding moments of the velocity distribution. Thus the generalized form of (19) is

$$S_n = 4\pi r_e^2 \int \frac{u_n \overline{N'^2} |E_0 \cdot G_0|^2 S(k_e) dV}{1+(\nu/\omega)^2} \qquad (21)$$

where S_n is the n^{th} moment of the doppler spectrum and u_n is the n^{th} moment of the electron velocity spectrum at a given point in the wake. Of course the radar cross section σ, as given by (19), is the zeroth moment ($u_0 \equiv 1$).

*See Section III C, top of page 42.

10. F. Lane, "Frequency Effects in the Radar Return from Turbulent, Weakly Ionized Missile Wakes", AIAA J., Vol. 5, No. 12, pp 2193-2200, December 1967.
11. R.L. Schapker, "Frequency Effects of Electromagnetic Scattering from Underdense Turbulent Plasmas", AIAA J., Vol. 8, No. 9, pp. 1582-1590, September 1970.

E. Representation of Axial Variations

Up to this point the wake has been treated as an infinite cylinder, so provision must be made for axial variations in its properties. This is done simply by breaking the wake up into a series of axial stations, each of which is assumed to fit the uniform cylinder representation. When the scattering from any given station is calculated, we carry out the volume integration in (21) over only the radial and angular coordinates. The result is the quantity dS_n/dz, which represents, for example if n = o, the radar cross section per unit length of wake.

An integration must be performed over the axial coordinate z to get the total scattering. In doing this we assume that the radar signal is pulsed and that the entire wake lies within the main beam of the radar antenna. Then the scattering is a function of the apparent wake station (time delay), which is given by a convolution integral. Thus

$$S_n(z) = \int_{-\infty}^{\infty} \frac{dS_n}{dz}(z')P(z - z')dz' \tag{22}$$

where $S_n(z)$ is the n^{th} doppler moment of the scattered pulse shape function versus apparent wake station z and P(z) is the effective transmitted radar pulse shape. For backscattering P(z) is equal to the relative transmitted pulse power at a time $(2z/c)\cos\alpha$ during the pulse, normalized such that the peak value is unity. In this model, the principal lobe of a cosine squared function is used to represent P(z). Its width is defined in terms of the parameter range resolution, which is the distance between half-power points when α = o.

III. DETAILED INFORMATION FOR THE USER

A. General

This computer program was developed and checked out using the Honeywell 6060 at the General Electric Company, Space Systems Division Computer Center, Valley Forge, Pa. A complete deck of punched cards (in 26-punch and fully interpreted in column alignment) has been supplied to the contract monitor (RADC/ETEP). A corresponding listing is included herewith in Appendix A. This listing contains the same statements as the punched cards. The deck and the listing are both in the form developed for the Honeywell 6060, however no control cards are included. This subsection gives certain general information about the program, including how to revise its central memory requirements to do the problem at hand economically and how to make it run on the CDC computers.

The language is FORTRAN-Y and complex, single precision arithmetic is used. The only kind of type statement used is COMPLEX; all integer variables are typed by the initial letter, from I through N, of their names. No mixed mode arithmetic expressions involving complex variables are used, despite the fact that the Honeywell 6060 FORTRAN-Y compiler permits them, in order to avoid any ambiguity for the user and to avoid difficulties with other compilers. All statement numbers increase as one reads down in each routine, and none is superfluous. Format statements are all numbered 1000 or greater. Output formats contain at least one space or a new page at the beginning of each line, to leave room for carriage control, even though the Honeywell 6060 does not need it. With certain exceptions noted below the program calls only the built-in and library functions listed in Table 1.

All common blocks are segregated according to variable type and labeled with a name which indicates the type as well as the routines containing the common. The first letter of the label indicates the variable type (C for complex, I for integer, and R for real) with one exception, ABCKLW, which would be too long if the R were prefixed. The other letters in the label denote the routines in which the common appears. The code letter of each routine appears in column 8 of its initial comment card. The 13 subroutines are denoted a through m, and the main program is denoted w for "wake". Thus, for example, COMMON/RBCW/ consists of real variables and appears in subroutines PROFS and WFP as well as in MAIN.

Most of the dimensions for array variables, and hence to a certain extent the central memory requirements, are dictated by the choices of certain more or less arbitrary limits on the problem description. The coding is designed to make it very easy to change these limits. The limiting factors are the number of layers, the number of angular modes, the number of axial stations, and the detail with which radial profiles can be input. The radial distribution of wake properties is currently represented by a series of 50 concentric cylindrical layers. The variable LAYERS which appears in MAIN, FIT, PROFS, RINT, WFP, BCO, STORF, PHINT, FFSUM, and AVGS has this value. The dimension of any subscript in the entire program which now has the value 50 also is determined by this quantity. The data statements for the arrays ROR and YIP must of course conform to this number; but see the detailed description below (subsections IIB2a) and IIB2c)). Note that YIP is dimensioned one less than this number.

Table 1. Mathematical Functions Called By The Program

NAME	DEFINITION	NUMBER OF ARGUMENTS	TYPE OF	
			ARGUMENT	FUNCTION
ABS(A)	$\|A\|$	1	real	real
AIMAG(C)	Imaginary part of C	1	complex	real
ALOG(A)	Natural log of A	1	real	real
ALOG10(A)	Common log of A	1	real	real
CABS(C)	$\|C\|$	1	complex	real
CMPLX(A,B)	A+iB	2	real	complex
COS(A)	cos(A), for A in radians	1	real	real
CSQRT(C)	$\sqrt{C}$	1	complex	complex
EXP(A)	e^A	1	real	real
FLOAT(I)	Convert integer to real	1	integer	real
IABS(I)	$\|I\|$	1	integer	integer
IFIX(A)	Truncate real to integer	1	real	integer
MAXO(I,J,...)	Maximum value of all arguments	>1	integer	integer
MOD(I,J)	I minus the product of J with the truncated value of (I/J)	2	integer	integer
REAL(C)	Real part of C	1	complex	real
SIN(A)	sin(A), for A in radians	1	real	real
SQRT(A)	$\sqrt{A}$	1	real	real

The em fields in the mean wake are currently represented by up to 64 angular modes. Thus the variable MODES has this value, which must be an integral power of two, in subroutines WFP and HANK. All variables which are now dimensioned 64 correspond to this requirement. The variable CN(65) in subroutine HANK must be dimensioned at least one greater than MODES. The dimension 256 for the variables G, H and WW in subroutines FFSUM and AVGS must be four times the value of MODES. In AVGS the variables EDS, U and V are dimensioned one greater than twice MODES.

Currently one can input up to 20 axial stations, which relates to all quantities now dimensioned 20. Note also that the data statement for MUTZ in MAIN must conform to the maximum number of axial stations, which is denoted ISTAT in subroutine ZINT. Also, in ZINT, the variable P must be dimensioned at least 19 or one less than ISTAT, whichever is greater. The quantities dimensioned 240 relate not only to the maximum number of axial stations but also to the fact that, currently, a given radial profile function can be input in terms of up to eleven numbers. Thus the dimensions of all quantities now dimensioned 240 must be the maximum number of axial stations times one more than the number of quantities which may be used to specify an input radial profile. If it is desired to input the radial profiles in terms of more than eleven numbers, one must also change the dimension of, and the data statement for, the variable G in subroutine FIT (see subsection IIB2a))*.

This program should require only slight modification to make it run on machines other than the Honeywell 6060. A preliminary version has been converted and run successfully on the CDC6600 at AFGL, Hanscom AFB, MA. The forerunner of this program was run extensively on the CDC7600 at the Army HMDATC-ARC in Huntsville, AL. The CDC (FORTRAN extended) compiler is a bit more particular than the Honeywell (FORTRAN-Y), in that certain changes had to be made to avoid warnings or fatal errors where none had previously occurred. All such changes are compatible with FORTRAN-Y and they have already been incorporated into the code as a general policy.

Certain statements (in MAIN, BCO, STORF, and FFSUM) must be omitted to make the program run on the CDC machines. All such statements are identified in columns 73 to 80 by a comment, which denotes the reason for their presence in the Honeywell version. This computer uses a word of only 36 bits limited to magnitudes between approximately $10^{\pm 38}$. Thus exponent underflow occurs occasionally, although it has a negligible effect on the accuracy of the output. The library subprogram FXOPT(67,1,1,0) suppresses the printing of this error message and proceeds as usual with execution. A second peculiarity in the Honeywell version is the use of scratch random disc for storage of certain quantities. Among the reasons for this are the facts that the number of locations required depends on the input and that the Honeywell execution cost is proportional to both central memory and time, while the latter is hardly affected by disc access. The library subroutine RANSIZ(lfn,n) defines the local file lfn as a random disc having n words per record. The read and write functions are READ(lfn'n)list and WRITE(lfn'n)list, where n is the location of the record.

* A caveat is in order regarding any changes to FIT which involve either the number of inputable profile points or the number LAYERS. If any of the possible input points is exactly the same as one of the values of the independent variable for either mesh point or layer profiles, special programming techniques must be used to avoid an indefinite condition.

The third and final peculiarity is the use of overlays to minimize core storage requirements*. The library routine LLINK('name') loads all routines denoted by certain control cards as belonging to "name" into an area where previous calls may have loaded other routines. (The program has been run with LINKA consisting of subroutines WFP, HANK, BIN, PROP, BCO, and STORF and LINKB containing PHINT, FFSUM, and AVGS.) In addition there is one labeled common block which is common only to the two overlaid areas, so it is included in the main program to avoid its loss during overlaying. This card may be removed from MAIN if overlays are not used. In general only those cards having an identifier in columns 73 to 80 need to be removed for the CDC computers. No other cards have anything in these columns.

Certain cards must be added to make the program run on the CDC machines. The Honeywell computer does not take a PROGRAM card. Also, a common block must be defined to replace the variable stored on disc. The following is a suggested program:

```
      PROGRAM WAKE(INPUT,OUTPUT,TAPE5=INPUT,TAPE6=OUTPUT)

      COMMON/RGHJN/EE(x)

      CALL MAIN

      STOP

      END
```

The quantity x must be specified according to the inputs for the case being run, so this approach permits one to control the amount of central memory required without recompiling the entire program. The value of x must be at least 12*N*(LAYERS+1), where N is defined by the fourth comment card of MAIN. The present main program should be headed by the card SUBROUTINE MAIN; and the card COMMON/RGHJN/EE(1) should be placed in subroutines BCO, STORF, and FFSUM. Also, the appropriate do-loop, transferring the array E into the array EE (or vice versa) replaces the statements writing (or reading) E on disc. For example,

```
      L = 12*NFILE - 11
      DO 300 I=1,12
      EE(L) = E(I)
300   L = L + 1
```

could be used in both BCO and STORF in place of the card identified by "DISC", in columns 73-76 although the index I need run only to 8 in BCO. If the middle statement is reversed, the same loop could be used in FFSUM. It is estimated that approximately 100000 octal central memory locations will be needed for this program in its present form on the CDC machines, not counting the space needed for the EE array. The latter could be anywhere from 3454 to 114400 octal as a function of the inputs, provided that 50 layers and up to 64 modes are used.

* The program requires 30K memory in the Honeywell 6060 when disc and overlays are used, where one K is defined as 1024 decimal locations.

Although it is probably not necessary to do so, one may want to change the values of certain threshold quantities which are used to guard against errors like exponent overflow or exponentials with outside argument, in view of the fact that 10^{38} is roughly the limit for the Honeywell 6060. Such quantities are THRESH in MAIN and subroutines HANK, AVGS, FFSUM and ZINT; EPSO, STP and TEST in subroutine WFP; DBT in subroutines FFSUM and ZINT; and EXA in subroutine AVGS.

B. Description of the Program

In this subsection we give detailed accounts of the mathematical and logical techniques used. The listings in Appendix A may be followed along with these accounts.

1. Main Program

The principal function of this routine is to direct the calculations by calling the major subroutines, WFP, which calculates the em fields in the mean wake, PHINT and RINT, which perform the integrations over ρ and ϕ in (21), and ZINT, which does the convolution (22). Another function, which occupies a large portion of the executable statements, is to generate the radial profiles of collision frequency, electron density, and velocity on the standard grid of layers and boundaries between layers. The logic is very simple. There are two principal nested loops. The outer one is an implicit loop over input cases, between statement number 1 and the statement immediately before the STOP statement. The inner loop iterates over all axial stations. Let us now go through the listing explaining each part in order.

After reading and writing the title and input data, certain constant quantities are calculated. CAY represents k, the free-space wavenumber (per meter). WO and VO represent the absolute values of the sine and cosine, respectively, of the aspect angle α. CS, SS, SC, and SMC represent certain combinations of the sine and cosine of the polarization angle, which are needed in subroutine AVGS. EMC is the critical electron density N_c (per cubic centimeter).

In the loop over the axial stations, EMNCO is the axial mean electron density divided by critical, N_e/N_c, RW is the radius of the wake r_w, CAYR is kr_w, and both VCM and VCOM are the axial collision frequency ratio ν/ω.

Shkarofsky[12] has defined a generalized spectrum function for isotropic turbulence which, when defined by (20), has the following equations:

$$S(k) = \frac{(2\pi)^{3/2} r_i^3 (r_i/r_o)^{\gamma} K_{\psi}(U)}{U^{\psi} K_{\gamma}(r_i/r_o)} \tag{23}$$

$$U = (r_i/r_o)\sqrt{1 + (kr_o)^2} \tag{24}$$

In these equations r_i and r_o are the inner and outer scales of turbulence, respectively, $K_{\gamma}(x)$ is the modified Bessel function of the second kind of order γ, and the parameters γ and ψ are interrelated with the parameter μ, which defines the shape of the spectrum function.

12. I.P. Shkarofsky, "Generalized Turbulence Space - Correlation and Wave-Number Spectrum - Function Pairs", Can. J. Phys., Vol. 46, No. 19, pp. 2133-2153, 1 October 1968.

$$\gamma = (\mu - 1)/2 \tag{25}$$

$$\psi = (\mu + 2)/2 \tag{26}$$

Now in order to obviate both the need for calculating modified Bessel functions and the evaluation of an indeterminate form when the inner scale vanishes, we have used the following equation in place of (23):

$$S(k) = \frac{8\pi\sqrt{\pi}r_o^3\Gamma(\psi)/\Gamma(\gamma)}{[1 + (kr_o)^2]^{\psi}\exp[(kr_i/\pi)^2]} \tag{27}$$

A comparison between (23) and (27) is shown in Figure 2.

The program has the spectrum function (27) built in for six values of μ. The input quantity MUTE and its representative MUT in the loop over axial stations are defined as $3(\mu - 1)$. Thus one can specify μ from 4/3 to 3 in steps of 1/3. The Kolmogorov spectrum function, which is obtained by default, is represented by $\mu = 5/3$. The variable GAMR and its representative GAR are the quantity $\sqrt{\pi}\Gamma(\psi)/\Gamma(\gamma)$. The meanings of the other FORTRAN names for the spectrum function parameters are obvious.

One can see from the listing that the five sets of profile functions are each generated in the same manner. An integer, for example LC for collision frequency, keeps count of the location in the input array where the data for the profile begin. If the initial data point is zero the process is skipped, leaving the profiles as specified at the previous axial station. Most of the profiles are generated both for mesh points (IND>0) and for layers (IND<0), the need for which will be apparent below.

At statement number 6 the variables WS and EMNC represent the values of $\sin^2\alpha$ and N_e/N_c to be used by subroutine WFP. The reason for these new variables is that subroutine PROFS changes their values and also the value of VS, which is $\cos^2\alpha$. TZCS is used by subroutine AVGS.

Statement numbers 8 through 70 represent output of the parameters for the current axial station including all profile functions. After the wake field penetration calculation, MINL (and also L) is the number of the innermost layer reached, all em fields in layers within it being set equal to zero, AN is $[N_e/(N_c\sin^2\alpha)]^2$, and BN is the denominator of (27) for $S(2k)$, where k is the free-space wavenumber. Thus BN represents the reciprocal of the non-constant parts of the backscattering spectrum function in the Born approximation.

After integration over ϕ and ρ (the comment, "integrate over 2RDR", refers to the latter integral), the quantities, S0, S1, S12, and S2, represent the normalized moments of the scattering per unit length for each of five polarization combinations. There are two kinds of normalization, which are removed by the "do 80". A represents the Born approximation for a collisionless uniform wake of radius r_w in which the electron density fluctuation equals the mean electron density. Also, each normalized spectrum moment, when calculated by (21), uses the appropriate electron velocity profile, all of which are normalized by the axial wake velocity/body velocity, VVBZ. The absolute first moment, as seen by the radar, requires multiplication by the cosine of the aspect angle as well as by this normalizing velocity. The second moment comes from $\cos^2\alpha$ times the "first squared" moment plus the true second moment of the fluctuations. The

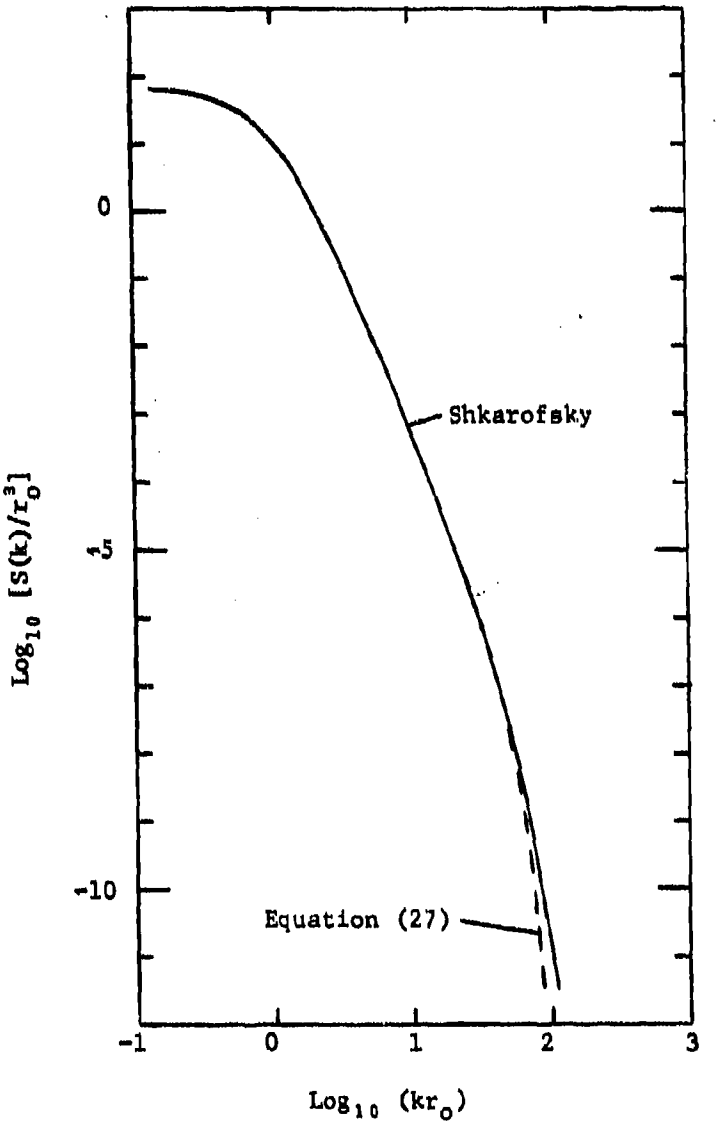

FIGURE 2. COMPARISON OF SHKAROFSKY'S SPECTRUM FUNCTION WITH EQUATION (27). THE SPECTRUM FUNCTION PARAMETERS ARE AS FOLLOWS: $\psi = 5/2$, $r_1 = 0.1r_o$.

quantity S12, representing the "first squared" moment, is the result of integrating over the square of the mean velocity profile. In the "do 90" loop, the moments are converted into velocity mean and spread, where the square of the latter is defined as the difference between the mean square velocity (second moment divided by the zeroth moment) and the square of the mean.

2. Subroutines

In this subsection we follow an outline in which the nomenclature is exactly the same as used in the program listing; i.e., the code letter for each subroutine denotes the paragraph heading for its description here.

a) Subroutine FIT(N,M,IND,F,Y) has the purpose of fitting the input data to a profile on a grid of either layers or layer boundaries. N is the number of points input, M is the location in the input array where the last of these N points is located (M - N + 1 is the location of the first data point), IND is a control variable, F is the array of input data, and Y is the array of output data. The array F must be dimensioned in the calling program at least as large as the value of M. IND controls two aspects of the routine. If IND>0 the profile is calculated for points located in the layers; otherwise the points are at mesh points (boundaries between layers). If $|IND|<2$ it is assumed that the input data are the values of a smooth function at N equally spaced points starting at the axis and ending at the outer edge of the wake. Otherwise the data represent a step function defined by the height of the first step (at the axis), the relative radius of the first step, the height of the next step, the relative radius of the next step, etc. Except, of course, for Y, the values of all variables in the calling sequence are returned unaltered.

A second function of this routine is to define the array ROR, which represents the relative radius, ρ/r_w, of each layer boundary. Note that the layers are not uniform in thickness. In fact they are defined so as to place a definite ceiling on the relative thickness of any given layer. Thus, except of course for the axial layer, the relative thickness, $(\rho_{i+1}-\rho_i)/\rho_i$ is not greater than 0.28519903. If the value of LAYERS were changed, the data for ROR would have to be changed. Let c represent the limit on the relative thickness. (See the discussion of subroutine PROP, where it is shown that c should not exceed 0.3.) The value of c is minimized if there is an integer j for which

$$(c + 1)^j = (c + 1)/c \tag{28}$$

Then

$$\rho_i = \begin{cases} (c + 1)^{i-1}b, & 0<i<j + 2 \\ \rho_{i-1} + b, & j<i<n \\ r_w, & i = n \end{cases} \tag{29}$$

where

$$b = r_w/(n - j + 1/c) \tag{30}$$

and where n is the total number of layers. Of course j is the number of layers having uniform relative thickness and the $(j+1)^{th}$ is the first layer to have the uniform absolute thickness, b, possessed by the remaining layers. In the present program, $j = 6$ and $b = 0.021049829r_w$. Thus relatively few layers have nonuniform thickness and of the fifty layers none has a thickness greater than about 2.1% of the wake radius.

Figure 3 gives a block diagram of this routine. As indicated by the comment card, the location of the independent variable for profiles belonging to points in the layers is defined to be at the midpoint of ρ^2 for each of the layer boundaries (rms value of the radius of the layer). This convention more or less guarantees conservation of line density in the layered cylinder approximation of a smooth profile. Note also that, for profiles on mesh points, the last data point is automatically the value of the last profile point.

As the comment card indicates, N-point Lagrange interpolation is used to give the output values of Y when the input represents a smooth function of the independent variable X. This approach was adopted only after abandoning one which consisted of a least squares fit to a polynomial of degree (N - 1). The least squares approach encountered numerical difficulties, resulting in rapid divergence of the result, when more than seven points were used to define the input function. This difficulty occurred even when the input function was actually an N^{th} degree polynomial. The Lagrange interpolation technique, on the other hand, is numerically quite stable. For example when the input represents a typical Gaussian at eleven points, the output is no more than one unit off in the third decimal place at any of the values of the array ROR.

The theory of the Lagrange interpolation for uniformly spaced data is right out of Abramowitz and Stegun[13]. A bit of manipulation reduces those formulas to the following:

$$Y = \sum_{J=1}^{N} F_J P(X)/[G_J A_J(X)] \tag{31}$$

$$A_J(X) = -(-)^J E_J(X) \tag{32}$$

$$E_J(X) = J - 1 - (N - 1)X \tag{33}$$

$$P(X) = \prod_{K=1}^{N} E_K(X) \tag{34}$$

13. M. Abramowitz and I. A. Stegun, editors, "Handbook of Mathematical Functions", U.S. National Bureau of Standards, Washington, D.C., 1964 (page 878).

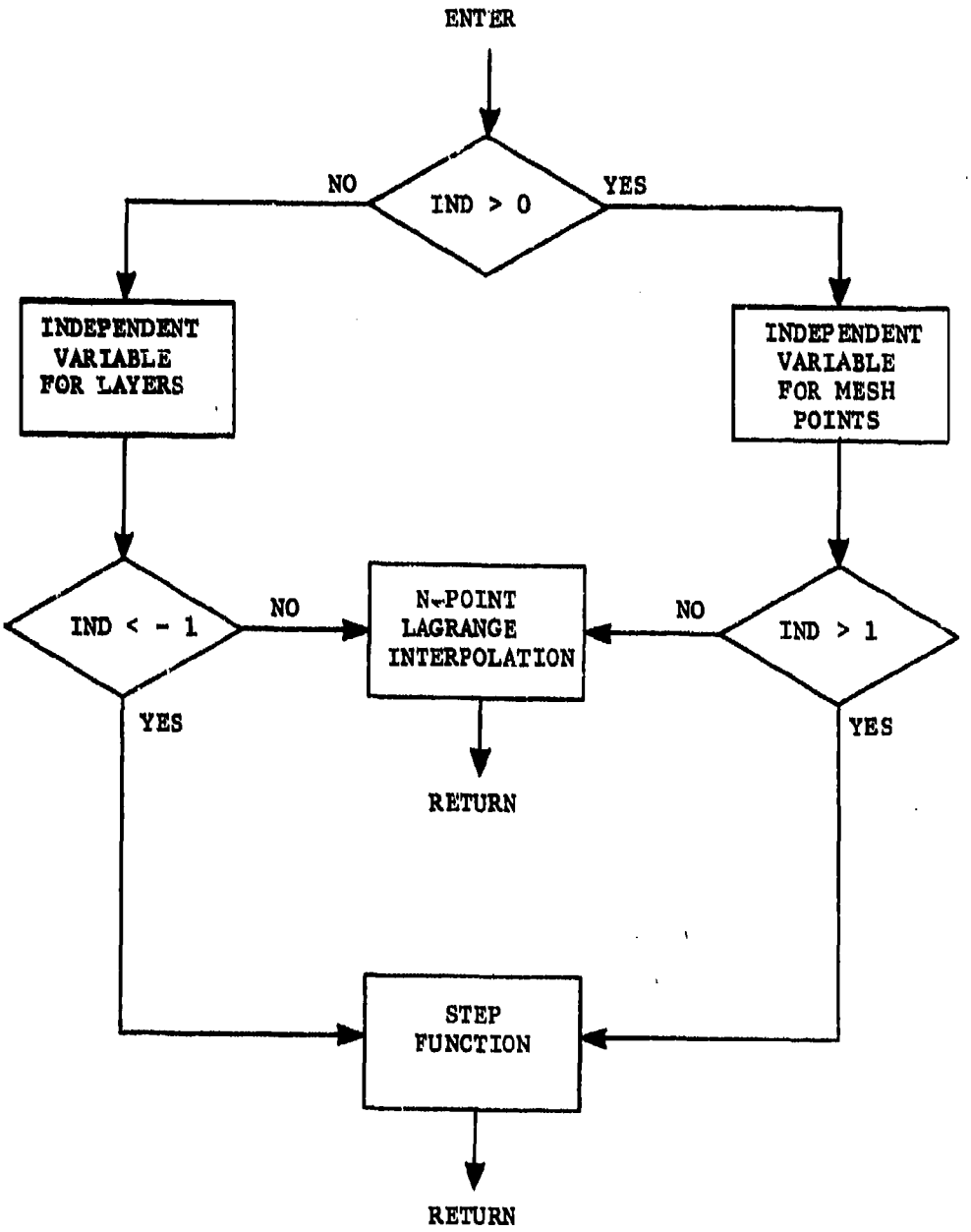

FIGURE 3. SIMPLIFIED FLOW DIAGRAM FOR SUBROUTINE FIT.

The quantity G_J is a symmetric function of J about the midpoint of 1,...,N, where

$$G_J = (J - 1)!(N - J)! \ , \ J < 1 + N/2. \tag{35}$$

Except for P(X) the FORTRAN names follow the above notation. The array G takes advantage of the symmetry of G_J and stores the data from (35) in triangular form. The numbers 1,2,2,3,3,4,4,5,5,6 count off the locations of G_J for N = 2,...,11, respectively. The variable L is the location immediately prior to the first one needed in a given calculation. The "do 10" loop covers all values of the independent variable X defined above. The symmetry of G is utilized in breaking up the sum into the sequential "do 7" and "do 9" loops. The variable B is used to accumulate the dependent variable Y, which is not permitted to be negative since it represents a profile function for a non-negative physical quantity. The routine could in principle give division by zero at the two locations where D is set equal to F divided by the quantity G times A. This will happen if any of the values of X is precisely equal to the value corresponding to one of the uniformly spaced input data. This cannot happen in the present program because the data for ROR and the rms values of adjacent pairs are not rational fractions for numbers up to ten. However, it is not likely to happen even if LAYERS were changed as long as equations (28) to (30) are used to define the values for ROR and c is not allowed to exceed 0.3. Obviously, of course, even if it happens, one would simply code the routine to take the input data value (Y = F) at such singular points.

The step function routine simply searches for X values which fit on a given step (the if statement in the do-loop), setting Y equal to the height of the step for all those that do. The steps can go up or down or both.

b) Subroutine PROFS(IRE,KRIT,MUT,PSI) has the primary purpose of computing the effects of scattering by turbulence on the propagation of the coherent wave in the mean wake. Other functions of this routine, which are included because of their logical relation to either this function or the point in MAIN where PROFS is called, are the coefficient of depolarization by second scattering, the adjustment of the aspect angle and electron density to make the critical points lie at layer boundaries, and the profile of the reciprocal of the dielectric constant at layer boundaries.

The variables IRE, MUT and PSI, in the calling sequence, are inputs, which are unaltered by the routine. IRE = 1 implies that the profile of mean electron density is a smooth function and that readjustment of the axial electron density and the aspect angle is necessary for reasons given below. MUT and PSI pertain to the turbulence spectrum function in precisely the same way as in MAIN. KRIT is returned as zero if IRE ≠ 1 or if there is no point at which the real part of the adjusted complex dielectric constant vanishes. Otherwise it is the number of the layer boundary at which this critical point occurs. The logic of this routine is very simple. It starts with a do loop over all layers, in which the scattering attenuation and depolarization are

calculated and the effect of scattering attenuation on the mean plasma is accounted for. Then the adjustment of aspect angle and electron density are made, if required, in two do loops over the layers. Finally there is a do loop generating the profile of the reciprocal of the dielectric constant at layer boundaries and placing the adjusted values of plasma properties in the appropriate arrays for use by subroutine WFP. The five tasks covered by the last three sentences are each denoted by comment cards.

The coefficients of attenuation by scattering and of depolarization by second Born are calculated from, for example, the theory given by Shkarofsky[14]. Thus

$$\alpha_s = \frac{r_e^2 \overline{N_e'^2}}{4[1 + (\nu/\omega)^2]} \int_{-1}^{\cos\beta_m} (1 + x^2) S(k_e \sqrt{2(1-x)}) dx \tag{36}$$

$$\beta = \frac{2^5 \pi r_e^2 \overline{N_e'^2}}{1 + (\nu/\omega)^2} \int_0^1 x^5 (1-x^2)^2 S(2k_e x) dx \tag{37}$$

where α_s is the scattering attenuation and β is the depolarization rate.* In the argument of the spectrum function S, the symbol k_e represents the effective wavenumber in the mean medium, which could be evaluated as half the gradient of the argument of $E_0 \cdot G_0$. But this would lead to an iterated problem, so we let k_e equal the free-space wavenumber k times the real part of the square root of the complex dielectric constant. In (36) the angle β_m represents a cutoff angle for omitting the effect of forward scattering from the extinction coefficient α_s. The idea for, and the form of, β_m are taken from Guthart and Graf[15]. Thus we use the following equation:

$$\cos\beta_m = 1 - [1 + (k + k_e)(r_w - \rho)/(2\pi \sin\alpha)]^{-1} \tag{38}$$

where k_e is k times the real part of the square root of the complex dielectric constant at the local value of the radius ρ in the mean wake.

Of course the spectrum function (27) is used in the above integrals, except that the exponential cutoff involving the inner scale r_i is replaced by a sharp cutoff. The integrals reduce to the following:

$$\alpha_s/k = D/(16\pi) \int_Y^X (1 - 2x + 2x^2)(1 + ax)^{-\psi} dx \tag{39}$$

$$\beta = kD \int_0^X x^2 (1-x)^2 (1 + ax)^{-\psi} dx \tag{40}$$

14. I.P. Shkarofsky, "Modified Born Backscattering from Turbulent Plasmas: Attenuation Leading to Saturation and Cross-Polarization", Radio Science, Vol. 6, Nos. 8, 9, pp. 819-831, August-September 1971.
15. H. Guthart and K. Graf, "Attenuation Due to Scatter in Random Media", Physics of Fluids, Vol. 15, No. 7, pp. 1292-1299, July 1972.

* Note that β is the two way depolarization; i.e., it is twice Shkarofsky's β.

$$D = \frac{\sqrt{\pi}\Gamma(\psi)(2kr_o)^3\overline{N_e'^2}}{\Gamma(\gamma)N_c^2[1 + (\nu/\omega)^2]} \tag{41}$$

$$Y = (1 - \cos\beta_m)/2 \quad , \quad a = (2k_e r_o)^2 \tag{42}$$

The upper limit X is equal to either unity or the quantity, $[\pi/(2k_e r_1)]^2$, whichever is smaller, the latter quantity representing the cutoff at the inner scale. The integrals in (39) and (40) are evaluated, if the quantity a is not too small, by repeated integration by parts to the point where the polynomial in x is reduced to a constant by the repeated differentiations. These formulas are represented in the FORTRAN statements prior to statement number 2, and they differ when ψ is integral (MUT = 3), as at statement number 1. These equations lead to indefinite conditions when a is small, so in that case we integrate by replacing the binomial in ax by $(1 - a\psi x)$, which is done between statements 2 and 3. In all statements FJ denotes the integral in (39) and GJ denotes that in (40). The quantity D at statement number 3 is D in the above formulas. AK represents α_s/k and BOK, $\beta/(k\sin\alpha)$.

The attenuation owing to scattering, α_s, is a concept from geometric optics theories. As such it is not easy to fit to the present theory, which is a full wave theory. In optical theories one integrates α_s along ray paths to get the total scattering attenuation to a given point, which is in close analogy with the phenomenology of collisional attenuation. However in this theory we get the local field at a given point by rigorous expansions of solutions of Maxwell's equations. In order to use a representation of scattering attenuation which is consistent with this theory, we adopt the approach of adding to the mean plasma properties in such a way that scattering attenuation is automatically accounted for. Ideally it would be preferable simply to add a quantity to the collision frequency since collisions cause attenuation, but it can be shown that this is not possible to do in a consistent way. Therefore we add quantities to both the electron density and collision frequency. These quantities must give an attenuation coefficient which is identical with α_s and they must vanish when α_s vanishes. There are many different sets of equations which have these properties, but we use the following:

$$G = 1/(1 + \sqrt{\alpha_s/k}) \tag{43}$$

$$D = 1 + (\alpha_s/k)^2 - G^2 \tag{44}$$

$$\nu/\omega = 2G\alpha_s/(kD) \tag{45}$$

$$N_e/N_c = [1 + (\nu/\omega)^2]D \tag{46}$$

These equations are used, down to statement number 6, to give EMS and CFS, which represent normalized profile function arrays for these added electrons and collisions. The arrays EM and CFL are temporarily used for the total profile functions at mesh points (layer boundaries).

In previous studies it was found that wave propagation in a layered

plasma can often be seriously affected by the method in which the layers are chosen to represent a given smooth distribution. This effect is related to the fact that the smooth distribution has critical density at only an isolated point, while the layered approximation, if selected at random, might have critical density in an entire layer. It was found that all spurious effects of layering could be avoided if the two critical density points are made to lie at layer boundaries. These two critical densities are defined as that for which the real part of the dielectric constant K vanishes (intrinsically critical density) and that for which the real part of K is equal to $\cos^2\alpha$ (critical density for refraction). The "do 10" loop adjusts EMNC to meet the first criterion and the "do 15" loop adjusts WS (defined as $\sin^2\alpha$) to satisfy the second. Additional conditions satisfied by these loops are that the electron density be a decreasing function of radius ρ at each critical point and that the outer edge be underdense.

It will be seen below that the radial component of the electric field is related to the tangential magnetic field components and to the reciprocal of the complex dielectric constant. The arrays ROK and AOK are the real and imaginary parts of 1/K at mesh points.

At the end of the routine the arrays EM and CFL are given their permanent meaning, for use in subroutine WFP, as the profile functions for electron density and collision frequency in the layers. EMO and CFO are the corresponding quantities without enhancement owing to scattering attenuation.

c) Subroutine WFP(JMIN,NHP) calculates the em fields in the mean wake plasma*. In the calling sequence, JMIN is the number of the innermost layer boundary reached, all fields within this point being assumed to vanish. NHP is the total number of angular modes used to represent the fields. Both variables are, of course, outputs of the routine.

The array YIP is defined as the thickness of a given layer divided by its inner radius, starting, of course, at the second layer (i.e., excluding the axial layer). Its values depend on the values of ROR in subroutine FIT. The first executable statements define the array RK as $k\rho$ for the outer boundaries of all layers and set up a few constants for later use.

The problem of em wave propagation in the cylindrical mean wake plasma is solved by separation of variables and superposition. Thus the vector electric field E at an arbitrary point (ρ,ϕ,z) is written as follows:

$$E = \exp(ikz\cos\alpha) \sum_{n=-\infty}^{\infty} e(n,\rho)e^{in\phi} \qquad (47)$$

The quantity $e(n,\rho)$ is the partial electric field vector for the n^{th} order mode and is a spatial function of only the radial coordinate. The magnetic field H has the same representation except that h replaces

* The name of this routine derives from the name Wake Field Penetration.

e. In free space the functions e and h involve Bessel functions of argument $k\rho\sin\alpha$ and order n. The incident wave includes only the ordinary Bessel functions and the scattered wave has the Bessel function of the second kind as well. The asymptotic behavior of these functions at large orders is such that the function of the second kind increases while the ordinary Bessel function decreases. If the modal series (47) is to converge at all, its convergence must depend on the ratio of these two functions. Therefore, in consonance with the 36-bit computer word (approximately eight place accuracy) we truncate the series when the ratio of the two functions of argument $kr_w\sin\alpha$ is greater that 10^9. In the section, "determine the number of modes to use", A represents this argument and NHP is the number of modes which satisfies this criterion. The equation for NHP is a good fit to the above criterion for values of the argument between about 0.5 and 35, and it is conservative at all other values. (Note that negative orders are not distinguished from positive ones in this discussion because of the symmetry properties which obtain. Thus NHP is one greater than the largest value of n used in (47).)

The complex dielectric constant K and the propagation constant γ determine the solution for em wave propagation. Their forms, which are used in the "do 100" loop, are as follows:

$$K = 1 - N_e/[N_c(1 + i\nu/\omega)] \tag{48}$$

$$\gamma = k\sqrt{K - \cos^2\alpha} \tag{49}$$

In these equations N_e and ν are the electron density and collision frequency in a given layer. The array DIEL represents K and the array GAM, γ/k.

The logic of this subroutine is very simple. It consists of two nested loops over the angular modes and the cylindrical layers. The separation of variables (47) allows the solutions e and h to be obtained as functions of ρ for each n independently, so we iterate over modes (NP = n + 1) in the outer loop ("do 600"). In this loop EYEN$\equiv i^n$, SGN$\equiv(-)^n$, and EN$\equiv$n.

The solutions for e and h for a given value of n come from substituting both (47) and its magnetic analog into Maxwell's equations, which for $\exp(-i\omega t)$ time dependence are

$$\nabla\times E = ikH \quad ; \quad \nabla\times H = -ikKE \tag{50}$$

where we have assumed a system of units in which the characteristic impedance of free space is unity, for convenience*. These equations give six linear first order ordinary differential equations in each of which are three of the six cylindrical coordinates components of e and h. These six equations reduce to four by elimination of the radial components, but each of these four equations contains in general three of the four tangential components. The easiest way to

* The system of units is immaterial since all results will eventually be expressible in nondimensional terms.

solve these is to suppose that all fields are the sums of two kinds, TE and TM, where T denotes transverse to the axis and E and M refer to electric and magnetic. Thus, for TE, when $e_z = 0$ is substituted one gets, by elimination of the ϕ - components, a second order differential equation in h_z. A similar equation for e_z results from assuming $h_z = 0$. These two equations differ only in terms of the effect of gradients of K, so in our layered approximation they are identically the same equation, which is Bessel's equation for order n and argument ξ, where

$$\xi \equiv \gamma\rho \tag{51}$$

The four simultaneous differential equations can also be solved for the ϕ - components as functions of the z - components. The results are expressible in terms of the following variables:

$$p \equiv ik/\gamma \tag{52}$$

$$q \equiv nk\cos\alpha/(\gamma\xi) \tag{53}$$

Thus

$$e_\phi = -qe_z - ph_z' \tag{54}$$

$$h_\phi = -qh_z + Kpe_z' \tag{55}$$

where prime denotes differentiation with respect to ξ.

Each tangential field component must be continuous across boundaries between layers. A matrix representation is a convenient way to keep satisfying this condition from layer to layer. Thus we arbitrarily adopt the following tangential fields vector F:

$$F \equiv \begin{bmatrix} e_z \\ h_\phi \\ h_z \\ -e_\phi \end{bmatrix} \tag{56}$$

Now, for the time being, we restrict the discussion to the behavior of F within any given layer. Since the z - components are each independent linear combinations of two independent solutions of Bessel's equation, let $F = UA$, where A is a column vector of undetermined coefficients and the square matrix U comes from the equations for each component of F. Let

$$U = \begin{bmatrix} u & v & o & o \\ Kpu' & Kpv' & -qu & -qv \\ o & o & u & v \\ qu & qv & pu' & pv' \end{bmatrix} \tag{57}$$

where u and v are the two solutions of Bessel's equation. Let subscript 0 denote the value of a quantity at the inner boundary of a given layer, unsubscripted variables denoting either constants or the values of the variables at the outer edge of the layer. There must exist a square matrix P such that $F = PF_0$, which implies that $UA = PU_0A$ since A is constant throughout the layer. Thus $U = PU_0$ or $P = UU_0^{-1}$. Now if we require of the two solutions that $v_0 - u_0' = 0$, then U_0 has only two nonzero off-diagonal elements and is easy to invert. The result is

$$P=\begin{bmatrix} u/u_o & v/(Kpv_o') & q_ov/(Kpv_o') & 0 \\ [Kpu'/u_o+qq_ov/(pv_o')] & v'/v_o' & (q_ov'/v_o'-qu/u_o) & -qv/(pv_o') \\ -q_ov/(pv_o') & 0 & u/u_o & v/(pv_o') \\ (qu/u_o-q_ov'/v_o') & qv/(Kpv_o') & [qq_ov/(Kpv_o')+pu'/u_o] & v'/v_o' \end{bmatrix} \quad (58)$$

Three of the fourteen nonzero elements of this matrix are repeated, so the arrays PP, PQ, ..., PZ represent the eleven unique elements in their order of appearance reading across rows. The variables P, Q, R, and S, which are calculated in subroutine PROP, represent u/u_o, v/v_o', u'/u_o, and v'/v_o', respectively.

Now the boundary condition between layers is automatically satisfied if F is matched. Therefore F at the outer edge of a given layer is identical with F at the inner edge of the next layer. Thus, since P represents the propagation of F through a layer, cumulative matrix multiplication of the P matrices for each layer gives the propagation of F through all layers. This cumulative product has the FORTRAN name QQ(i,j) for the element of the i^{th} row and j^{th} column. Initially it is the identity matrix (the "do 200" loop) and it is updated in the "do 300" loop. One will note that QQ is replaced by QQ times P as the layers are iterated from the outside in. Thus, since P represents propagation of F from the inside to the outside of the layer, QQ is the propagation of F from the currently reached inner boundary to the outermost boundary.

The overall propagation matrix (let us call it Q instead of QQ in this discussion) tends to diverge in cases in which there is strong cutoff of the em fields in the central regions of the layered cylinder. Owing to the nature of the Wronskian, the inverse representation Q^{-1}, which gives propagation inward from the outside edge, also diverges. Thus, no matter how one calculates propagation, there can be a point at which exponential overflow will occur, especially in case of a limited computer word. In the computer model we insert a perfectly conducting boundary just before that point is reached. Three criteria are used. The first is the if statement near the beginning of the "do 500" loop, which guards against the fact that the layer propagation matrix P tends to increase exponentially with the argument ξ. The second is the two if statements in the "do 400" loop, which guard against overflow of $|Q|^2$. The third criterion, which is exercised just after the latter loop, is based on the supposition that ϵ (called EPSO) represents the smallest field intensity of any practical

significance. Then the greatest value of Q of any interest is such that $|Q|^2\varepsilon$ has about the magnitude of the field intensity at the outer edge, which is approximately proportional to the square of the ordinary Bessel function of argument $kr_w\sin\alpha$. The Bessel function is in the neighborhood of unity for small orders and at large orders it drops off according to well known asymptotic forms. Combining these limits into a single expression gives the criterion

$$|Q|^2\varepsilon\{1 + \sqrt{2\pi n}[2n/(ekr_w\sin\alpha)]^n\}^2<1 \qquad (59)$$

where e is the base of natural logarithms. The magnitude squared of Q is estimated from its average value for all sixteen elements.

The section of this routine which involves boundary conditions is closely related to subroutines BIN and BCO. The theory is detailed under those routines rather than here because this routine merely calculates certain parameters for, or from, those routines.

d) Subrountine HANK(NP,X,HNK,HNKP) calculates the Hankel functions of the first kind and their derivatives for use in the outer boundary condition. NP is the number of orders to be calculated (n = o to NP - 1) and X is the argument, a real variable. The complex arrays HNK and HNKP contain the output Hankel functions and their derivatives and must be dimensioned at least NP by the calling program. The method used is downward recurrence on the Bessel function, normalization based on the value unity for the generating function, the Neumann expansion of $Y_0(x)$ in terms of $J_n(x)$ for all even values of n, the use of the Wronskian to get $Y_1(x)$, and finally upward recurrence on the function of the second kind, $Y_n(x)$. Refer to chapter 9 of Abramowitz and Stegun (op. cit., ref. 13) for the equations, which are readily located in the listing with the aid of the comment cards.

The form of the convergence criterion, which identifies the order at which to begin the downward recurrence, is based on the behavior of Bessel functions, for which it can be shown from tabulated values and asymptotic forms that $J_n(x)<10^{-y}$ if n is approximately equal to or greater than $[y - 4.5 + \sqrt{3|x|(|x| + 8)}]$. The value 12 for y was derived from experimental (checkout) runs using the 36-bit computer word.

e) Subroutine BIN(X,NP,B1) calculates $J_n'(X)/J_n(X)$ for complex X and for orders n = 0 to NP - 1. The results are placed in the complex array B1, which must be dimensioned at least NP in the calling routine. The method used is downward recurrence; i.e.,

$$J_n'(X)/J_n(X) = n/X - C_{n+1}(X)/C_n(X) \qquad (60)$$

$$C_n(X) = 2(n + 1)C_{n+1}(X)/X - C_{n+2}(X) \qquad (61)$$

where the C_n's are started with arbitrary values at the order given by the convergence criterion, which was derived as in subroutine HANK. Of course normalization using a generating function is not required. Also, there is no danger of division by zero as long as the imaginary part of X does not vanish (collision frequency not

identically zero in the axial layer), because all zeros of $J_n(X)$ are real.

The raison d'etre of this routine is the inner boundary condition. In case, in subroutine WFP, the axial layer is reached in the propagation calculation, the boundary condition at its surface must account for the presence of only the Bessel function of the first kind. We state this boundary condition in the following form in terms of the two unknown constants A_1 and A_2:

$$F_1 = \begin{bmatrix} A_1 B_{11} \\ A_1 - q A_2 \\ A_2 \\ A_2 B_{12} + q A_1 B_{11} \end{bmatrix} \tag{62}$$

$$B_{12} = ikB_1/\gamma \tag{63}$$

$$B_{11} = 1/(B_{12}K) \tag{64}$$

$$B_1 = J_n'(\xi)/J_n(\xi) \tag{65}$$

where the dielectric constant K and the quantities γ, ξ and q, which are defined by (49), (51) and (53), are for the axial layer at its outer edge. Of course F_1 represents the tangential fields vector F at this boundary. This normalization is used, rather than one in which J_n and J_n' appear separately in all terms of (62), because B_1 is easier to calculate and because this form is compatible with the perfectly conducting boundary condition, in which B_{11} and B_{12} are zero to account for the vanishing of the tangential electric fields.

f) Subroutine PROP(EN,XZR,XZI,Y,C,D,CP,DP) calculates the four basic quantities which comprise the nonzero elements of the propagation matrix P for a given layer. The first four variables in the calling sequence represent inputs and the last four, outputs. EN is the floating point value of the mode order n. XZR and XZI are the real and imaginary parts of the quantity ξ_0, which represents $\gamma\rho$ at the inner boundary of the layer. Y is the relative layer thickness. For the purposes of the derivations, let C, D, C', and D' represent C, D, CP, and DP, which are called P, Q, R, and S in subroutine WFP.

In the limit of zero layer thickness the propagation matrix must approach the identity matrix. In this limit the quantities C and D', which are on the diagonal, must go to unity and the quantities D and C' must vanish. Supposing that this limit is approached continuously, we use series expansions in the layer thickness to calculate these quantities. The limiting forms serve to determine the forms of these series up to the second order. Thus let

$$C = 1 + \xi_0 Y \sum_{j=1}^{\infty} c_j \tag{66}$$

$$D = \xi_0 Y[1 + \sum_{j=1}^{\infty} d_j] \tag{67}$$

$$C' = \sum_{j=1}^{\infty} (j + 1)c_j \tag{68}$$

$$D' = 1 + \sum_{j=1}^{\infty} (j + 1)d_j \tag{69}$$

In these equations c_j and d_j are each equal to a complex number, which depends on j, times the j^{th} power of the relative layer thickness Y. The recurrance relation for these terms is derived by substitution of either the C or the D series in Bessel's equation, for which the independent variable is $\xi = \xi_0(1 + Y)$, and requiring that the result apply independently for each power of Y. Thus

$$j(j + 1)a_j + (2j - 1)jYa_{j-1} + [(j - 1)^2 - n^2]Y^2a_{j-2} + \xi_0^2Y^2(a_{j-2} + 2Ya_{j-3} + Y^2a_{j-4}) = 0 \tag{70}$$

where a_j represents either c_j or d_j. This recurrence relation applies liberally as long as the following initial conditions are used:

$$a_j = 0 \ , \ j < -1 \tag{71}$$

$$c_0 = d_{-1} = 0 \tag{72}$$

$$c_{-1} = 1/(\xi_0 Y) \tag{73}$$

$$d_0 = 1 \tag{74}$$

In the program the approximate convergence criterion represents a fit to the minimum number of terms needed in the infinite series to guarantee convergence in all of more than 500 runs of this routine which were made during checkout. These sums also have an internal convergence criterion following the "do 8" loop. The array AJ(I,J,K) represents c_j for I = 1 and d_j for I = 2. The real and imaginary parts are for J = 1 or 2, respectively. The five locations in the third subscript represent the values needed for recurrance. The values of these locations are denoted L, LA, LB, LC, and LD and are updated in each iteration. The first three terms of (70) have real coefficients and these are represented temporarily in terms of the array P. The coefficient of the complex variable ξ_0^2 is temporarily placed in the array Q. After updating the a_j the sums used in C and D are accumulated in U and those used in C' and D', in W, but not before P and Q are temporarily used for the old values of U and W to facilitate convergence testing. At the end the outputs are calculated as in (66) to (69).

The present form of this routine is believed to be the optimum for a multi-layered medium. These four matrix elements are, of course, identical with the cross products of the first and second kinds of Bessel functions for the complex arguments for either boundary of the layer. But the method of calculation based on this fact would require much more memory and would have great inefficiency in thin

layers. The recurrence relations for these cross products were tried, but no way was found to eliminate the fatal round off error which was accumulated. A detailed study of series expansions whose leading terms are designed to fit the various asymptotic forms of Bessel functions was done also, however all of these failed in some regime where the above scheme worked. With the constraint that Y be not greater than 0.3 this algorithm works in the Honeywell 6060 for values of the outer-edge argument $|\xi_0(1 + Y)|$ as large as 88. This is exceptionally good performance because the result tends to be exponential in this argument and exp(88) is at the limit of the computer word. Note that the implicit series in Y, in which Y^j is part of c_j and d_j, is largely responsible for this good performance. When explicit power series were used we could not get past about 50, instead of 88, without exponent overflow.

g) Subroutine BCO(M) applies the boundary conditions to get the local fields at all mesh points from layer M out to the outer edge.

The outer boundary condition is the sum of the tangential fields for the incident and scattered waves. Standard Fourier-Bessel expansions of the vector incident fields given by (16), (17) and (18) produce expressions for the tangential components of e in the incident wave. The incident waves are so defined that the magnetic field for transverse polarization is identical with the electric field for parallel while the magnetic field for parallel is the negative of the electric field for transverse. The result is

$$F^i = \begin{bmatrix} F_1 \\ F_2 \\ 0 \\ b\,F_1 \end{bmatrix}_{\text{parallel}} \quad \text{or} \quad \begin{bmatrix} 0 \\ -b\,F_1 \\ F_1 \\ F_2 \end{bmatrix}_{\text{transverse}} \tag{75}$$

$$F_1 = i^n \; J_n(kr_w \sin\alpha) \sin\alpha \tag{76}$$

$$F_2 = i^{n+1} J_n'(kr_w \sin\alpha) \tag{77}$$

where F^i denotes the contribution of the incident wave to the tangential fields vector, defined by (56), at the outer edge and b is q, defined by (53), evaluated in free space at the outer edge.

$$b = n \cos\alpha/(kr_w \sin^2\alpha) \tag{78}$$

The axial components of the scattered waves must be proportional to the Hankel function of the first kind, so we let the scattered tangential fields vector F^s have the following form:

$$F^s = \begin{bmatrix} A_1^s \\ A_1^s B_2 - b A_2^s \\ A_2^s \\ A_2^s B_2 + b A_1^s \end{bmatrix} \tag{79}$$

$$B_2 = i \; H_n'(kr_w \sin\alpha)/[\, H_n(kr_w \sin\alpha) \sin\alpha] \tag{80}$$

where A_1^s and A_2^s are unknown scattering coefficients.

The boundary conditions are expressible as the following matrix equation:

$$F^i + F^s = Q\, F_i \tag{81}$$

where one will recall that F_i is the inner boundary condition, given by (62), and that Q represents propagation of F from the inner boundary point to the outer edge. Because it involves the four unknown coefficients in F_i and F^s, this equation is equivalent to another matrix equation as follows:

$$\begin{bmatrix} S_{11} & S_{12} & -1 & 0 \\ S_{21} & S_{22} & -B_2 & b \\ S_{31} & S_{32} & 0 & -1 \\ S_{41} & S_{42} & -b & -B_2 \end{bmatrix} \begin{bmatrix} A_1 \\ A_2 \\ A_1^s \\ A_2^s \end{bmatrix} = F^i \tag{82}$$

where

$$S_{j1} = B_{11}\,(Q_{j1} + q\, Q_{j4}) + Q_{j2} \tag{83}$$

$$S_{j2} = Q_{j3} + B_{12}\, Q_{j4} - q\, Q_{j2} \tag{84}$$

It is not necessary to solve this equation for A_1^s and A_2^s because A_1 and A_2 determine the fields at all points via the propagation matrix P for each layer. Equation (82) represents the equation $SA = F^i$, which is transformed by the matrix

$$T = \begin{bmatrix} B_2 & -1 & -b & 0 \\ b & 0 & B_2 & -1 \end{bmatrix} \tag{85}$$

into the following equation of rank two:

$$TS \begin{bmatrix} A_1 \\ A_2 \end{bmatrix} = \begin{bmatrix} F_3 \\ 0 \end{bmatrix}_{\text{parallel}} \quad \text{or} \quad \begin{bmatrix} 0 \\ F_3 \end{bmatrix}_{\text{transverse}} \tag{86}$$

The quantity F_3 is $(B_2F_1 - F_2)$, but the Wronskian gives

$$F_3 = -\, 2i^n/[\pi\, kr_w\, H_n(kr_w \sin\alpha) \sin\alpha] \tag{87}$$

The two systems of equations represented by (86) are readily solved for the two alternative sets of values of A_1 and A_2. Note that all results are proportional to the quantity F_3. The complex exponential $e^{in\phi}$ is used in the modal expansion (47) because it represents all field components simultaneously. However each cylindrical coordinate component of each (electric and magnetic) field for each incident wave polarization has either even or odd symmetry in n and ϕ. Thus (47) is actually a summation over positive n involving either 2 cos(nϕ) or 2i sin(nϕ), as well as the term for n = 0. Therefore we take care of the factor 2 for n>0 by multiplying F_3 by two in subroutine WFP, where this quantity is calculated. (The quantity F_1, which is needed to give the coherent scattering coefficients, is likewise doubled at the same point.)

Now, to interpret the FORTRAN, the variable C7 represents b and B represents q. C5 and C6 are temporarily used for S_{11} and S_{31}, and C1 and C2 are the elements in the first column of TS. Then C5 and C6 are S_{12} and S_{32}, and C3 and C4 are the second column of TS. The two sets of simultaneous equations (86) are then solved and, after the "do 10" loop the arrays FJA(K), FJB(K), FJC(K), and FJD(K) are the four elements, in order, of the tangential fields vector F. The first set (K = 1) is for a parallel polarization incident wave and the second (K = 2) is for transverse. After this the "do 200" loop generates the tangential fields at each layer boundary by iterated matrix multiplication by the stored propagation matrix P for each layer.

The final function of this routine is to generate, output, and store (on disc) the coherent scattering coefficients, starting at statement number 210. Note from the definition (56) of F that according to (79) and (75) the scattering coefficients are fully characterized by the z-components of the fields at the outer boundary after F_1 has been subtracted from e_z for parallel polarization and h_z for transverse. Now in free space the four z-components each propagate as $H_n(k\rho \sin\alpha)$, so their values at any point may be gotten by multiplying the ratio of this quantity to its value at the wake edge by their values at the wake edge. In the far field this ratio has the asymptotic form

$$\frac{2 \exp[i(+\pi/4 + k\rho \sin\alpha)]}{\sqrt{2\pi k\rho \sin\alpha}\; i^n\; H_n(kr_w \sin\alpha)}$$

Now see subroutine WFP, where Z is $0.5\, i^n \sin^2\alpha\, H_n(kr_w \sin\alpha)$. Also noting that the slant range r from the origin of the wake is equal to $\rho/\sin\alpha$, this implies, for example, that in the far scattered field for

parallel polarization

$$E_z \sim \frac{\sin\alpha \exp[i(kr - \pi/4)]}{\sqrt{2\pi\, kr}} \sum_{n=o}^{\infty} C3 \cos n\phi \qquad (88)$$

where C3 is the FORTRAN variable which is output and stored (on disc) at this point in the program. Now, seeing that the scattered wave propagates in the direction making angle α to the z-axis,

$$E_{\text{scattered parallel}} \sim \frac{e^{i(kr - \pi/4)}}{\sqrt{2\pi kr}} \sum_{n=o}^{\infty} C3 \cos n\phi \qquad (89)$$

This is a component of the coherent far electric field scattered by a wave incident in the plane of the axis (as defined above). This component also lies in the plane of the axis, where the positive direction is as defined for the incident wave. The same component of the scattered magnetic field for transverse incident wave polarization has identically the same equation with C6 replacing C3. These two field components have even symmetry. The other two, having odd symmetry, use i sin $n\phi$ in place of cos $n\phi$. The axial plane magnetic field for parallel incident wave polarization has C4 in the summation and the axial plane electric field for transverse polarization has C5. The fact that half of these results are magnetic fields presents no problem conceptually since in the far field the electric vector is equal to the cross product $\mathbf{H}\times\hat{\mathbf{r}}$, where $\hat{\mathbf{r}}$ is a unit vector in the direction of scattering. Thus the transverse (ϕ - component) electric field scattered by a parallel incident field is the sum in C4 and the transverse electric field for transverse incident field uses C6. The write statement, then, gives the coefficients for parallel and transverse in order, first for parallel incident field and then for transverse. For reasons of convenience below, the real and imaginary parts of the field components are stored in odd, even order, where the odd components have the coefficient multiplied by i so that the Fourier sums are over either sin $n\phi$ or cos $n\phi$. This order is E_{tp}, E_{tt}, E_{pt}, E_{pp}, where the first subscript is the incident wave polarization and the second is the scattered. The storage location implies that these are scattered fields in that one extra "layer" is saved for this (LAYERS + 1).

h) Subroutine STORF(NP,J,ENKR,V) stores in odd, even order the local electric fields components. All elements of the calling sequence are inputs, which are unaltered by the routine. NP is (n + 1), J is the number of the layer boundary, ENKR is $n/(k\rho)$ for this boundary, and V is cos α. All components having odd symmetry are multiplied by i in order that all total fields be straight Fourier sums. The order of storage is real, imaginary; ρ, ϕ, z - component; transverse, parallel incident wave; where the first set of things varies the most rapidly and the last varies the least rapidly.

The radial electric fields are given by the following equation, which is one of the six resulting from substitution of the modal expansions (47) in Maxwell's equations:

$$e_\rho = \{ h_\phi \cos\alpha - [n/(k\rho)]\, h_z \}/K \qquad (90)$$

The general storage location denotes both the layer boundary and the mode order.

i) Subroutine PHINT(LS,MM) directs the analysis of the ϕ - dependence of all field quantities for the mean wake. One of the most important aspects of these calculations is the integration over ϕ for equation (21), whence the name PHINT. In the calling sequence LS is the number of the innermost layer boundary reached in the field penetration calculation. MM is the total number of modes used in the expansions of the fields.

The first part of this routine sets up the grid of angles to use for representing the variation of all fields with ϕ. The criterion is that the number of uniformly spaced angles be a power of two which is at least four times the number of modes used in the field expansions. This criterion derives from the fact that the integral over all angles ϕ of any m^{th} order Fourier sum is precisely represented by the trapezoidal rule for evenly spaced values of ϕ as long as the number of angles is greater than or equal to m. The product $|E_0 \cdot G_0|^2$ represents a Fourier sum of order 4m if E_0 and G_0 are each of order m. In the routine, IM is the number of angles and M is the power of 2 to which it is equal.

The routine calls for the summation of the coherent scattered fields before going to the loop over layer boundaries, at each of which the ϕ - dependence is analyzed.

j) Subroutine FFSUM(LYR,MM,N,M,LTH) uses the FFT algorithm to evaluate the various Fourier sums which represent the components of the electric field in the mean wake. LYR is the number of the layer boundary or, if greater than LAYERS, an indication that the coherent scattered fields are to be evaluated. MM is the number of modes for which the Fourier coefficients of the fields have been calculated. N is the number of angles, which must be the M^{th} power of 2. If LTH = 0 the routine assumes that sin ϕ and cos ϕ for all ϕ on the grid of angles have not been calculated before. These quantities are placed in the array WW during execution and LTH = 1 is returned. If LTH = 1 it is assumed that these values already are stored in WW. (These assumptions are valid as long as the calling routine (PHINT) does not change the values of N and M without resetting LTH = 0 and as long as the array WW is not changed by the routine (AVGS) with which it has this variable in common.)

This routine is based in greater part on the subroutine FFCPLX by Martin.[16] In the present notation, the arrays G and H represent both input and output. Thus the FFT, between "*bit inversion" and statement number 40, represents the following:

16. M.A. Martin, "Frequency Analysis of Real Sampled Data by the Fast Fourier Transform Technique", General Electric Co., Technical Information Series, Report No. 69SD267, May 1969.

$$G(I,K) + iH(I,K) = \sum_{J=1}^{N} [G(I,J) + iH(I,J)]e^{i(J-1)\phi} \qquad (91)$$

where $\phi = 2\pi(K-1)/N$ and K also runs from 1 through N. The bit inversion part of the routine, in which the locations of all variables are changed to the location whose binary digits are the reverse, permits the output to occupy the same places as the input. The economized Fourier summation is essentially the Cooley and Tukey[17] method.

Note that the imaginary part of the right hand side of (91) is a cosine series if the G's are all zero or a sine series if the H's are zero. Thus we apply the fast Fourier sum by inputting all even functions to the H array and all odd ones to G; the output is then in H in all cases. All members of both arrays are initially set to zero and then the data for the modes calculated by WFP are read in. The data are missing, of course, if the innermost layer boundary reached by WFP, which is denoted INLAY, is outside of the point currently being considered. The arrays G and H are doubly subscripted to permit the fast Fourier sums to be evaluated simultaneously for all 8 or 12 field components which were stored by BCO or STORF. Alternating pairs of these components are odd and even, so alternating pairs are input to G and H in the "do 2" loops.

If the point in question is within the wake boundaries, the routine proceeds to the evaluation of the integral over ϕ involving $|E_0 \cdot G_0|^2$ Otherwise it outputs the coherent scattering versus ϕ, which goes from 0 to 180°, the other half of the space being symmetrical with this half. Referring back to g) Subroutine BCO, the complex parallel polarization scattering is in the arrays H(7, J) and H(8, J). Likewise elements 3 and 4 are for transverse. Linear orthogonal, which is X(3), is taken as the rms value of E_{pt} and E_{tp}. Circular polarization is straightforward also since the transmitted field is composed of one linear polarization plus i multiplied by the other. We then define principal circular polarization scattering as the conjugate combination; i.e.,

$$E_{principal} = \frac{1}{2}[E_{tt} + i\,E_{pt} - i\,(E_{tp} + i\,E_{pp})] \qquad (92)$$

and orthogonal is therefore

$$E_{orthogonal} = \frac{1}{2}[E_{tt} + i\,E_{pt} + i\,(E_{tp} + i\,E_{pp})] \qquad (93)$$

These equations are used to give X(4) and X(5) in the program. Of some interest in calculating far field diffraction into the shadow of the wake is the coherent forward scattering. The complex coefficients of E_{pp} and E_{tt} for $\phi = 0$ are output, after accounting for $e^{-i\pi/4}$ in (89), in the variables A, B, C, and D.

17. J.W. Cooley and J.W. Tukey, "An Algorithm for the Machine Calculation of Complex Fourier Series", Mathematics of Computation, Vol. 19, pp 297-301, 1965.

k) Subroutine AVGS(H,IK,N,LAYR) has the main purpose of performing the integral in (21) over all angles ϕ. The variable H in the calling sequence represents the IK components of the electric field at N equally spaced values of ϕ from 0 to 360°. IK must be equal to 12 but N can be as large as 256 in the current version of the program. LAYR is the number of the layer boundary where the field points are located, and it is the only one of the variables which may be altered on return to the calling program. This is the only subroutine in this program which relies on memory for quantities calculated during previous calls of it.

The logic of this routine is not complicated when it is broken down into the parts headed by comment cards. The first part evaluates the line integral of β given by (40). This line integral is taken along a straight line parallel to the direction of incidence to the point (ρ, ϕ) in question. A given path of integration intercepts a given radius ρ at two values of ϕ which are symmetric about 90°, so the range of ϕ covered by "do 6" is 90°. The line integrals at a given value of ϕ are calculated in implicit loops over the radial grid points. Between statements 2 and 3 the line integral for $\phi < 90°$ is accumulated in the variable A as ρ goes through all radial grid points from r_w down to the one in question. The variable B accumulates the line integral from this point down to but not including the point of closest approach, which is represented by the variable RS. (One will recognize that the equations for A and B have the form of the line integral in polar coordinates when the radial coordinate is the variable of integration.) The contribution up to the point of closest approach is added after statement number 5. Statement number 6 takes account of the fact that the integral for $\phi > 90°$ is that for $\phi < 90°$ plus twice the integral from that point to the point of closest approach. Multiplication by CAYR (kr_w) removes the normalization by r_w, and the fact that BOK is $\beta/(k \sin \alpha)$ implies that the array BDS is $\int \beta \, ds$ for the grid of angles from 0 to 180°.

In the volume integral in (21) we need the effective wavenumber k_e, which is the gradient of the phase angle of $E_0 \cdot G_0$. This derivative is obtained numerically in terms of the values of this scalar product at five points in the radial and angular grids. Thus the point in question in the integration for (21) must always be retarded by one in both directions as we iterate ρ and ϕ, or else we would not have the required five points about the point in question. Thus LM is the layer boundary in question and if it is not inside of MINL, the innermost point at which the fields were calculated, NM is set equal to one greater than the number of angles needed to cover the region 0 to 180° in the average over angles. In the "do 30" loop over these angles we usually (unless it is logically superfluous) start by evaluating the scalar products $E_0 \cdot G_0$ for five polarization combinations. The arrays U and V are the real and imaginary parts of these products and their middle subscript denotes the polarization in the order vertical, horizontal, linear orthogonal, circular, and circular orthogonal. The last subscript pertains to the angle grid and the first is designed to save the value for the current radial grid point, the previous one and the one before that in locations L, LA, and LB, respectively. To interpret further, the ten values of S, after completion of the "do 9" loop, are the ten possible dot products between

the real and imaginary parts of the fields induced by each of the two principal plane incident wave polarizations. Refer to the definition of the 12 components of E given in h) subroutine STORF, which applies also to the components of the H array in this routine, to decode these equations. In the "do 25" loop UA and VA are the real and imaginary parts of $E_0 \cdot G_0$ at the point in question for evaluation of the integral over ϕ. The variable T is the square of the magnitude of this quantity.

The effective wavenumber k_e is the gradient of the argument of

$$E_0 \cdot G_0 = (U + i\ V)\ e^{2ikz \cos \alpha} \tag{94}$$

where U and V have the meaning of the corresponding FORTRAN variables. Elementary analysis gives

$$k_e^2 = (2k \cos \alpha)^2 + [(U \frac{\partial V}{\partial \rho} - V \frac{\partial U}{\partial \rho})^2 + (U \frac{\partial V}{\partial \phi} - V \frac{\partial U}{\partial \phi})^2/\rho^2]/|E_0 \cdot G_0|^4 \tag{95}$$

DUR and DVR represent r_w times the partial derivatives with respect to ρ; DUP and DVP represent r_w/ρ times the partial derivatives with respect to ϕ. Note that the radial grid is nonuniform, so generally three-point numerical differentiation, except when only two points are had at the edges, is used for the radial variation. The angular grid being uniform, the two points surrounding the point in question are used and $\Delta\phi = 4\pi/N$. As we indicated above, the contribution of the critical point (LM = KRIT) is ignored if $|E_0 \cdot G_0|$ is possibly resonant (T>1).

When "accumulate averages" is reached, A represents $|E_0 \cdot G_0|^2$ times the nonconstant part of $S(k_e)$. The variable FGS accumulates that quantity's integral over ϕ by the trapezoidal rule and the variable DEP accumulates the same quantity weighted by the depolarization by second Born. Multiplication by F at completion of the integrals normalizes them by S(2k), the free-space spectrum function. Both are printed out layer by layer, so one can see the relative magnitude of the second Born depolarization. Then DEP is added to FGS using the logic that the depolarization in the orthogonally polarized wave scattering adds to the principally polarized wave scattering and vice versa.

Finally, if the layer boundary called is the outermost (LAYR = LAYERS), we add one more layer and run through almost the entire routine again because of the lag in the layer boundary of interest.

1) Subroutine RINT(JM) is designed to calculate the normalized moments of the scattering per unit length of wake, by performing the integration in (21) over the radial coordinate. The argument JM is the number of the innermost layer boundary at which the integral over ϕ has been completed by subroutine PHINT.

The output of this routine is a set of 20 integrals, defined as follows:

$$I \equiv \frac{1}{N_e^2} \int_0^{\infty} \frac{u_n N'^2}{1 + (\upsilon/\omega^2)} \{\phi\} \; d(\rho/r_w)^2 \tag{96}$$

where

$$\{\phi\} \equiv \frac{1}{2\pi S(2k)} \int_0^{2\pi} |E_0 \cdot G_0|^2 \; S(k_e) \; (1 + d) \; d\phi \tag{97}$$

N_e is the axial value of the mean electron density and, in the definition of $\{\phi\}$, d is symbolic of the depolarization by second Born. The precise definition of (97) is such that $|E_0 \cdot G_0|^2$ multiplying d is for the opposite polarization to that multiplying unity (See paragraph k) Subroutine AVGS). The quantity $\{\phi\}$, which is the input, is represented by the array FGS. The output S0 takes $u_n = 1$ in (96), S1 takes v/v_0, S2 takes v'^2/v_0^2, and S12 takes $(v/v_0)^2$. The quantity v is the mean velocity profile, v' is the velocity fluctuation, and v_0 is the axis velocity. Each output has five values, one for each of the five polarization combinations carried through from AVGS. Before returning to the calling routine we print out these 20 integrals for each of two normalizations. The first represents normalization by the first Born approximation for principal polarization, in terms of the quantities BN, CN, DN and EN; i.e., these normalizing factors are the results of (96) if $\{\phi\} = 1$. Since it is interesting to examine refraction effects, the 20 integrals are also printed out in terms of their normalization by the values of the first Born at critical density for refraction. (Recall that in MAIN, AN is $[N_e/(N_c \sin^2\alpha)]^2$.)

m) Subroutine ZINT(NZ,V) performs the convolutions defined by (22), where NZ is the number of axial stations at which input values of dS_n/dz exist and V is $\cos\alpha$.

The variables DSDZ, DTDZ, and DVDZ are the input values of dS_n/dz for n = 0, 1, and 2, respectively. Referring back to MAIN,whence these quantities come, one can see that essentially all normalizations have been removed. DSDZ is radar cross section per unit length of wake in units of meters. The other two quantities, when divided by DSDZ, are the mean and mean square doppler velocity at the axial station in question, in units of the body velocity and the square of the body velocity.

The logic of this routine is based on the various situations which can arise. Thus there is a special form of result for normal incidence ($|\cos\alpha| < 10^{-5}$), as follows:

$$S_n(0) = \int_{-\infty}^{\infty} \frac{dS_n}{dz} \; dz \tag{98}$$

where only one output axial station is required since the backscattered pulse shape is identical with the transmitted pulse. If only one axial station is input, including the case of normal incidence, then the output is simply set equal to the input since the convolution is meaningless. In all other situations the convolution is represented as follows:

$$S_n(z) = \int_{-a}^{a} \frac{dSn}{dz} (z - z') \cos^2\left(\frac{\pi z'}{2a}\right) dz' \qquad (99)$$

where a is the range resolution (distance between half-power points for the pulse backscattered from a point target) divided by cos α. Note that the pulse is assumed to have the shape of the cosine squared function. This integral is evaluated at a set of uniformly spaced values of z regardless of whether or not the input is on a uniform grid. The number of points used to calculate it by the trapezoidal rule depends on the relative widths of the scattering function (the distance between the first and last input stations) and the pulse (between zero points). If the pulse width dominates we use the larger of 20 or the maximum allowable number of axial stations. If the scattering function dominates we use an odd number which approaches unity as the relative width of the pulse approaches zero and which is identical with the number used in the other case when the pulse width approaches the width of the scattering function. The limits of the range of z for the output generally cover the points where the result goes to zero, where it is assumed that the input scattering function drops to zero at either end of its range of stations.

Interpolation of the scattering function dS_n/dz is required in general because the grid of input will not necessarily match the integration grid. The form of the interpolation has been designed to try to account for situations where the function varies either linearly or exponentially. If either interpolated value is zero or if they are within an order of magnitude of each other, linear interpolation is used. Otherwise the interpolation is exponential; i.e., it is linear with respect to the logarithm.

C. Input and Output

The listing for MAIN gives a complete definition of the input requirements, so very little need be added. A title card, which can contain any symbols one wishes in all columns, must precede each set of input data. One will notice that certain conventions are used in naming the input variables. All dimensional quantities contain a reminder of their units at the end of their name. With the exception of FMHZ, all names which contain Z refer to axially varying quantities and all but NZ are arrays. MUTZ is defined as $(6\psi - 9)$ in the spectrum function; thus ψ can take any of the values 5/3, 11/6, 2, 13/6, 7/3, and 5/2. The program will return to the beginning of MAIN and look for new data if, after completion of all calculations for a given case, the number of cases so far done in this run is less than whatever value KASES has been given. In the Honeywell 6060 one need not repeat namelist inputs which are no different from what is currently in memory, so KASES needs to be input only with the first set of data. In the definition of POLAD, "plane of incidence" is the plane containing both the wake axis and the radar line of sight. All profile functions, which are denoted by PRO at the end of the name, are defined as the given quantity at some radius divided by a normalizing quantity. For both EMPRO and EPPRO the normalizing quantity is the axial value of the mean electron density. The collision frequency and velocity profiles are normalized by the axial value of collision frequency and velocity, respectively. In general, however, it does no harm to use inconsistent normalizations; e.g., one could input a set of

values of EMPRO which represents a profile which is different from unity at the axis with no adverse effect on program operation. The EPPRO often will differ from unity at the axis if $N' \neq N_e$. The methods of inputting various types of profile functions are detailed on the listing. Note that when a smooth profile function is to be input, the data correspond to evenly spaced radial points starting with the axis and ending with the outer edge. When using this option it is best to go to the limit and input eleven points in the profile. Obviously the meaning of the variable VVEZ is arbitrary and some other velocity than that of the re-entry body could be used as a normalizing factor.

Other than those already mentioned, there are relatively few restrictions on the values of the input quantities. ASPECD must not be zero (or such that its sine is zero). CZPSEC, EMZPCC, FMHZ, RESM, and RZM must be greater than zero. The values of EPPRO may not be such that the profile of electron density fluctuation is identically zero. Finally, the array ZM must have unequal, increasing values.

Appendix B is a copy of the complete output for a sample case, which can serve as a user's test case. The output starts on a new page. The top line gives the case number in this run and the title card characters. The format for this line is given in statement number 5000 of MAIN. We have used a title card spanning all 80 columns, to illustrate where they appear on this line. All data for the input variables are then written in NAMELIST format.

The next new page gives the data used for the first axial wake station. The meanings of most of the items should be obvious. Each "changed to" entry refers to the item to its left, which has been adjusted by PROFS to avoid spurious effects of nearly critical density in a layer (format, including column headings: 1000, MAIN). In the profile functions the relative radius refers to the layer boundaries, which are called "mesh pt." in the listing. The next three columns fall under the heading of electron density. All other columns are self-explanatory (format for each row of data: 2000, MAIN). Note that various possible kinds of input profiles are illustrated by the inputs used for this case. The mean electron density is approximately equal to a Gaussian and the rms fluctuation is a step function to half the wake radius. The collision frequency is uniform and the two velocity profiles linearly decrease by a factor of ten.

The next page of output gives the summary of the results of the calculation of em fields in the mean wake (format for heading: 3000, MAIN). The first column shows the mode orders used. The next eight columns give each of the two scattering coefficients for each incident wave polarization. In each pair of columns the first is the real part and the second, the imaginary. These scattering coefficients are defined in the discussion on subroutine BCO concerning equation (89). The last column shows that the wave propagation was not cut off in this case (format for each row of data: 1000, BCO).

The next page gives the far field coherent scattering pattern, where "azimuthal angle" refers to ϕ and the first row of the table is for the forward scattering (format for headings: 2000, PHINT; format for rows of numbers: 1000, FFSUM). The complex forward scattered fields, with the phase relative to the incident wave, are written at the bottom of the table (format: 2000, FFSUM).

The next page is the output of subroutine AVGS. It shows the average over ϕ of $|E_0 \cdot G_0|^2 S(k_e)/S(2k)$ for each polarization combination. The five columns of depolarization factors include the second Born in this average as well (format for headings: 4000, PHINT; format for data: 1000, AVGS). The data for this sample case show a very interesting phenomenon on this page. The critical point in the mean electron density profile is at point #33, where AVGS has set all results equal to zero to avoid the resonance effect. However this wake is in the diffraction regime, which permits wave propagation without cutoff all the way to the axis. Diffraction also spreads the resonance effect over a band of radii about critical. But, as can be seen from the data either side of critical, the phase varies so rapidly in this region that the spectrum function drops off as the critical point is approached.

The next page gives the lowest three moments of the scattering spectrum (format for page headings: 1000, RINT). In the two normalizations by the Born approximation, even the cross polarized results are divided by the first Born approximation for direct polarization. Also, "first squared" refers to the contribution to the second moment of the profile of the square of the mean velocity (formats: 2000 and 3000, RINT). The heading "absolute" means, for the zeroth moment, radar cross section per unit length of wake in meters. For the first or second moment the units are meters times the body velocity or its square, respectively (format: 6000, MAIN). In "doppler/body velocity", the term "mean" is self explanatory. "Spread" is defined as the standard deviation of the doppler spectrum in units of the body velocity; i.e.,

$$\text{"spread"} \equiv \sqrt{\overline{v^2} - \bar{v}^2}/v_{body} \tag{100}$$

The above five pages of output are repeated for each axial station which was input. Note that in the sample run we have illustrated a three-step function radial profile in the second axial station. Also, note that in the second and third stations we have used electron densities which decrease by four orders of magnitude. The results show that, indeed, the Born approximation is approached in this limit.

The final pages of output give the backscattered pulse shape functions for each of the five polarizations (format for headings: 1000, ZINT). The pulse shapes are expressed in terms of radar cross section (dBsm) and doppler mean and spread (as defined above) versus apparent axial station (format 2000, ZINT). A page is turned after the first 13 stations and then after each 14 more (format 3000, ZINT).

D. Summary of Checkout Procedures Used

The reliability of this computer code for doing the calculations for which it was designed has been proven by a series of checkout runs during its development. The checkout was done at various levels in the program, starting with subroutines which do not call other subroutines and working up to the entire program.

The Lagrange interpolation in subroutine FIT was checked by exercising it on two profile functions, a Gaussian and a Gaussian multiplied by a quadratic. The input data were taken from the appropriate points on the true underlying function. The number of points used was varied from one through eleven and the accuracy and reasonableness of the output were verified by Calcomp plots as well as numerical printout. For each of these functions, one can not

visually detect any difference from the true curve, on a graph scale of about 13 cm height, as long as eight or more points are input. The sample output discussed above verifies that the step-function type of output is correct also.

Subroutine PROFS was checked out by hand calculation of its outputs for a few selected cases.

Subroutine HANK was checked out by comparing its output with tabulated values for a number of arguments ranging from 0.2 to 50. The results were accurate to within one part in at least 10^6 or within an absolute value of 10^{-6} or less if the result is much less than 10^{-6}. In the process of these checkout runs we developed the convergence criterion which is built into this routine. These same statements apply to subroutine BIN as well, except that imaginary and complex arguments also were used.

Subroutine PROP was checked out by comparing its results with the direct calculation of the cross-products of Bessel functions, p_n, q_n, r_n, and s_n in 9.1.32 on page 361 of Abramowitz and Stegun (op. cit.). ($C = -\pi\xi_0 r_n/2$, $D = \pi\xi_0 p_n/2$, $C' = -\pi\xi_0 s_n/2$, $D' = \pi\xi_0 q_n/2$, $a = \xi_0$, $b = \xi$) Subroutine HANK was the standard of comparison for real arguments; library routines for modified Bessel functions were the standard for imaginary arguments; and selected tabulated values were the standard for certain real, imaginary, and complex (using Kelvin functions) arguments. Initially the series expansions of the matrix elements in PROP were formulated in terms of power series in Y with the coefficient of Y^j calculated by recurrence relations. This approach began to lose accuracy when $|\xi_0|$ exceeded 10 or 20, and it encountered exponent overflows in the Honeywell 6060 for arguments greater than 50. The formulation described above, in which the power of Y is included in the coefficient which is calculated by recursion, significantly improved the performance. Now, as stated above, we can go to values of $[|\xi_0|(1 + Y)]$ up to 88, which is the ultimate single precision limit of the Honewell 6060, with accuracy generally of 10^{-6} or better. Values of Y used in these runs were 0.02, 0.05, 0.1, 0.2, and 0.3. An earlier series of experimental runs using a more primitive formulation had shown that the series would not always converge if Y was greater than 0.3, however this conclusion may now be conservative.

Subroutine WFP and the routines it calls (HANK, BIN, PROP, BCO, and STORF) were checked out by doing a set of calculations for a uniform cylinder. The standard of comparison was a specially written routine using Bessel functions inside the cylinder. It was found that, even for zero collision frequency, the accuracy is consistent with the computer word size.

Subroutine FFSUM was checked out by putting in the Fourier expansion coefficients for the incident plane wave and noting that its output faithfully reproduced the plane wave.

Subroutine PHINT, which calls FFSUM and AVGS, was checked by doing the case of zero electron density in subroutine WFP and calling PHINT. This, of course, produces the incident wave as the output of FFSUM. AVGS should produce results which are unity for the three principal polarizations and zero for the orthogonal. This result was obtained except that zero is about 10^{-15} for linear orthogonal and 10^{-8} for circular orthogonal.

Subroutine RINT was checked out by input of analytical functions for which the integrals are known in closed form.

Subroutine ZINT was checked out by putting in various functions of z which can be convolved with the pulse shape function in closed form. These runs included cases in which the scattering function ranged from much shorter to much longer than the radar pulse. They included cases in which the scattering function was specified in terms of as few as one point to as many as 20. Cases were done also to verify the program's logic for normal incidence.

The sample run discussed above serves as a checkout for the entire program. At the third axial station the electron density is less than 10^{-7} of critical density and the principal polarization results are 1.0005 times the Born approximation while those for linear and circular orthogonal are down by at least 10^{16} and 10^{13}, respectively. The factor 1.0005 comes from the numerical differentiation to obtain the effective wavenumber, which therefore does not exactly equal 2k.

IV. SAMPLE RESULTS

A. Comparisons with Experimental Data

Shkarofsky et al.[18] have reported experimental data on microwave scattering from a turbulent arc jet. Their paper is an excellent subject for analysis by our theory since it gives all the necessary information on the plasma. Radial and axial variations of mean and rms electron density are given in terms of graphs of the profiles at nine axial stations, and the turbulence spectrum function also is given. Figure 4 shows the comparison of this theory with Shkarofsky's data. Note that they reported the absolute backscatter power while our model gives radar cross section per unit length, so we have displaced their data to force it to agree with the Born approximation at low electron density. The polarization is the one parameter not explicitly stated in ref. 18; but even in the worst case that the polarization was parallel to the plane of incidence, the agreement between this theory and the data is excellent. (Note that in these calculations fifty angular modes were used on a grid of 256 angles.)

Cross-polarized backscatter results are shown in Figure 5 in terms of the ratio to the principal polarization. The agreement with the data is still good, although only within a factor of three. The most satisfying aspect of both sets of results is the very good agreement in the shapes of the curves all the way through critical density. Note that the background medium contributes to depolarization also, a fact which has been noted by Halseth and Sivaprasad.[19] The dashed lines in Figure 5 show that this contribution is quite significant in this case, being about equal to that from the second Born approximation when the plasma is overdense. (Special changes were made in the program to output these results.)

Graf et al.[20] have studied the effects of incidence angle on refraction in a turbulent laboratory plasma. Their data for backscattering at 40° aspect angle (between the line of incidence and the plasma axis) follow the first Born square law dependence on the rms electron density. These data points extend up to an rms electron density of 0.7 times critical density. They do not show backscatter data for 20° aspect angle although they state, "At an aspect angle of 20°, the backscatter cross sections deviated ... from the slope-of-two curve ... about 3db when n' was 0.15 n_c." Regrettably, they do not report much detail about the conditions of their experiment, especially regarding the background (average) electron density distribution, which is so important in this theory. We have made calculations using radially Gaussian electron density distributions, where the standard deviation of the Gaussian is 2.1 cm for the average electron density and 2.5 cm for the fluctuations. The results of calculations using this theory are shown in Table 2.

---

18. I.P. Shkarofsky, A.K. Ghosh, and E.N. Almoy, "Direct and Cross-Polarized Backscatter Power from a Turbulent Plasma", Plasma Physics, Vol. 14, pp. 935-950, October 1972.
19. M.W. Halseth and K. Sivaprasad, "Depolarization of Singly Scattered Radiation in a Turbulent Plasma", Phys. of Fluids, Vol. 15, No. 6, pp. 1164-1166, June 1972.
20. K.A. Graf, H. Guthart, and D.G. Douglas, "Refraction Effects in Turbulent Media", Radio Science, Vol. 9, Nos. 8, 9, pp. 777-787, August-September 1974.

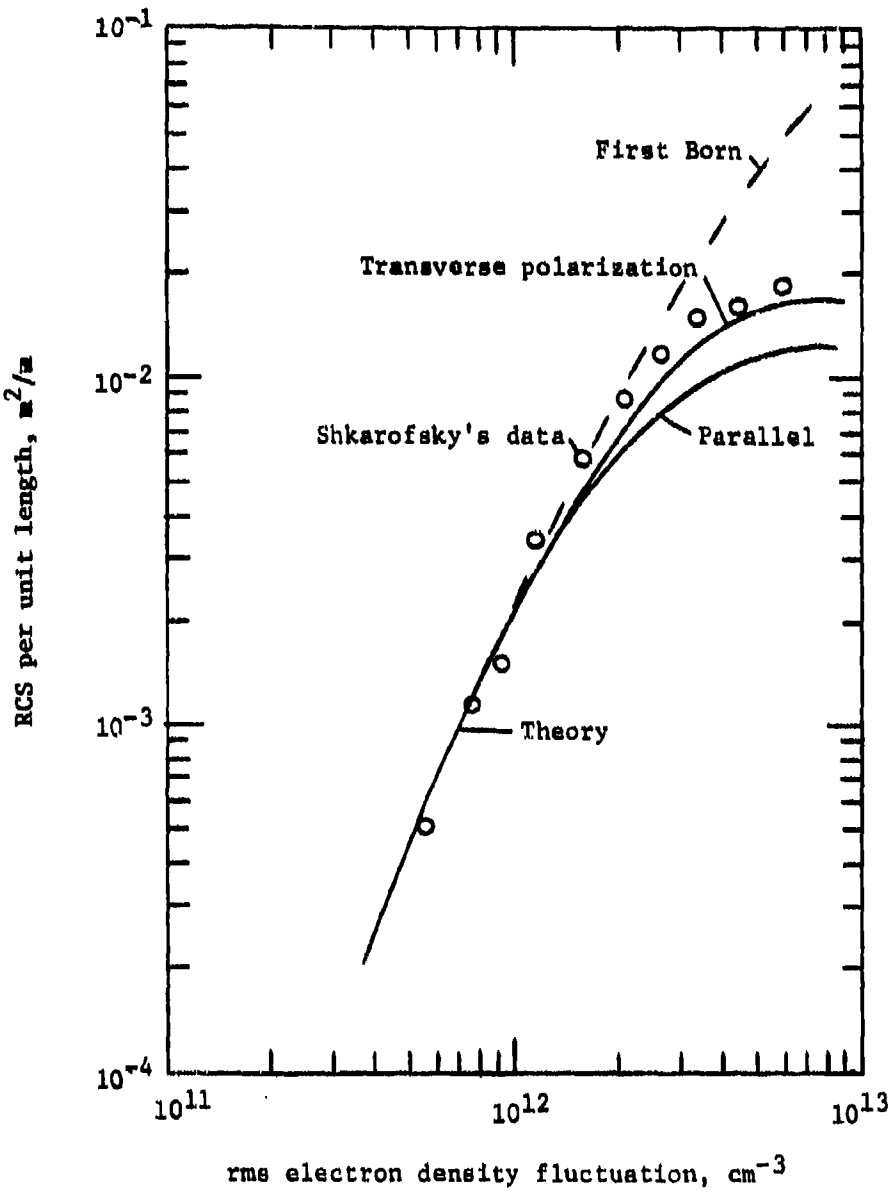

FIGURE 4. COMPARISON OF THIS THEORY WITH SHKAROFSKY'S DATA FOR BACKSCATTERING AT 16GHz FROM A TURBULENT ARC JET.

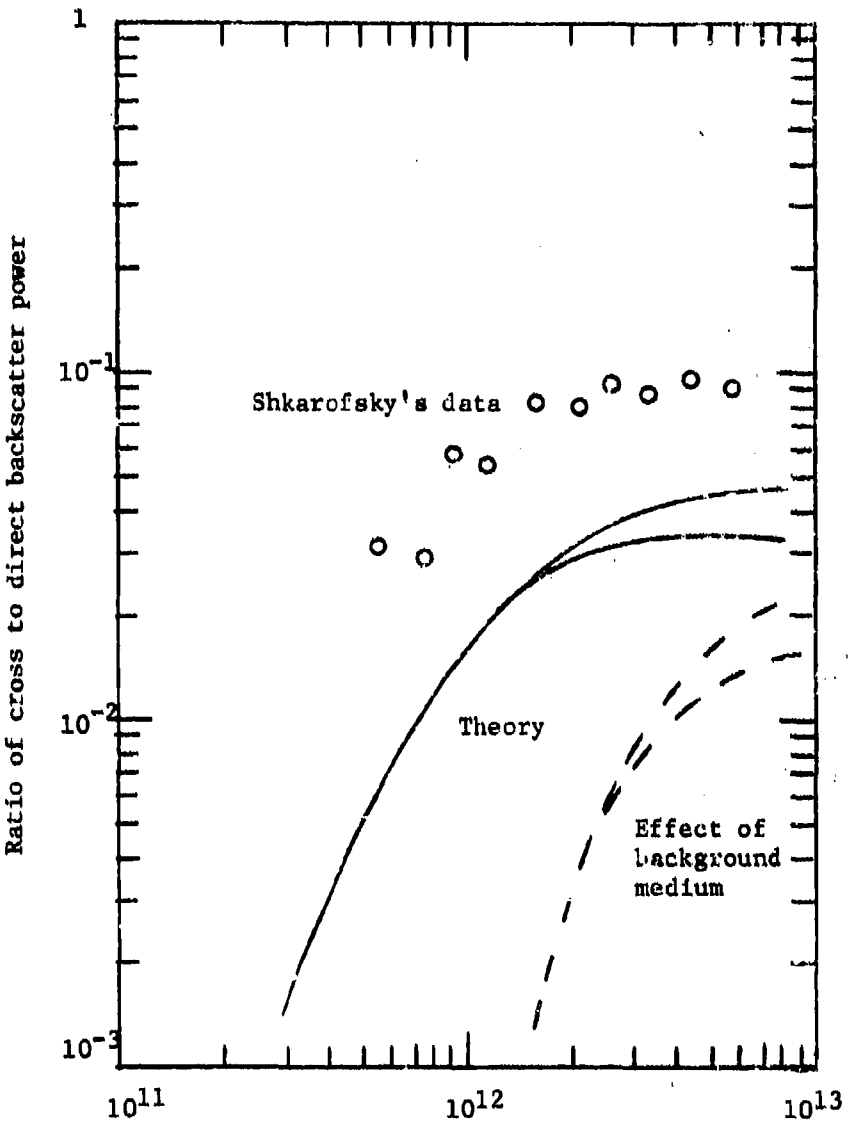

FIGURE 5. COMPARISON OF THIS THEORY WITH SHKAROFSKY'S DATA FOR THE RELATIVE DEPOLARIZATION OF THE BACKSCATTERING.

TABLE 2. THEORETICAL RESULTS FOR GRAF'S EXPERIMENT

ASPECT ANGLE	N'/N_c	$N'/\bar{N}$	BACKSCATTERING AMPLITUDE/BORN (dB) PARALLEL POLARIZATION	TRANSVERSE POLARIZATION
40°	0.7	0.5	-8.4	-5.3
40°	0.7	1	-4.7	-2.4
20°	0.15	0.5	-7.0	-6.0
20°	0.15	1	-3.5	-2.8

The parameter $N'/\bar{N}$ represents the axial value of the ratio of the rms electron density fluctuation to the mean electron density, and it can be seen that this is an important parameter in the theory. Although the nominal value is given as 0.5, the theory agrees with the experiment better for a larger value.

Graf et al.[20] have given results of coherent field measurements also. Figure 6 reproduces their result for measured field intensity at a distance of 156 cm from the transmitter when the plasma axis was a perpendicular bisector of the line of sight. The theory gives the coherent forward scattered field as a byproduct, which falls off as the inverse square root of the far-field distance because of the assumption of cylindrical symmetry. The points plotted on the graph show the results of the theory for the total field intensity, assuming that the incident field falls off as 1/r. The square symbol denotes parallel polarization and the circle, transverse. The open symbols show the results of accounting for only the mean electron density, neglecting the effect of scattering attenuation. The filled symbols show the results when the mean plasma properties are enhanced to account for scattering attenuation, assuming that $N'/\bar{N} = 0.5$. The theory gives more diffraction than the data show, although the trend with electron density is similar. It would appear to be anamalous that the transmitted field is increased when scattering attenuation is accounted for; but this result is caused by the manner in which the calculation is done, in that quantities are added to the mean electron density and collision frequency. Apparently, more diffraction than attenuation is added.

Attwood[21,22] has reported the results of backscattering experiments for a wide range of aspect angles and electron densities either side of critical. But this theory comes nowhere near explaining the extreme degree of dependence of his data on these parameters, especially at and above critical density. This is probably caused by the fact that his plasma does not fit the description assumed herein, of a random medium embedded in a steady, cylindrical background medium.

21. D. Attwood, "Microwave Scattering from Underdense and Overdense Turbulent Plasmas", Physics of Fluids, Vol. 15, No. 5, pp. 942-944, May 1972.
22. D. Attwood, "Microwave Scattering from an Overdense Turbulent Plasma", Physics of Fluids, Vol. 17, No. 6, pp. 1224-1231, June 1974.

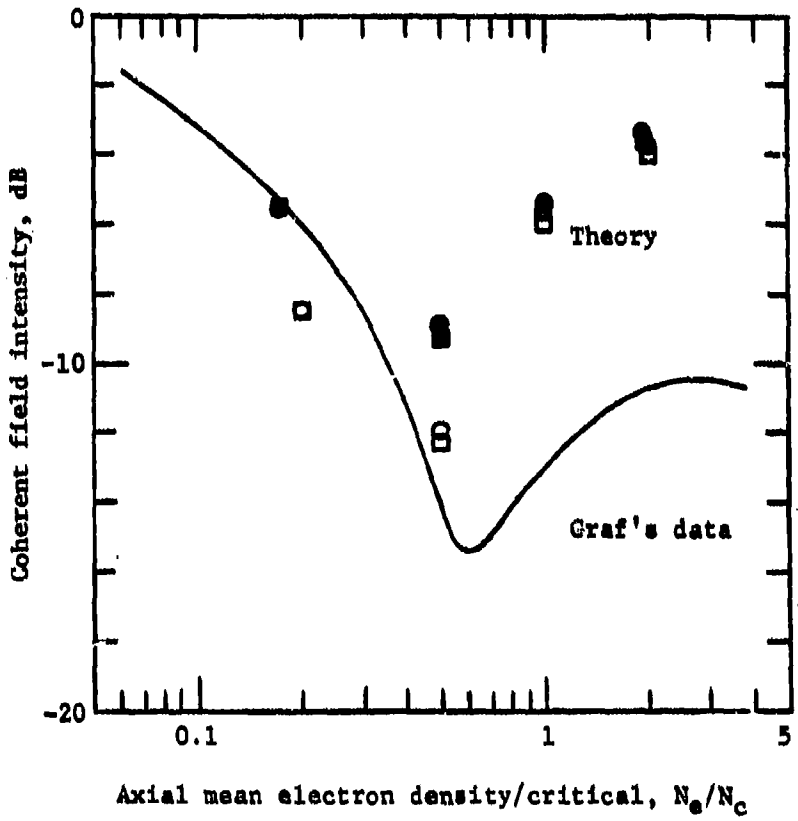

FIGURE 6. COMPARISON OF THIS THEORY WITH GRAF'S DATA ON THE COHERENT FIELD INTENSITY TRANSMITTED THROUGH A TURBULENT FLAME AT NORMAL INCIDENCE.

B. Some Parametric Results

In the previous study (see Ref. 1) the importance of finite wavelength effects was evaluated in some detail. These effects refer to many of the considerable differences which are found when the results of rigorous em wave propagation in a cylindrical plasma are compared with the results of ray tracing. Thus that study identified the diffraction effect, which was so named because it represents the departure from geometrical optics laws as the wavelength is increased. Furthermore, in that study, it was shown that the diffraction regime occurs when the parameter $k\sigma_e \sin\alpha$ is small, where σ_e is the width (standard deviation) of the radial profile of the mean electron density distribution. In other words the standard of comparison for the wavelength is the width of the electron density distribution projected onto the line of incidence. An important corollary of this result is the fact that low radar aspect angle can be a sufficient condition for diffraction. Our objective in this subsection is to determine how significantly the improvements embodied in the present model affect the results both in the diffraction regime and in the transition between diffraction and geometrical optics.

To permit direct comparisons we have used the same radial profile functions as for most of the prior parametric studies. Thus the mean electron density is a Gaussian with $\sigma_e = 0.3r_w$; i.e., $\exp[-\rho^2/(0.18r_w^2)]$. The rms electron density fluctuation is equal to the mean multiplied by $[1 + \rho^2/(0.18r_w^2)]$; i.e., it has an incipient off-axis peak. The mean velocity profile is Gaussian with $\sigma_v = 0.9478\ \sigma_e$. The rms velocity fluctuation has an incipient off-axis peak and the standard deviation of its Gaussian part $\sigma_{v'} = 1.0787\ \sigma_e$. We use a moderately collisionless condition ($\nu/\omega = 0.1$) and a low aspect angle ($\sin\alpha = 1/18$). The scales of turbulence are $kr_i = 0.021$ and $kr_o = 0.21$.

Figures 7 through 10 show the RCS (radar cross section), the ratio of orthogonal/principal RCS, the mean doppler and the contribution of velocity fluctuations to the doppler second moment as functions of axial electron density for circular polarization. These figures are all for $k\sigma_e \sin\alpha = 0.03$, so they represent the diffraction regime. The dashed line in each figure represents the results from the previous study and we conclude that the improvements which the new model incorporates (effective wavenumber calculation, scattering attenuation, and depolarization from turbulence) make little difference in the diffraction regime.

Figures 11 through 14 show the same four quantities as functions of $k\sigma_e \sin\alpha$ at a value of $N_e/(N_c \sin^2\alpha) = 100$. The only significant difference between the old and the new results is the polarization ratio for $k\sigma_e \sin\alpha$ greater than about 2. Thus it appears that in the diffraction regime the depolarization by the mean wake plasma dominates that by second Born scattering from the turbulence.

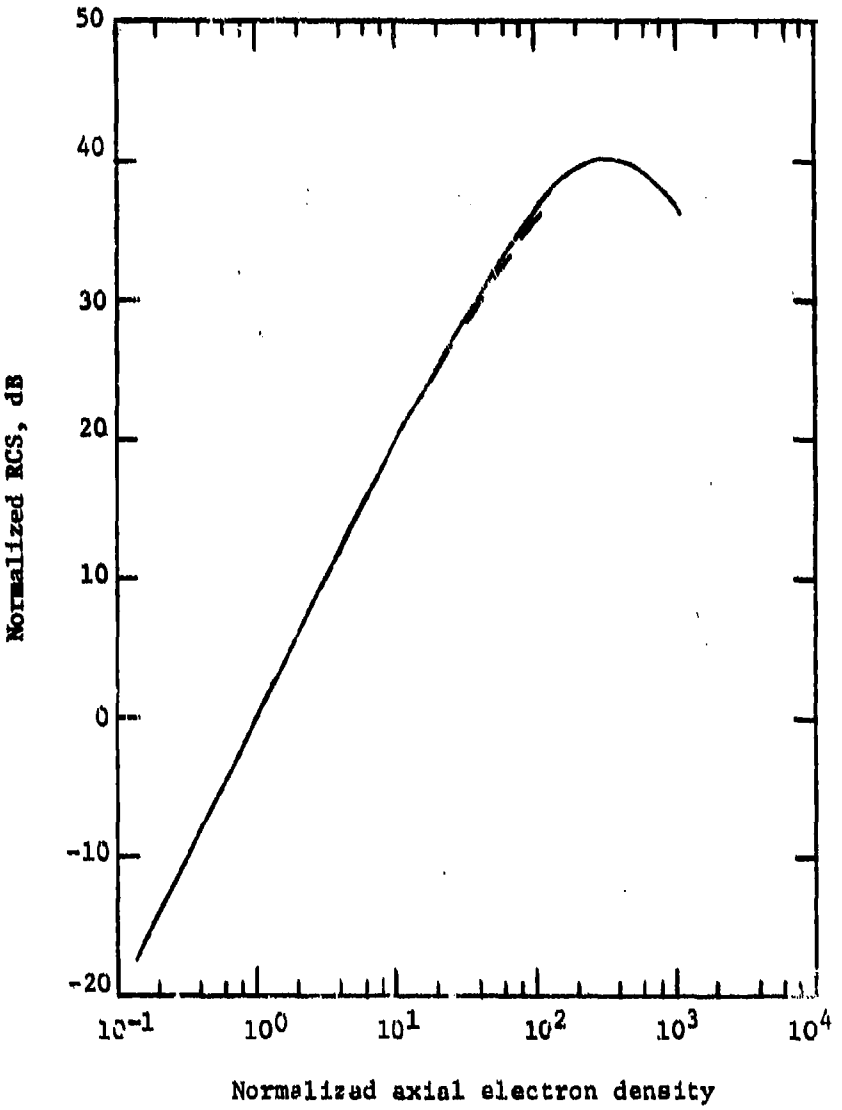

FIGURE 7. RCS VERSUS ELECTRON DENSITY IN THE DIFFRACTION REGIME. THE NORMALIZATION IS WITH RESPECT TO THE REFRACTION EFFECT; I.E., THE NORMALIZING ELECTRON DENSITY IS $N_c \sin^2\alpha$ AND THE NORMALIZING RCS IS THE BORN APPROXIMATION AT THIS ELECTRON DENSITY. (FIGURES 7 THROUGH 14 ARE FOR CIRCULAR POLARIZATION AND THE DASHED CURVE IS FROM REFERENCE 1.)

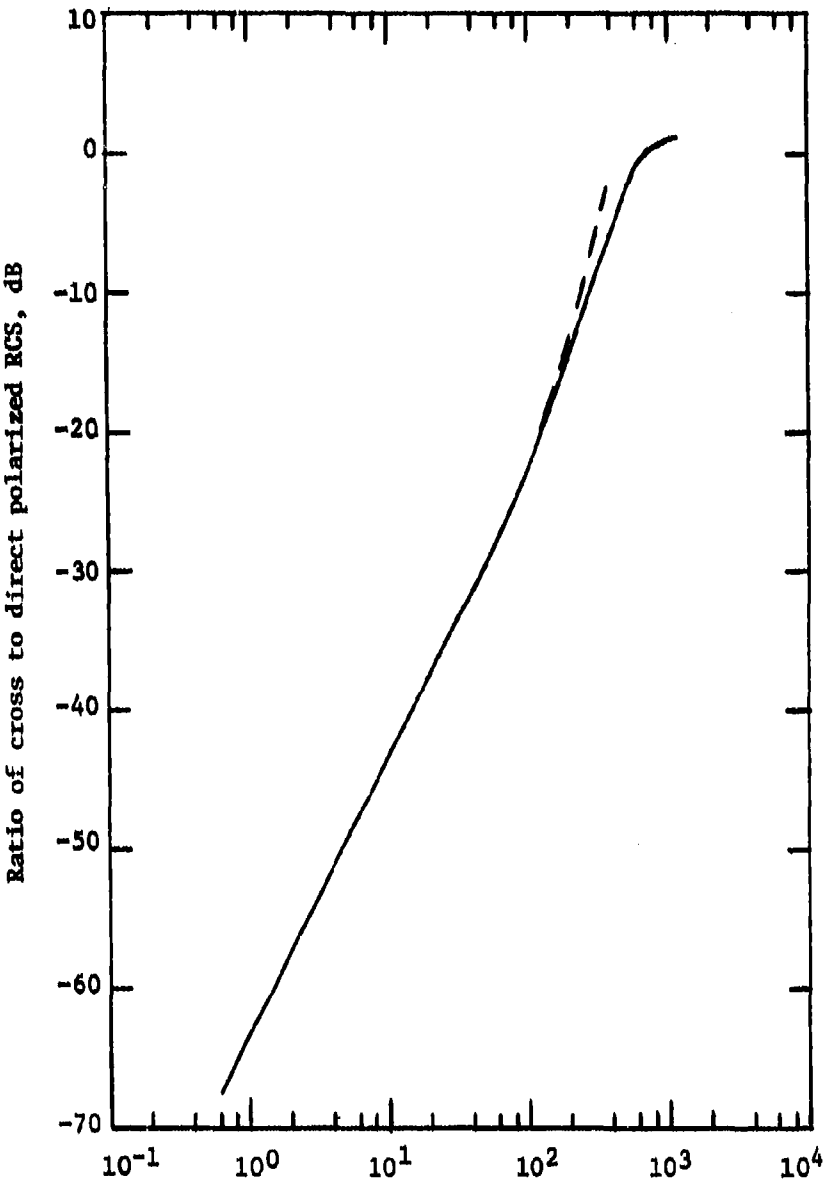

FIGURE 8. ORTHOGONAL/PRINCIPAL POLARIZATION RCS IN THE DIFFRACTION REGIME.

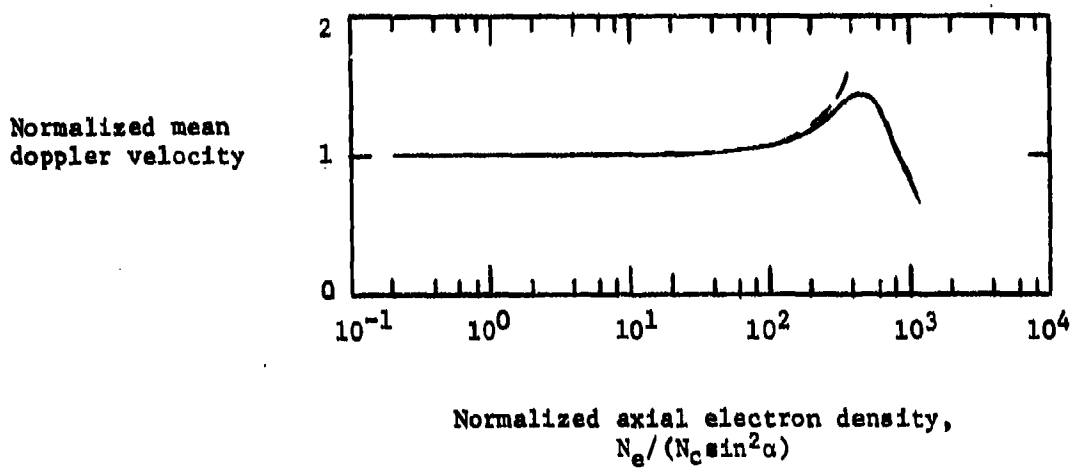

FIGURE 9. MEAN DOPPLER VELOCITY IN THE DIFFRACTION REGIME. THE NORMALIZING VELOCITY IS THE BORN APPROXIMATION; I.E., THE VELOCITY PROFILE WEIGHTED BY $N^{1/2}$.

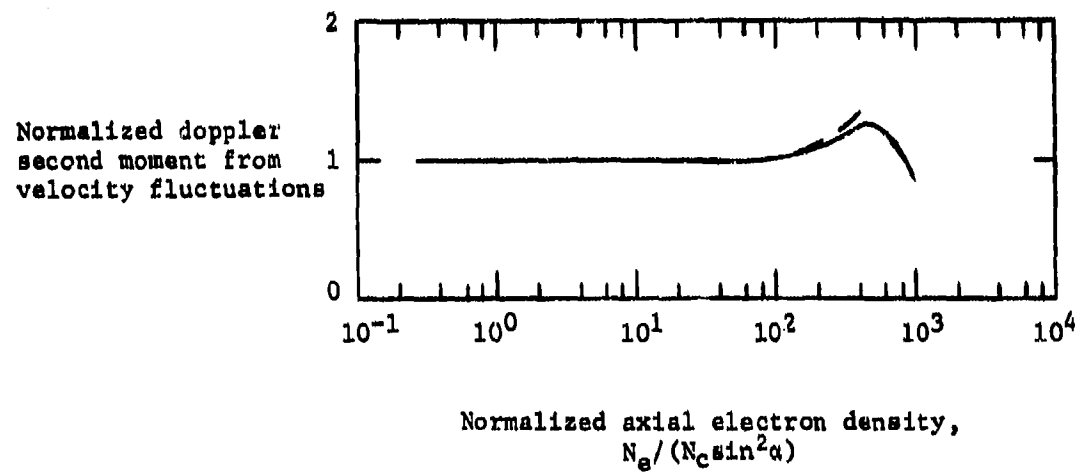

FIGURE 10. CONTRIBUTION OF VELOCITY FLUCTUATIONS TO THE DOPPLER SECOND MOMENT IN THE DIFFRACTION REGIME.

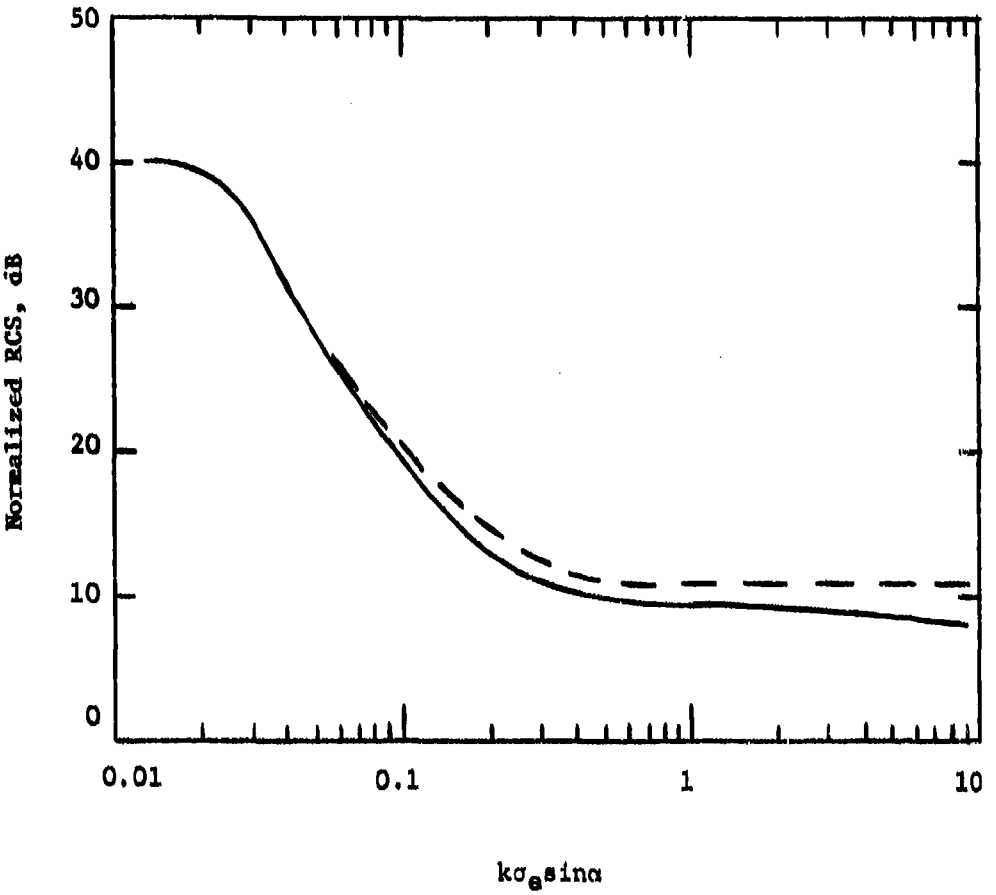

FIGURE 11. NORMALIZED RCS AS A FUNCTION OF THE ELECTRONIC WAKE WIDTH PROJECTED ONTO THE LINE OF INCIDENCE AND COMPARED WITH THE WAVELENGTH. (IN FIGURES 11 THROUGH 14 $N_e/(N_c \sin^2\alpha) = 100.$)

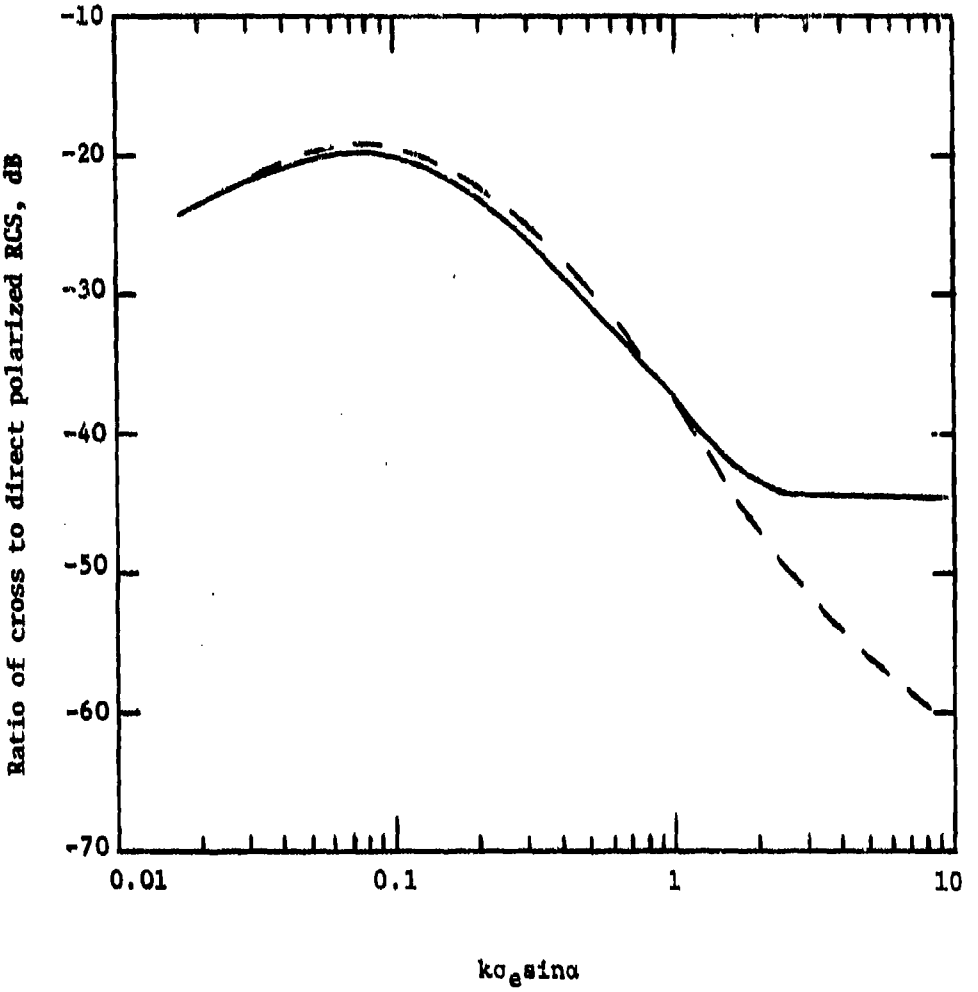

FIGURE 12. ORTHOGONAL/PRINCIPAL POLARIZATION RCS VERSUS NORMALIZED ELECTRONIC WAKE WIDTH.

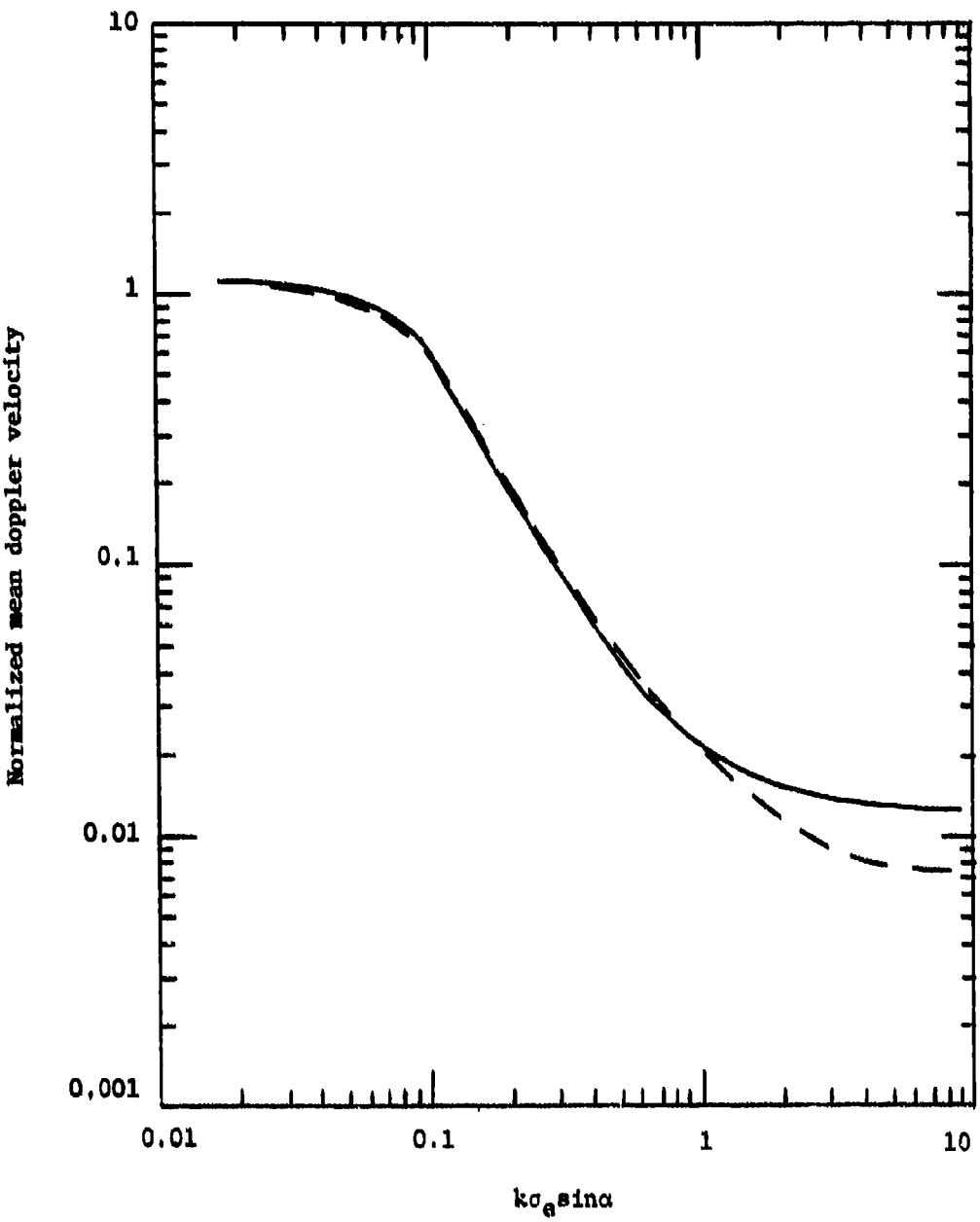

FIGURE 13. NORMALIZED MEAN DOPPLER VELOCITY VERSUS NORMALIZED ELECTRONIC WAKE RADIUS.

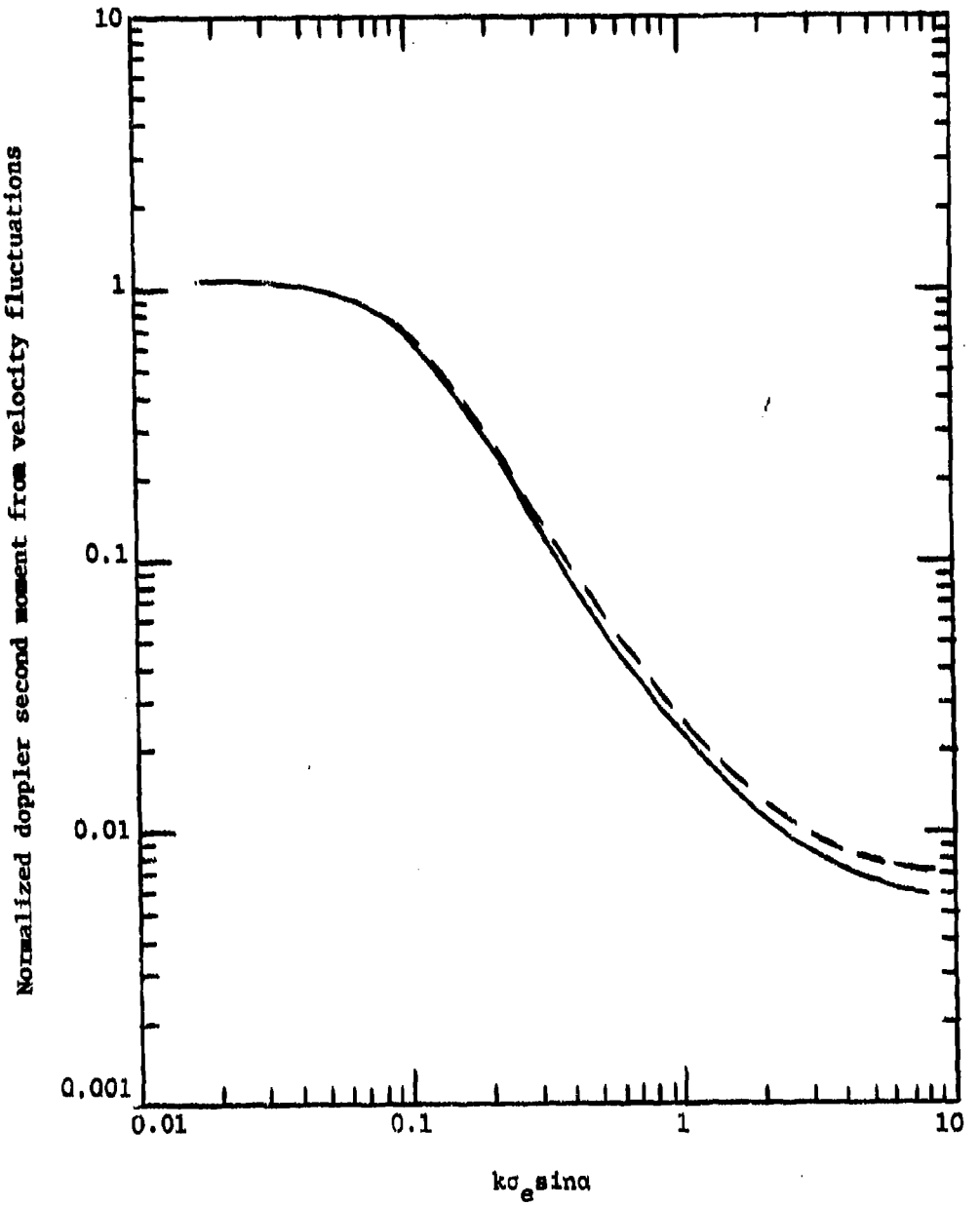

FIGURE 14. CONTRIBUTION OF VELOCITY FLUCTUATIONS TO THE DOPPLER SECOND MOMENT VERSUS NORMALIZED ELECTRONIC WAKE RADIUS.

V. CONCLUSION

A sophisticated computer model for the radar backscattering from turbulent re-entry-induced ionized wakes has been described in sufficient detail to permit the user to modify the program as desired. This model uses the basic concept that propagation in the background, average electron density distribution determines both the local fields and the Green's function for scattering; and this effect is formulated in a rigorous and general way by assuming that this background is a cylindrical medium. At this stage of development, however, the application of this model to the turbulence scattering is relatively crude, being of the type generally used in so-called distorted wave Born theories. Thus much room for improvement exists.

Many improvements and modifications are possible without basic theory changes. For example, one could generalize the program for bistatic scattering. This would take major programming changes but it does not require any new theory. Generalization for anisotropic turbulence would be relatively straightforward, and allowance for various types of radar pulses is almost trivial. The same can be said for including the effects of antenna patterns; i.e., nonuniform illumination.

This model probably could also be applied to the problem of radar scattering from the turbulent plume of a rocket exhaust. The main constraint would be that it be in a regime of flow that simulates the turbulent wake flow. At high altitude, where the plume is laminar and spherical, the canonical problem to be solved would be scattering from spheroidal media. The presence of strong, nonrandom irregularities in the plume, such as those created by shock diamonds, would require yet different techniques such as, perhaps, the geometric theory of diffraction.

Various basic theory improvements are possible in the problem of turbulent, cylindrical wake scattering. There is every reason to expect that, with the known rigorous solution for the effect of the background, one could do the statistics of the scattering from the random component of the medium in a rigorous way. At least one could do a Monte Carlo calculation. Also, the quasi-optical approximations (and their accompanying *ad hoc* assumptions) borrowed from the distorted wave Born approximation could be removed by carrying out higher order iterations in the Neumann series. Of course the difficulties of doing this are not trivial because one would have to get near-field solutions for propagation in the background medium. Obviously this is easier to do in the diffraction regime, where fewer angular modes are needed, but this is where the significance of this model is the greatest.

In conclusion, this model provides not only a valuable tool for applications but also a framework for future research in the theory of scattering from random media.

APPENDIX A

FORTRAN LISTINGS

```
*MAIN  WAKE ELECTROMAGNETIC SCATTERING MODEL
*THIS PROGRAM REQUIRES M LINKS OF SCRATCH RANDOM DISC,                    DISC
*WHERE M IS NOT GREATER THAN 10 BUT IS AT LEAST 6K/38,                    DISC
*WHERE N IS GREATER THAN (2+SQRT(2A(A+12))), AND WHERE A=KRSIN(ASPECD),   DISC
*K IS THE RADAR WAVENUMBER, AND R IS THE MAXIMUM VALUE OF RZM.            DISC
*A TITLE CARD MUST PRECEDE THE INPUT DATA FOR EACH CASE
*NAMELIST INPUT QUANTITIES (NAMELIST NAME = INPUT)
*     ASPECD = ASPECT ANGLE IN DEGREES, RELATIVE TO WAKE AXIS
*     CPRO   = PROFILES OF COLLISION FREQUENCY VERSUS RADIUS
*     CZPSEC = COLLISIONS PER SECOND VERSUS AXIAL STATION
*     EMPRO  = PROFILES OF MEAN ELECTRON DENSITY VERSUS RADIUS
*     EMZPCC = MEAN ELECTRON DENSITY VARIATION ALONG THE AXIS IN
*              ELECTRONS PER CUBIC CENTIMETER
*     EPPRO  = PROFILES OF RMS ELECTRON DENSITY FLUCTUATION NORMALIZED
*              BY EMZPCC VERSUS RADIUS
*     FMHZ   = RADAR FREQUENCY IN MHZ
*     KASES  = NUMBER OF CASES TO BE INPUT
*     MUTZ   = SPECTRUM FUNCTION FORM FACTOR VERSUS AXIAL STATION, WHICH
*              MUST BE AT LEAST 1 BUT LESS THAN 7 (DEFAULT = 2)
*     MZ     = NUMBER OF INPUT AXIAL STATIONS
*     POLAD  = POLARIZATION ANGLE IN DEGREES, DEFINED AS THE ANGLE BE-
*              TWEEN THE PLANE OF INCIDENCE AND THE VERTICAL RADAR PLANE
*     RESM   = RADAR RANGE RESOLUTION IN METERS
*     RZM    = WAKE RADIUS IN METERS VERSUS AXIAL STATION
*     SIZM   = INNER SCALE OF TURBULENCE IN METERS VERSUS AXIAL STATION
*     SOZM   = OUTER SCALE OF TURBULENCE IN METERS VERSUS AXIAL STATION
*     VMPRO  = MEAN VELOCITY PROFILES VERSUS RADIUS
*     VPPRO  = PROFILES OF RMS VELOCITY FLUCTUATION VERSUS RADIUS
*     VVBZ   = MEAN VELOCITY NORMALIZED BY BODY VELOCITY VERSUS AXIAL
*              STATION
*     ZM     = LOCATIONS OF AXIAL STATIONS IN METERS
*FOR ALL PROFILE FUNCTIONS INPUT LINEAR ARRAYS IN ORDER OF AXIAL STATION
*     THE FIRST ELEMENT IN EACH ARRAY MUST BE LESS THAN 12. AND ITS
*          ABSOLUTE VALUE IS THE NUMBER OF DATA REMAINING IN THE ARRAY,
*          WHICH REPRESENT
*        IF GREATER THAN 1., THE PROFILE AT UNIFORMLY SPACED POINTS
*        IF ZERO, THE PREVIOUS PROFILE IS REPEATED
*        IF +1. OR -1., A UNIFORM PROFILE
*        IF AN ODD NUMBER LESS THAN -1., A SERIES OF STEP FUNCTIONS
*          DEFINED ALTERNATELY BY THE HEIGHT OF THE STEP AND BY THE
*          LOCATION OF THE STEP
      COMMON/ABCKLW/ROR(50)
      COMMON/ICJW/INLAY(64)                                              OVERLAYS
      COMMON/IKW/KRIT,MINL
      COMMON/RBCW/CAYR,EMMC,VCOM,VS,WS
      COMMON/RBLW/CFM(50),EP(50)
      COMMON/RBW/CFO(50),CFS(50),CRS,EMM(50),EMO(50),EMS(50),GAR,TKR,WO
      COMMON/RKW/BN,CAY,CS,PSI,RI,RO,RW,SC,SMC,SS,TZCS
      COMMON/RLW/AN,S0(5),S1(5),S12(5),S2(5),VCM,VM(50),VP(50)
      COMMON/RMW/DSDZ(5,20),DTDZ(5,20),DUDZ(5,20),RESM,ZM(20)
      DIMENSION CPRO(240),CZPSEC(20),EMPRO(240),EMZPCC(20),EPPRO(240),
```

```
     1GAMR(6),MUTZ(20),RZM(20),SIZM(20),SOZM(20),TITLE(16),VMPRO(240),
     2VPPRO(240),VVBZ(20)
      NAMELIST/INPUT/ASPECD,CFRO,CZPSEC,EMPRO,EMZPCC,EPSRC,FMHZ,KASES,
     1MUTZ,NZ,POLAD,RESM,RZM,SIZM,SOZM,VMPRO,VPPRO,VVBZ,ZM
      DATA BORNC/7.87785E-15/,PI/3.1415927/,RADP/.0174532
      DATA GAMR/.257457,.622362,1.,1.41671,1.86958,2.35619/
      DATA LAYERS/50/,MUTZ/20*2/
      DATA THRESH/1.E-30/
      CALL RANSIZ(15,12)                                          DISC
      CALL FXOPT(67,1,1,0)                                        UNDERFLO
      KASE=0
    1 KASE=KASE+1
      READ(5,4000)TITLE
      WRITE(6,5000)KASE,TITLE
      READ(5,INPUT)
      WRITE(6,INPUT)
      CAY=.02095845*FMHZ
      A=RADP*ASPECD
      WO=ABS(SIN(A))
      WSO=WO*WO
      VSO=1.-WSO
      VO=SQRT(VSO)
      A=RADP*POLAD
      B=SIN(A)
      A=COS(A)
      CS=A*A
      SS=B*B
      SC=A*B
      SMC=SS-CS
      EMC=2.82413E7*CAY*CAY
*ITERATE ALL AXIAL STATIONS (IZ = 1 TO NZ)
      LC=0
      LEM=0
      LEP=0
      LVM=0
      LVP=0
      DO 100 IZ=1,NZ
      EMNCO=EMZPCC(IZ)/EMC
      RW=RZM(IZ)
      CAYR=CAY*RW
      VCOM=1.591549E-7*CZPSEC(IZ)/FMHZ
      VCM=VCOM
*SPECTRUM FUNCTION PARAMETERS
      RO=SOZM(IZ)
      RI=SIZM(IZ)
      MUT=MUTZ(IZ)
      GAR=GAMR(MUT)
      PSI=FLOAT(MUT)/6.+1.5
      TKR=(2.*CAY*RO)**2
      CRS=(2.*CAY*RI/PI)**2
*GENERATE COLLISION FREQUENCY PROFILES
```

```
      LC=LC+1
      N=CPRG(LC)
      IF(N.EQ.0)GO TO 3
      IND=3-N+IABS(N-2)
      N=IABS(N)
      LC=LC+N
      CALL FIT(N,LC,IND,CPRO,CFM)
      IND=-IND
      CALL FIT(N,LC,IND,CPRO,CFO)
*GENERATE MEAN ELECTRON DENSITY PROFILES
    3 LEM=LEM+1
      N=EMPRO(LEM)
      IF(N.EQ.0)GO TO 5
      C=EMPRO(LEM+1)
      IND=3-N+IABS(N-2)
      IRE=IND
      N=IABS(N)
      LEM=LEM+N
      CALL FIT(N,LEM,IND,EMPRO,EMM)
      IND=-IND
      CALL FIT(N,LEM,IND,EMPRO,EMO)
*GENERATE ELECTRON DENSITY FLUCTUATION PROFILE
    5 LEP=LEP+1
      N=EPPRO(LEP)
      IF(N.EQ.0)GO TO 6
      IND=3-N+IABS(N-2)
      N=IABS(N)
      LEP=LEP+N
      CALL FIT(N,LEP,IND,EPPRO,EP)
*ACCOUNT FOR TURBULENCE SCATTERING IN MEAN PROFILES
    6 WS=WSO
      EMNC=EMNCO
      CALL PROFS(IRE,KRIT,MUT,PSI)
      TZCS=4.*CAY*CAY*VS
*GENERATE MEAN VELOCITY PROFILE
      LVM=LVM+1
      N=VMPRO(LVM)
      IF(N.EQ.0)GO TO 7
      IND=3-N+IABS(N-2)
      N=IABS(N)
      LVM=LVM+N
      CALL FIT(N,LVM,IND,VMPRO,VM)
*GENERATE VELOCITY FLUCTUATION PROFILE
    7 LVP=LVP+1
      N=VPPRO(LVP)
      IF(N.EQ.0)GO TO 8
      IND=3-N+IABS(N-2)
      N=IABS(N)
      LVP=LVP+N
      CALL FIT(N,LVP,IND,VPPRO,VP)
    8 WRITE(6,1000)ZM(IZ),EMNCO,EMNC,CAYR,WSO,WS,VCON,VVBZ(IZ)
```

```
      DO 70 I=1,LAYERS
   70 WRITE(6,2000)I,ROR(I),EMO(I),EMM(I),EP(I),CFO(I),CFM(I),EMS(I),
     1CFS(I),VM(I),VP(I)
      WRITE(6,3000)
*WAKE FIELD PENETRATION
      CALL LLINK('LINKA')                                          OVERLAYS
      CALL WFP(L,M)
      MINL=L
      AN=(C*EMMC/WS)**2
      A=CRS+PSI*ALOG(1.+TKR)
      BN=EXP(A)
      CALL LLINK('LINKB')                                          OVERLAYS
*INTEGRATE OVER PHI
      CALL PHINT(L,K)
*INTEGRATE OVER 2RDR
      CALL RINT(L)
*MOMENTS OF THE SCATTERING PER UNIT LENGTH
      A=GAR*BORNC*RO**3*(RW*EMZPCC(IZ))**2/BN
      DO 80 I=1,5
      DSDZ(I,IZ)=A*SO(I)
      DTDZ(I,IZ)=A*VO*VVBZ(IZ)*S1(I)
      DUDZ(I,IZ)=A*VVBZ(IZ)**2*(VSO*S12(I)+S2(I))
   80 CONTINUE
      WRITE(6,6000)(DSDZ(I,IZ),I=1,5),(DTDZ(I,IZ),I=1,5),(DUDZ(I,IZ),
     1 I=1,5)
      DO 90 I=1,5
      A=DSDZ(I,IZ)
      S1(I)=0.
      S2(I)=0.
      IF(A.LT.THRESH)GO TO 90
      S1(I)=DTDZ(I,IZ)/A
      B=DUDZ(I,IZ)/A-S1(I)**2
      IF(B.GT.0.)S2(I)=SQRT(B)
   90 CONTINUE
      WRITE(6,7000)S1,S2
  100 CONTINUE
*COMPLETION OF ITERATION OF AXIAL STATIONS
*CONVOLVE OVER Z
      CALL ZINT(M2,VO)
      IF(KASE.LT.KASES)GO TO 1
      STOP
 1000 FORMAT(1H1,2X,'AXIAL STATION (M) =',F7.2,6X,'MEAN ELECTRON DENSITY
     1/CRITICAL =',1PE12.5,6X,'CHANGED TO',1PE12.5,7X,'KRW ='1PE10.3//3X
     2,'(SIN ALPHA)**2 =',1PE12.5,5X,'CHANGED TO',1PE12.5,5X,'NU/OMEGA =
     3',1PE12.5,5X,'MEAN VELOCITY/BODY VELOCITY =',1PE10.3//3X,'PROFILE
     4FUNCTIONS**'/28X,'ELECTRON DENSITY',15X,'COLLISION FREQUENCY',10X,
     5'ALLOWANCE FOR',16X,'VELOCITY'/7X,'RELATIVE',6X,'MEAN',9X,'MEAN',
     610X,'RMS',8X,'LAYER',7X,'MESH PT.',5X,'SCATTERING ATTENUATION',6X,
     7'MEAN',9X,'RMS'/8X,'RADIUS',6X,'(LAYER)',4X,'(MESH PT.)',3X,
     8'FLUCTUATION',28X,'ELECTRONS',4X,'COLLISIONS',15X,'FLUCTUATION'//)
 2000 FORMAT(2X,I2,3X,F7.4,1X,1P9E13.4)
```

```
 3000 FORMAT(1H1,5X,'MEAN WAKE FIELD'//53X,'SCATTERING COEFFICIENTS'/
     128X,'PARALLEL POLARIZATION',30X,'TRANSVERSE POLARIZATION'/
     215X,'LAYERS'/6X,'MODE',12X,'ELECTRIC',18X,'MAGNETIC',
     318X,'ELECTRIC',18X,'MAGNETIC',10X,'USED'//)
 4000 FORMAT(16A5)
 5000 FORMAT(1H1,'CASE',I3,20X,16A5//)
 6000 FORMAT(5X,'ABSOLUTE'//6X,'ZEROTH',9X,1P3E15.4,5X,1P2E15.4/
     16X,'FIRST',10X,1P3E15.4,5X,1P2E15.4/6X,'SECOND',9X,1P3E15.4,5X,
     21P2E15.4///)
 7000 FORMAT(5X,'DOPPLER/BODY VELOCITY'//6X,'MEAN',11X,1P3E15.4,5X,
     11P2E15.4/6X,'SPREAD',9X,1P3E15.4,5X,1P2E15.4)
      END



*      A)  INTERPOLATION FOR RADIAL PROFILES
      SUBROUTINE FIT(N,M,IND,F,Y)
      COMMON/ABCKLW/ROR(50)
      DIMENSION F(M),G(35),X(50),Y(50)
      DATA G/1.,2.,1.,6.,2.,24.,6.,4.,120.,24.,12.,720.,120.,48.,36.,
     15040.,720.,240.,144.,40320.,5040.,1440.,720.,576.,362880.,40320.,
     2100B0.,4320.,2880.,3628800.,362880.,80640.,30240.,17280.,14400./
      DATA ROR/0.021049929,0.027053221,0.034768773,0.044684793,
     10.057428853,0.073807506,0.094857335,0.11590716,0.13695699,
     20.15800682,0.17905665,0.20010648,0.22115631,0.24220614,0.26325597,
     30.28430580,0.30535563,0.32640546,0.34745529,0.36850512,0.38955496,
     40.41060479,0.43165462,0.45270445,0.47375428,0.49480411,0.51585394,
     50.53690377,0.55795360,0.57900343,0.60005325,0.62110308,0.64215290,
     60.66320273,0.68425256,0.70530239,0.72635221,0.74740204,0.76845187,
     70.78950170,0.81055152,0.83160135,0.85265118,0.87370100,0.89475083,
     80.91580066,0.93685049,0.95790032,0.97895014,1./
      DATA LAYERS/50/
      MN=M-N
      IF(IND.GT.0)GO TO 3
*INDEPENDENT VARIABLE FOR LAYERS (MIDPOINTS OF R**2)
      A=0.
      IM=LAYERS
      DO 2 I=1,IM
      B=ROR(I)*ROR(I)
      X(I)=SQRT(.5*(A+B))
    2 A=B
      IF(IND+1)11,5,5
*INDEPENDENT VARIABLE FOR MESH POINTS
    3 IM=LAYERS-1
      DO 4 I=1,LAYERS
    4 X(I)=ROR(I)
      Y(LAYERS)=F(M)
      IF(IND.GT.1)GO TO 11
*N-POINT LAGRANGE INTERPOLATION OF F TO GIVE Y AT X
```

```
      5 I=N/2
        MM=(N+1)/2
        JM=MM+1
        L=(I*(I+1)+MM*(MM-1))/2-1
        NPO=I+L
        ENM=N-1
        DO 10 I=1,IM
        B=0.
        C=-ENM*X(I)
        A=C
        S=1.
        DO 7 J=1,MM
        D=F(J+MM)/(G(J+L)*A)
        A=-(A+S)
        S=-S
        E=C
        DO 6 K=1,N
        D=D*E
      6 E=E+1.
      7 B=B+D
        NP=NPO
        DO 9 J=JM,N
        D=F(J+MM)/(G(NP)*A)
        NP=NP-1
        A=-(A+S)
        S=-S
        E=C
        DO 8 K=1,N
        D=D*E
      8 E=E+1.
      9 B=B+D
        IF(B.LT.0.)B=0.
     10 Y(I)=B
        RETURN
  *STEP FUNCTION
     11 I=1
     12 MM=MM+1
        A=F(MM)
        IF(MM.LT.M)GO TO 13
        B=2.
        GO TO 14
     13 MM=MM+1
        B=F(MM)
     14 K=I
        DO 15 I=K,LAYERS
        IF(X(I).GT.B)GO TO 12
     15 Y(I)=A
        RETURN
        END
```

```
*      B)  TURBULENCE EFFECTS ON PROPAGATION
       SUBROUTINE PROFS(IRE,KRIT,MUT,PSI)
       COMMON/ABCKLW/ROR(50)
       COMMON/RBC/CFL(50),EM(50),V
       COMMON/RBCW/CAYR,EMNC,VCON,VS,WS
       COMMON/RBH/AOK(50),ROK(50)
       COMMON/RBK/BOK(50)
       COMMON/RBLW/CFM(50),EP(50)
       COMMON/RBW/CFO(50),CFS(50),CRS,EMM(50),EMO(50),EMS(50),GAR,TKR,WO
       DATA LAYERS/50/
       XR=6.283185*WO/CAYR
       DO 7 I=1,LAYERS
*CALCULATE COEFFICIENTS OF ATTENUATION AND DEPOLARIZATION BY TURBULENCE
       VC=VCON*CFM(I)
       VCS=1.+VC*VC
       A=EMM(I)*EMNC/VCS
       B=VC*A
       A=1.-A
       GS=.5*(A+SQRT(A*A+B*B))
       G=SQRT(GS)
       Y=.5*XR/(XR+(1.+G)*(1.-ROR(I)))
       FJ=0.
       A=GS*TKR
       B=GS*CRS
       X=1.
       IF(B.GT.1.)X=1./B
       D=A*PSI
       IF(D*X.LT..1)GO TO 2
       C=1./A
       VX=C+X
       VY=C+Y
       UX=ALOG(1.+A*X)
       UY=ALOG(1.+A*Y)
       D=1.-PSI
       IF(MUT.EQ.3)GO TO 1
       AA=EXP(D*UX)*C/D
       GJ=AA*((X*(1.-X))**2-VX*(X*(2.+X*(4.*X-6.))-VX*(2.+X*(12.*X-12.)
      1-24.*VX*(X-.5-VX/(D+4.))/(D+3.))/(D+2.))/(D+1.))
       GJ=GJ-C*C*C*(2.+24.*C*(.5+C/(D+4.))/(D+3.))/(D+2.)/(D+1.)/D
       IF(Y.GE.X)GO TO 3
       FJ=AA*(1.+X*(X+X-2.)-4.*VX*(X-.5-VX/(D+2.))/(D+1.))
       FJ=FJ-C*EXP(D*UY)*(1.+Y*(Y+Y-2.)-4.*VY*(Y-.5-VY/(D+2.))/(D+1.))/D
       GO TO 3
     1 AA=C*C
       GJ=(2.+X*(4.*X-6.))*X*UX-(X*(1.-X))**2/VX-VX*((2.+X*(12.*X-12.))
      1*(UX-1.)-VX*((12.*X-6.)*(UX-1.5)-VX*(4.*UX-22./3.)))
       GJ=AA*(GJ-C*(2.+C*(9.+22.*C/3.)))
       IF(Y.GE.X)GO TO 3
```

```
      FJ=(4.*X-2.)*UX-(1.+X*(X+X-2.))/VX-VX*(4.*UX-4.)
      FJ=AA*(FJ-(4.*Y-2.)*UY+(1.+Y*(Y+Y-2.))/VY+VY*(4.*UY-4.))
      GO TO 3
    2 GJ=X*X*X*(1./3.+X*(X*(.2+B*(.4-X/6.))-.5-.25*B))
      IF(Y.GE.X)GO TO 3
      A=.5*B
      B=2.*(1.+B)/3.
      C=1.+A
      FJ=X*(1.+X*(X*(B-A*X)-C))-Y*(1.+Y*(Y*(B-A*Y)-C))
    3 B=GAR*TKR*SQRT(TKR)*(EP(I)+EMNC)**2/VCS
      AK=.01989*FJ*B
      IF(AK.LT.0.)AK=0.
      B=GJ*B/WO
      IF(B.LT.0.)B=0.
      BOK(I)=B
*ELECTRON DENSITY AND COLLISION FREQUENCY FOR SCATTERING ATTENUATION
      B=SQRT(AK)
      IF(AK.LT.1.E-4)GO TO 5
      G=1./(1.+B)
      GS=6*6
      B=1.+AK*AK-GS
      B=2.*6*AK/B
      EMS(I)=B*(1.+B*B)/EMNC
      GO TO 6
    5 EMS(I)=2.*B/EMNC
    6 CFS(I)=B/VCOM
      EM(I)=EMM(I)+EMS(I)
      CFL(I)=CFM(I)+CFS(I)
    7 CONTINUE
      KRIT=0
      IF(IRE.NE.1)GO TO 16
*ADJUST ASPECT AND DENSITY TO MAKE CRITICAL POINTS LIE AT MESH POINTS
      JM=LAYERS-1
      B=EM(LAYERS)/(1.+(CFL(LAYERS)*VCOM)**2)
      D=EMNC*B
      IF(D.GT.1.)GO TO 16
      DO 10 J=1,JM
      I=LAYERS-J
      A=EM(I)/(1.+(CFL(I)*VCOM)**2)
      C=EMNC*A
      IF(C.LT.D.OR.C.LT.1.)GO TO 9
      IF(C+D.GT.2.*C*D)GO TO 8
      I=I+1
      A=B
    8 EMNC=1./A
      KRIT=I
      IF(I.GT.JM)GO TO 16
      GO TO 11
    9 B=A
   10 D=C
   11 B=EMNC*EM(LAYERS)/(1.+(CFL(LAYERS)*VCOM)**2)
```

```
      IF(B.GT.WS)GO TO 16
      DO 15 J=1,JM
      I=LAYERS-J
      A=EMNC*EM(I)/(1.+(CFL(I)*VCON)**2)
      IF(A.LT.B.OR.A.LT.WS)GO TO 15
      IF(A+B.GT.WS+WS.OR.A.GT.1.)A=B
      WS=A
      GO TO 16
   15 B=A
   16 WS=1.-WS
      V=SQRT(WS)
*PROFILE OF 1/K AT MESH POINTS
      DO 20 I=1,LAYERS
      VC=VCON*CFL(I)
      A=EM(I)*EMNC/(1.+VC*VC)
      B=A*VC
      A=1.-A
      C=A*A+B*B
      ROK(I)=A/C
      AOK(I)=-B/C
*TOTAL ELECTRON DENSITY AND COLLISION FREQUENCY PROFILE FUNCTIONS
      IF(EMN(I).GT.0.)EM(I)=EM(I)*EMO(I)/EMN(I)
      IF(CFN(I).GT.0.)CFL(I)=CFL(I)*CFO(I)/CFN(I)
   20 CONTINUE
      RETURN
      END
```

89

```
*       C)  EM FIELDS IN THE MEAN WAKE
      SUBROUTINE WFP(JMIN,NFP)
      COMMON/ABCKLW/ROR(50)
      COMMON/CCG/B11,B12,B2,CN,CV,CW,F1,F3,GAM(50),PP(50),PQ(50),PR(50),
     1 PS(50),PT(50),PU(50),PV(50),PW(50),PX(50),PY(50),PZ(50),QQ(4,4),Z
      COMMON/ICJW/INLAY(64)
      COMMON/RBC/CFL(50),EM(50),V
      COMMON/RCCW/CAYR,EMNC,VCON,VS,WS
      COMMON/RCG/RK(50)
      COMPLEX BT(64),B11,B12,B2,CN,CV,CW,C1,C2,C3,C4,C5,DIEL(50),EYE,
     1 EYEN,F1,F3,GAM,HNK(64),HNKP(64),ONE,P,PP,PQ,PR,PS,PT,PU,PV,PW,PX,
     2 PY,PZ,Q,QQ,R,RHO,S,SGN,Z,ZERO
      DIMENSION YIP(49)
      DATA YIP/6*0.28519903,0.22191040,0.18160939,0.15369664,0.13322102,
     10.11755961,0.10519314,0.095180776,0.086908736,0.079959553,
     20.074039395,0.068935455,0.064489820,0.060582844,0.057122216,
     30.054035584,0.051265427,0.048765445,0.046497952,0.044431957,
     40.042541744,0.040805793,0.039205963,0.037726846,0.036355276,
     50.035079936,0.033891040,0.032780089,0.031739660,0.030763245,
     60.029845113,0.028980196,0.028163598,0.027392515,0.026662171,
```

```
     70.025969761,0.025312404,0.024687504,0.024092715,0.023525912,
     80.022985165,0.022468718,0.021974969,0.021502481/
      DATA EYE/(0.,1.)/,ONE/(1.,0.)/,ZERO/(0.,0.)/
      DATA LAYERS/50/,MODES/64/
      DATA EPS0/1.E-30/,STP/88./,TEST/1.E18/
      DO 10 I=1,LAYERS
   10 RK(I)=CAYR*ROR(I)
      DELK=RK(1)
      W=SQRT(WS)
      CV=CMPLX(V,0.)
      CW=CMPLX(W,0.)
      K1=LAYERS-1
*DETERMINE THE NUMBER OF MODES TO USE
      A=W*CAYR
      ARG=1.359*A
      NHP=3+SQRT(2.*A*(A+12.))
      IF(NHP.GT.MODES)NHP=MODES
      CALL HANK(NHP,A,HNK,HNKP)
*CALCULATE THE DIELECTRIC CONSTANT AND PROPAGATION CONSTANT OF LAYERS
      C1=CMPLX(VS,0.)
      DO 100 J=1,LAYERS
      VC=VCOM*CFL(J)
      B=ENC*EM(J)/(1.+VC*VC)
      C4=CMPLX(1.-B,B*VC)
      DIEL(J)=C4
      C2=C4-C1
      GAM(J)=CSQRT(C2)
  100 CONTINUE
      C1=GAM(1)*CMPLX(DELK,0.)
      CALL BIN(C1,NHP,B1)
*ITERATE ALL MODES (NP = 1 TO NHP)
      EYEN=ONE
      SGN=ONE
      EN=0.
      EPS=EPS0
      JMIN=LAYERS
      DO 600 NP=1,NHP
      CN=CMPLX(EN,0.)
*ITERATE ALL LAYERS FROM THE OUTSIDE IN
      J=LAYERS
      DO 200 L=1,4
      DO 190 M=1,4
  190 QQ(L,M)=ZERO
  200 QQ(L,L)=ONE
      DO 500 K=1,K1
      C1=GAM(J)
      IF(RK(J)*CABS(C1).GT.STP)GO TO 410
*CALCULATE AND STORE THE PROPAGATION MATRIX FOR THE CURRENT LAYER
      JM=J-1
      DEL=TIP(JM)
      A=RK(JM)
```

```
            B=A*AIMAG(C1)
            A=A*REAL(C1)
            CALL PROP(EN,A,B,DEL,P,Q,R,S)
            PP(J)=P
            PT(J)=S
            C4=EYE*C1*Q
            PX(J)=-C4
            PQ(J)=-C4/DIEL(J)
            C2=CN*CV/(C1+CMPLX(A,B))
            PR(J)=C2*PQ(J)
            C5=C2*C4
            PW(J)=C5
            C3=CMPLX(RK(JM)/RK(J),0.)*C2
            PV(J)=C3*C4
            PY(J)=C3*PQ(J)
            PU(J)=C2*S-C3*P
            PS(J)=EYE*DIEL(J)*R/C1-C3*C5
            PZ(J)=PS(J)/DIEL(J)
      *ACCUMULATE THE OVERALL PROPAGATION MATRIX
            DO 300 L=1,4
            C2=QQ(L,1)*PQ(J)+QQ(L,2)*S+QQ(L,4)*PY(J)
            C3=QQ(L,1)*PR(J)+QQ(L,2)*PU(J)+QQ(L,3)*P+QQ(L,4)*PZ(J)
            QQ(L,1)=QQ(L,1)*P+QQ(L,2)*PS(J)+QQ(L,3)*C5-QQ(L,4)*PU(J)
            QQ(L,4)=QQ(L,2)*PY(J)-QQ(L,3)*C4+QQ(L,4)*S
            QQ(L,2)=C2
            QQ(L,3)=C3
        300 CONTINUE
            J=JM
            IF(K.EQ.K1)GO TO 510
      *ESTIMATE THE MAGNITUDE OF THE PROPAGATION MATRIX
            A1=0.
            DO 400 L=1,4
            DO 400 M=1,4
            A=REAL(QQ(L,M))
            IF(A.GT.TEST)GO TO 410
            A1=A1+A*A
            A=AIMAG(QQ(L,M))
            IF(A.GT.TEST)GO TO 410
            A1=A1+A*A
        400 CONTINUE
            A1=.0625*EPS*A1
            IF(A1.LT.1.)GO TO 500
      *IF THE PROPAGATION MATRIX DIVERGES, INSERT A PERFECT CONDUCTOR
        410 B11=ZERO
            B12=ZERO
            GO TO 520
        500 CONTINUE
      *APPLY THE BOUNDARY CONDITIONS
        510 B12=EYE*B1(NP)/GAM(1)
            B11=ONE/(B12*DIEL(1))
        520 J1=J
```

```
      B2=EYE*HNKP(NP)/(CW*HNK(NP))
      F1=EYEN*CMPLX(W*REAL(HNK(NP)),0.)
      A=-.636619772/(W*CAYR)
      F3=CMPLX(A,0.)*EYEN/HNK(NP)
      Z=CMPLX(.5*WS,0.)*EYEN*HNK(NP)
      IF(NP.EQ.1)GO TO 530
      F1=F1+F1
      F3=F3+F3
  530 CALL BCO(J1)
      INLAY(NP)=J1
      IF(J1.LT.JMIN)JMIN=J1
      IF(NP.EQ.NHP)RETURN
      EYEN=CMPLX(-AIMAG(EYEN),REAL(EYEN))
      SGN=-SGN
      EN=EN+1.
      A1=1.+SQRT(5.283*EN)*(EN/ARG)**NP
      EPS=EPSO*A1*A1
  600 CONTINUE
      RETURN
      END


C     9)  HANKEL FUNCTIONS AND DERIVATIVES
      SUBROUTINE HANK(NP,X,HNK,HNKP)
      COMPLEX HNK(NP),HNKP(NP)
      DIMENSION CN(65)
      DATA MODES/64/,THRESH/1.E-30/,TP/.636619772/
      IDIMP=MODES+1
C     *CONVERGENCE CRITERION
      B=ABS(X)
      M=7.5+SQRT(3.*B*(B+8.))
      M=MAXO(M,NP)
      MM=(M+1)/2
C     *DOWNWARD RECURRENCE
      A=2./X
      B=1.
      C=0.
      E=0.
      S=0.
      T=0.
      U=1.
      I=MM+MM
      DO 10 J=1,MM
      S=S+E
      EYE=I
      U=-U
      T=T+U*E/EYE
      C=A*EYE*B-C
```

```
      E=A*D*(EYE-1.)-B
      C=D
      B=E
      IF(I.GT.IDIMP)GO TO 10
      CN(I)=D
      CN(I-1)=E
   10 I=I-2
      S=S+S+E
*CALCULATE FUNCTIONS FOR FIRST TWO ORDERS
      B=E/S
      C=TP*(E*(.57721566-ALOG(A))+4.*U*T)/S
      D=D/S
      IF(ABS(B).LT.THRESH)GO TO 12
      E=(D*C-TP/X)/B
      GO TO 14
   12 E=((B-D/X)*C+TP/(X*X))/(D+D)
   14 HNK(1)=CMPLX(D,C)
      HNK(2)=CMPLX(D,E)
      HNKP(1)=-HNK(2)
      HNKP(2)=HNK(1)-CMPLX(D/X,E/X)
      IF(NP.LT.3)RETURN
*NORMALIZATION AND RECURRENCE FOR HIGHER ORDERS
      T=1./X
      I=1
      EYE=1.
      DO 20 J=3,NP
      U=A*E*EYE-C
      I=I+1
      EYE=I
      B=CN(J)/S
      HNK(J)=CMPLX(B,U)
      HNKP(J)=HNK(J-1)-CMPLX(T*EYE*B,T*EYE*U)
      C=E
   20 E=U
      RETURN
      END
```

```
*      E)  JN'(X)/JN(X) FOR COMPLEX X
      SUBROUTINE BIN(X,NP,B1)
      COMPLEX B1(NP),C,D,E,F,X
*CONVERGENCE CRITERION
      A=CABS(X)
      M=5.5+SQRT(3.*A*(A+8.))
      M=MAXO(M,NP)
*DOWNWARD RECURRENCE
      I=M
      EYE=I
```

```
      C=CMPLX(2.*(EYE+1.),0.)
      D=C/X
      E=(1.,0.)
      C=CMPLX(2.*EYE,0.)
      C=C/X-E/D
      DO 10 J=1,M
      EYE=EYE-1.
      F=CMPLX(EYE,0.)/X
      D=F-E/C
      C=D+F
      IF(I.LE.NP)BT(I)=D
   10 I=I-1
      RETURN
      END



*     F)  ELEMENTS OF PROPAGATION MATRIX
      SUBROUTINE PROP(EN,XZR,XZI,Y,C,D,CP,DP)
      COMPLEX C,CP,D,DP
      DIMENSION AJ(2,2,5),P(2,2),Q(2,2),U(2,2),W(2,2)
      A=XZR*XZR
      B=XZI*XZI
      E=A+B
      F=SQRT(E)
      G=F+.01
*APPROXIMATE CONVERGENCE CRITERION
      LIM=6.+.1*F+.2*EN/SQRT(G)+(41.+.4*F+.04*E+(4.6-.7*ALOG(G))*EN)*Y
      ENS=EN+.4
      XSA=A-B
      XSB=2.*XZR*XZI
      YS=Y*Y
      Z=Y*Y
*INITIALIZE THE SERIES
      AJ(1,1,3)=XZR/A
      AJ(1,2,3)=-XZI/A
      AJ(2,1,4)=1.
      AJ(2,2,4)=0.
      DO 3 K=1,2
      DO 2 J=1,2
      AJ(J,K,1)=0.
      AJ(J,K,2)=0.
      U(K,J)=0.
    2 W(K,J)=0.
      AJ(2,K,3)=0.
    3 AJ(1,K,4)=0.
      L=5
      LA=4
      LB=3
```

```
      LC=2
      LB=1
      A=1.
*EVALUATE THE SERIES
      DO 10 J=1,LIM
      G=YS/A
      A=A+1.
      G=G/A
      E=(3./A-2.)*Y
      F=(ENS-(A-2.)**2)*G
      DO 5 I=1,2
      DO 4 K=1,2
      P(K,I)=E*AJ(K,I,LA)+F*AJ(K,I,LB)
    4 Q(K,I)=(AJ(K,I,LB)+2.*Y*AJ(K,I,LC)+YS*AJ(K,I,LD))*G
    5 CONTINUE
      DO 7 K=1,2
      AJ(K,1,L)=P(K,1)-XSA*Q(K,1)+XSB*Q(K,2)
      AJ(K,2,L)=P(K,2)-XSA*Q(K,2)-XSB*Q(K,1)
      DO 6 I=1,2
      P(K,I)=U(K,I)
      Q(K,I)=W(K,I)
      U(K,I)=U(K,I)+AJ(K,1,L)
    6 W(K,I)=W(K,I)+A*AJ(K,I,L)
    7 CONTINUE
*TEST FOR CONVERGENCE
      E=0.
      DO 8 K=1,2
      DO 8 I=1,2
      E=E+(U(K,I)-P(K,I))**2+(W(K,I)-Q(K,I))**2
    8 CONTINUE
      IF(E.LE.0.)GO TO 11
      LB=LC
      LC=LB
      LB=LA
      LA=L
      L=1+MOD(LA,5)
   10 CONTINUE
*CALCULATE THE OUTPUTS
   11 A=Y+XZR
      B=Y+XZI
      C=CMPLX(1.+A*U(1,1)-B*U(1,2),A*U(1,2)+B*U(1,1))
      E=1.+U(2,1)
      D=CMPLX(A*E-B*U(2,2),A*U(2,2)+B*E)
      CP=CMPLX(W(1,1),W(1,2))
      DP=CMPLX(1.+W(2,1),W(2,2))
      RETURN
      END
```

```
*     G)  SOLUTION FOR LOCAL FIELDS
      SUBROUTINE BCG(M)
      COMMON/CCG/B11,B12,B2,CN,CV,CW,F1,F3,GAM(50),PP(50),PQ(50),PR(50),
     1 PS(50),PT(50),PU(50),PV(50),PW(50),PX(50),PY(50),PZ(50),QQ(4,4),Z
      COMMON/CGH/FJA(2),FJB(2),FJC(2),FJD(2)
      COMMON/RCG/RK(50)
      COMPLEX B,B11,B12,B2,C,CN,CV,CW,C1,C2,C3,C4,C5,C6,C7,FJA,FJB,FJC,
     1 FJD,F1,F3,GAM,PP,PQ,PR,PS,PT,PU,PV,PW,PX,PY,PZ,QQ,Z
      DIMENSION E(12)
      DATA LAYERS/50/
*INVERT THE MATRIX EQUATION FOR THE BOUNDARY CONDITIONS
      EN=REAL(CN)
      N=EN
      NP=N+1
      V=REAL(CV)
      A=RK(M)
      C=CMPLX(A,0.)
      C2=CMPLX(RK(LAYERS),0.)
      C5=CN*CV
      C6=GAM(M)
      C7=C5/(C2*CW*CW)
      B=C5/(C+C6+C6)
      C5=B11*(QQ(1,1)+B*QQ(1,4))+QQ(1,2)
      C6=B11*(QQ(3,1)+B*QQ(3,4))+QQ(3,2)
      C1=B2*C5-C7*C6-B11*(QQ(2,1)+B*QQ(2,4))-QQ(2,2)
      C2=B2*C6+C7*C5-B11*(QQ(4,1)+B*QQ(4,4))-QQ(4,2)
      C5=QQ(1,3)+B12*QQ(1,4)-B*QQ(1,2)
      C6=QQ(3,3)+B12*QQ(3,4)-B*QQ(3,2)
      C3=B2*C5-C7*C6-QQ(2,3)-B12*QQ(2,4)+B*QQ(2,2)
      C4=B2*C6+C7*C5-QQ(4,3)-B12*QQ(4,4)+B*QQ(4,2)
      IF(ABS(REAL(C4))+ABS(AIMAG(C4)).GT.0.)GO TO 1
      FJA(1)=(0.,0.)
      GO TO 2
    1 C5=C3/C4
      FJA(1)=F3/(C1-C2*C5)
    2 IF(ABS(REAL(C2))+ABS(AIMAG(C2)).GT.0.)GO TO 3
      FJC(1)=(0.,0.)
      GO TO 4
    3 C5=C4/C2
      FJC(1)=F3/(C3-C1*C5)
    4 IF(ABS(REAL(C3))+ABS(AIMAG(C3)).GT.0.)GO TO 5
      FJA(2)=(0.,0.)
      GO TO 6
    5 C5=C4/C3
      FJA(2)=F3/(C2-C1*C5)
    6 IF(ABS(REAL(C1))+ABS(AIMAG(C1)).GT.0.)GO TO 7
      FJC(2)=(0.,0.)
      GO TO 8
    7 C5=C3/C1
      FJC(2)=F3/(C4-C2*C5)
```

```
     $ DO 10 K=1,2
       FJB(K)=FJA(K)-B*FJC(K)
       FJA(K)=B11*FJA(K)
       FJB(K)=B12*FJC(K)+B*FJA(K)
    10 CONTINUE
       AA=EN/A
       CALL STORF(NP,M,AA,V)
       IF(M.EQ.LAYERS)GO TO 210
*ITERATE TO GIVE THE FIELDS AT EACH LAYER BOUNDARY
       JP=M+1
       DO 200 J=JP,LAYERS
       DO 100 K=1,2
       C2=PS(J)*FJA(K)+PT(J)*FJB(K)+PU(J)*FJC(K)+PV(J)*FJD(K)
       C3=PW(J)*FJA(K)+PP(J)*FJC(K)+PX(J)*FJD(K)
       FJD(K)=PT(J)*FJB(K)+PZ(J)*FJC(K)+PY(J)*FJB(K)-PU(J)*FJA(K)
       FJA(K)=PP(J)*FJA(K)+PQ(J)*FJB(K)+PR(J)*FJC(K)
       FJB(K)=C2
       FJC(K)=C3
   100 CONTINUE
       JI=J
       AA=EN/RK(J)
       CALL STORF(NP,JI,AA,V)
   200 CONTINUE
*COHERENT SCATTERING COEFFICIENTS
   210 C1=FJA(1)-F1
       C2=FJC(2)-F1
       C3=C1/Z
       C4=FJC(1)/Z
       C5=FJA(2)/Z
       C6=C2/Z
       MU=LAYERS-M+1
       WRITE(6,1000)N,C3,C4,C5,C6,MU
       E(1)=-AIMAG(C5)
       E(2)=REAL(C5)
       E(3)=REAL(C6)
       E(4)=AIMAG(C6)
       E(5)=-AIMAG(C4)
       E(6)=REAL(C4)
       E(7)=REAL(C3)
       E(8)=AIMAG(C3)
       NFILE=(LAYERS+1)*NP
       WRITE(15'NFILE)E                                          DISC
       RETURN
 1000  FORMAT(6X,I3,2X,4(2X,1P2E12.4),I6)
       END
```

```
*       H)  STORAGE OF FIELD PROFILES
        SUBROUTINE STORF(NP,J,ENKR,V)
        COMMON/CGH/FJA(2),FJB(2),FJC(2),FJD(2)
        COMMON/RBH/AOK(50),ROK(50)
        COMPLEX FJA,FJB,FJC,FJD
        DIMENSION E(12)
        DATA LAYERS/50/
        A=ROK(J)*V
        B=AOK(J)*V
        C=ROK(J)*ENKR
        D=AOK(J)*ENKR
        E(1)=D*REAL(FJC(2))+C*AIMAG(FJC(2))-B*REAL(FJB(2))-A*AIMAG(FJB(2))
        E(2)=D*AIMAG(FJC(2))-C*REAL(FJC(2))-B*AIMAG(FJB(2))+A*REAL(FJB(2))
        E(3)=-REAL(FJD(2))
        E(4)=-AIMAG(FJD(2))
        E(5)=-AIMAG(FJA(2))
        E(6)=REAL(FJA(2))
        E(7)=A*REAL(FJB(1))-B*AIMAG(FJB(1))-C*REAL(FJC(1))+D*AIMAG(FJC(1))
        E(8)=A*AIMAG(FJB(1))+B*REAL(FJB(1))-C*AIMAG(FJC(1))-D*REAL(FJC(1))
        E(9)=AIMAG(FJD(1))
        E(10)=-REAL(FJD(1))
        E(11)=REAL(FJA(1))
        E(12)=AIMAG(FJA(1))
        NFILE=J+(LAYERS+1)*(NP-1)
        WRITE(15'NFILE)E                                        DISC
        RETURN
77      END


*       I)  ANALYSIS OF FIELDS VERSUS PHI
        SUBROUTINE PHINT(LS,MM)
        DATA LAYERS/50/
*SET UP THE NUMBER OF ANGLES AS A POWER OF TWO
        K=1
        M=2
   10   M=M+1
        K=K+K
        IF(K.LT.MM)GO TO 10
        IM=4*K
*FAST FOURIER SUM FOR MEAN WAKE_SCATTERING
        WRITE(6,2000)
        LTH=0
        L=LAYERS+1
        CALL FFSUM(L,MM,IM,M,LTH)
*ANALYZE FIELDS AT EACH LAYER BOUNDARY
        WRITE(6,4000)
        DO 20 L=LS,LAYERS
```

```
      LL=L
      CALL FFSUM(LL,MM,IM,M,LTH)
   20 CONTINUE
      RETURN
 2000 FORMAT(1H1,'SCATTERING FROM MEAN WAKE PLASMA'//
     1 15X,'AZIMUTHAL',46X,'2*PI*KR*SCATTERED POWER (DB)'/2X,
     2'ANGLE'/45X,'LINEAR POLARIZATION',23X,'CIRCULAR POLARIZATION'/3X,
     3'NUMBER',3X,'DEGREES',17X,'PARALLEL',6X,'TRANSVERSE',5X,
     4'ORTHOGONAL',11X,'PRINCIPAL',5X,'ORTHOGONAL'//)
 4000 FORMAT(1H1,2X,'PROFILES OF WEIGHTED AVERAGES OF SQUARES OF SCALAR
     1PRODUCTS OF ELECTRIC FIELDS'//21X,'LINEAR POLARIZATION',15X,
     2'CIRCULAR POLARIZATION'/14X,'VERTICAL',4X,'HORIZONTAL',3X,
     3'ORTHOGONAL',5X,'PRINCIPAL',4X,'ORTHOGONAL',17X,
     4'DEPOLARIZATION FACTORS'//)
      END




*      J)  FIELDS AT N VALUES OF PHI BY FFT
      SUBROUTINE FFSUM(LYR,MM,N,M,LTH)
      COMMON/ICJW/INLAY(64)
      COMMON/RJK/WW(256)
      DIMENSION E(12),G(12,256),H(12,256),X(5)
      DATA DBT/-300./,THRESH/1.E-30/
      DATA LAYERS/50/
      LP=LAYERS+1
      IF(LTH.EQ.0)TH=6.2831853/FLOAT(N)
      N2=N/2
      IK=8
      IF(LYR.LT.LP)IK=12
      JM=IK-3
*INITIALIZE ALL LOCATIONS
      DO 1 I=1,N
      DO 1 J=1,IK
      G(J,I)=0.
    1 H(J,I)=0.
      DO 3 I=1,MM
      IF(INLAY(I).GT.LYR)GO TO 3
*READ DATA IN
      NFILE=LYR+LP*(I-1)
      READ(15'NFILE)E                                          DISC
      DO 2 J=1,JM,4
      JP=J+1
      DO 2 K=J,JP
      KP=K+2
      G(K,I)=E(K)
      H(KP,I)=E(KP)
    2 CONTINUE
    3 CONTINUE
```

```
      *BIT INVERSION
            DO 30 I=1,M
            K=I-1
            II=1
            DO 20 J=1,M
            MJ=M-J
            KK=K/2
            L=K-KK-KK
            K=KK
         20 II=II+L*2**MJ
            IF(I.GE.II)GO TO 30
            DO 25 J=1,IK
            A=G(J,I)
            B=H(J,I)
            G(J,I)=G(J,II)
            G(J,II)=A
            H(J,I)=H(J,II)
            H(J,II)=B
         25 CONTINUE
         30 CONTINUE
      *ECONOMIZED FOURIER SUMMATION
            L2=1
            LIM=M
            DO 40 L=1,M
            L21=L2
            L2=L2+L2
            LIM=LIM/2
            LPO=-1
            DO 40 LL=1,L21
            LPO=LPO+1
            IB=LIM*LPO
            IF(LIM.EQ.1)GO TO 32
            A=IB*TH
            IB=IB+1
            CST=COS(A)
            SNT=SIN(A)
            WW(IB)=CST
            IB=IB+N2
            WW(IB)=SNT
            GO TO 33
         32 IB=IB+1
            CST=WW(IB)
            IB=IB+N2
            SNT=WW(IB)
         33 L1=1-L2
            DO 40 KK=1,LIM
            L1=L1+L2
            KKA=L1+LPO
            KKB=KKA+L21
            DO 35 J=1,IK
            A=G(J,KK2)*CST-H(J,KKB)*SNT
```

```
      B=G(J,KKB)*SNT+H(J,KKB)*CST
      G(J,KKB)=G(J,KKA)-A
      H(J,KKB)=H(J,KKA)-B
      G(J,KKA)=G(J,KKA)+A
      H(J,KKA)=H(J,KKA)+B
   35 CONTINUE
   40 CONTINUE
      LTH=1
      IF(LYR.GT.LAYERS)GO TO 45
*EVALUATE NUMERICAL AVERAGES OVER PHI
      I=IK
      K=N
      CALL AVGS(M,I,K,LYR)
      RETURN
*OUTPUT THE COHERENT SCATTERING VERSUS PHI
   41 K=N2+1
      A=180./N2
      PHI=0.
      DO 60 J=1,K
      X(1)=H(7,J)**2+H(8,J)**2
      X(2)=H(3,J)**2+H(4,J)**2
      X(3)=.5*(H(1,J)**2+H(2,J)**2+H(5,J)**2+H(6,J)**2)
      X(4)=.25*((H(3,J)+H(7,J))**2+(H(4,J)+H(8,J))**2
     1      +(H(5,J)-H(1,J))**2+(H(6,J)-H(2,J))**2)
      X(5)=.25*((H(3,J)-H(7,J))**2+(H(4,J)-H(8,J))**2
     1      +(H(5,J)+H(1,J))**2+(H(6,J)+H(2,J))**2)
      DO 50 I=1,5
      B=BBT
      IF(X(I).LT.THRESH)GO TO 50
      B=10.*ALOG10(X(I))
   50 X(I)=B
      I=J-1
      WRITE(6,1000)I,PHI,X
   60 PHI=PHI+A
      D=.707107
      A=D*(H(7,1)+H(8,1))
      B=D*(H(8,1)-H(7,1))
      C=D*(H(3,1)+H(4,1))
      D=D*(H(4,1)-H(3,1))
      WRITE(6,2000)A,B,C,D
      RETURN
 1000 FORMAT(3X,I4,F12.3,9X,3F15.3,5X,2F15.3)
 2000 FORMAT(//6X,'SQUARE ROOT OF (2*PI*KR) TIMES THE COMPLEX FORWARD SC
     1ATTERED FIELD'//10X,'PARALLEL',1PE16.4,' ',1PE12.4//10X,'TRANSVER
     2SE',1PE16.4,' ',1PE12.4)
      END
```

```
C  K)  NUMERICAL AVERAGES OVER PHI
      SUBROUTINE AVGS(N,IK,M,LAYR)
      COMMON/ABCKLW/ROR(50)
      COMMON/IKW/KRIT,MINL
      COMMON/RBK/BOK(50)
      COMMON/RJK/WW(256)
      COMMON/RKW/BN,CAY,CS,PSI,RI,RO,RW,SC,SMC,SS,TICS
      COMMON/RKL/FGS(50,5)
      DIMENSION BDS(129),DEP(5),H(IK,M),JA(10),K(10),S(10),U(3,5,129),
     1V(3,5,129)
      DATA JA/1,2,1,7,8,7,1,2,1,2/
      DATA K/0,0,1,0,0,1,7,5,6,6/
      DATA EXA/88./,LAYERS/50/,THRESH/1.E-30/
      FM=M
      F=2.*BW/FM
      N2=M/2
      ML=1+N2
      MM=ML
      MN=ML+1
      LM=LAYR-1
      IF(LM.LT.MINL)GO TO 7
    1 MM=MN
C*CALCULATE THE LINE INTEGRAL OF THE DEPOLARIZATION RATE
      LL=1+N2/2
      CAYR=CAY*RW
      R=ROR(LM)
      DO 6 M=1,LL
      RS=R*WW(M+N2)
      RB=1.01*RS
      A=0.
      RA=1.
      I=LAYERS
    2 IF(I.EQ.LM.OR.RA.LT.RB)GO TO 3
      IM=I-1
      RB=ROR(IM)
      A=A+(RA-RB)*BOK(I)/SQRT(1.-(RS/RA)**2)
      RA=RB
      I=IM
      GO TO 2
    3 B=0.
    4 IF(I.EQ.1.OR.RA.LT.RB)GO TO 5
      IM=I-1
      RB=ROR(IM)
      B=B+(RA-RB)*BOK(I)/SQRT(1.-(RS/RA)**2)
      RA=RB
      I=IM
      GO TO 4
    5 I=MAXO(1,I-1)
      B=B+BOK(I)*SQRT(2.*RS*(RA-ROR(I)))
      I=MM-M
```

```
      BDS(I)=A*CAYR
    6 BDS(M)=(A+B+B)*CAYR
*BEGIN THE AVERAGE OVER ANGLES FROM 0 TO PI
    7 LB=LA
      LA=L
      L=1+MOD(LM,3)
      MM=0
      DO 30 M=1,MM
      IF(M.EQ.MM)GO TO 12
      IF(LAYR.GT.LAYERS)GO TO 10
*SCALAR PRODUCTS OF ELECTRIC FIELDS
      DO 9 I=1,10
      S(I)=0.
      J1=JA(I)
      J2=J1+4
      DO 9 J=J1,J2,2
      JP=J+K(I)
      S(I)=S(I)+H(J,M)*H(JP,M)
    9 CONTINUE
      S(1)=S(1)-S(2)
      S(4)=S(4)-S(5)
      S(7)=S(7)+S(8)
      S(9)=S(9)-S(10)
      A=2.*SC*S(9)
      U(L,1,M)=CS*S(4)+SS*S(1)+A
      V(L,1,M)=2.*(CS*S(6)+SS*S(3)+SC*S(7))
      U(L,2,M)=SS*S(4)+CS*S(1)-A
      V(L,2,M)=2.*(SS*S(6)+CS*S(3)-SC*S(7))
      U(L,3,M)=SMC*S(9)+SC*(S(4)-S(1))
      V(L,3,M)=SMC*S(7)+2.*SC*(S(6)-S(3))
      U(L,4,M)=.5*(S(4)+S(1))
      V(L,4,M)=S(6)+S(3)
      U(L,5,M)=.5*(S(4)-S(1))-S(7)
      V(L,5,M)=S(6)-S(3)+S(9)
      IF(LAYR.EQ.MINL)GO TO 30
   10 IF(M.NE.1)GO TO 11
      AA=ROR(LAYR)-ROR(LM)
      IF(LM.GT.MINL)AB=ROR(LM)-ROR(LM-1)
      AC=12.566371*ROR(LM)/FN
      GO TO 30
   11 MQ=MM-1
   12 DO 25 I=1,5
      UA=U(LA,I,MM)
      VA=V(LA,I,MM)
      T=UA*UA+VA*VA
      A=0.
      IF(T.LT.THRESH)GO TO 18
      IF(LM.EQ.KRIT.AND.T.GT.1.)GO TO 18
*EFFECTIVE WAVENUMBER AND SPECTRUM FUNCTION
      IF(LAYR.GT.LAYERS)GO TO 15
      IF(LM.EQ.MINL)GO TO 14
```

```
      DUR=.5*((U(L,I,MM)-UA)/AA+(UA-U(LB,I,MM))/AB)
      DVR=.5*((V(L,I,MM)-VA)/AA+(VA-V(LB,I,MM))/AB)
      GO TO 16
   14 DUR=(U(L,I,MM)-UA)/AA
      DVR=(V(L,I,MM)-VA)/AA
      GO TO 16
   15 DUR=(UA-U(LB,I,MM))/AB
      DVR=(VA-V(LB,I,MM))/AB
   16 DUP=0.
      DVP=0.
      IF(MM.EQ.1.OR.M.EQ.MM)GO TO 17
      DUP=(U(LA,I,M)-U(LA,I,M1))/AC
      DVP=(V(LA,I,M)-V(LA,I,M1))/AC
   17 B=T+RM
      B=T2CS*((UA+DVR-VA+DU2)/B)**2+((UA+DVP-VA+DUP)/B)**2
      B=.1013212*B*RI*RI*PSI*ALOG(1.+B*RO*RO)
      IF(B.LT.EXA)A=T/EXP(B)
C     *ACCUMULATE AVERAGES
   18 IF(MM.EQ.1)GO TO 19
      IF(M.EQ.MM)GO TO 20
      FGS(LM,I)=FGS(LM,I)+A
      DEP(I)=DEP(I)+A*BDS(MM)
      GO TO 25
   19 FGS(LM,I)=.5*A
      DEP(I)=.5*A*BDS(1)
      GO TO 25
   20 FGS(LM,I)=F*(FGS(LM,I)+.5*A)
      DEP(I)=F*(DEP(I)+.5*A*BDS(MM))
   25 CONTINUE
   30 MM=M
      IF(LM.LT.MINL)RETURN
      WRITE(6,1000)LM,(FGS(LM,I),I=1,5),DEP
      FGS(LM,1)=FGS(LM,1)+DEP(3)
      FGS(LM,2)=FGS(LM,2)+DEP(3)
      FGS(LM,3)=FGS(LM,3)+.5*(DEP(1)+DEP(2))
      FGS(LM,4)=FGS(LM,4)+DEP(5)
      FGS(LM,5)=FGS(LM,5)+DEP(4)
      IF(LAYR.NE.LAYERS)RETURN
      LM=LAYERS
      LAYR=LAYERS+1
      GO TO 1
 1000 FORMAT(5X,I3,2X,1P3E13.4,2X,1P2E13.4,5X,1PE9.1)
      END
```

```
*      L)  NORMALIZED MOMENTS OF SCATTERING
       SUBROUTINE RINT(JM)
       COMMON/ABCKLW/ROR(50)
       COMMON/RBLW/CFM(50),EP(50)
       COMMON/RKL/FGS(50,5)
       COMMON/RLW/AM,S0(5),S1(5),S12(5),S2(5),VCM,VM(50),VP(50)
       DIMENSION S(5),T(5),U(5),V(5)
       DATA LAYERS/50/
       LM=LAYERS-1
*INITIALIZE
       BM=0.
       CM=0.
       DM=0.
       EM=0.
       DO 10 I=1,5
       S0(I)=0.
       S1(I)=0.
       S12(I)=0.
    10 S2(I)=0.
*INTEGRATE OVER 2PHP
       J=1
       JP=2
       A=ROR(1)*ROR(2)
       GO TO 14
    11 A=ROR(J)*(ROR(JP)-ROR(JQ))
       GO TO 14
    12 A=1.-ROR(LM)
    14 VC=VCM*CFM(J)
       B=A*EP(J)*EP(J)/(1.+VC*VC)
       BM=BM+B
       C=VM(J)*B
       CM=CM+C
       D=C*VM(J)
       DM=DM+D
       E=D*VP(J)*VP(J)
       EM=EM+E
       IF(J.LT.JM)GO TO 21
       DO 20 I=1,5
       F=FGS(J,I)
       S0(I)=S0(I)+B*F
       S1(I)=S1(I)+C*F
       S12(I)=S12(I)+D*F
    20 S2(I)=S2(I)+E*F
    21 JQ=J
       J=JP
       JP=J+1
       IF(J-LAYERS)11,12,22
    22 WRITE(6,1000)
       DO 25 I=1,5
       IF(S0(I).LT.0.)S0(I)=0.
```

```
      IF(S1(I).LT.0.)S1(I)=0.
      IF(S2(I).LT.0.)S2(I)=0.
      IF(S12(I).LT.0.)S12(I)=0.
      S(I)=S0(I)/BN
      T(I)=S1(I)/CN
      U(I)=S2(I)/EN
   25 V(I)=S12(I)/DN
      WRITE(6,2000)S,T,U,V
      DO 30 I=1,5
      S(I)=AN*S(I)
      T(I)=AN*T(I)
      U(I)=AN*U(I)
   30 V(I)=AN*V(I)
      WRITE(6,3000)S,T,U,V
      RETURN
 1000 FORMAT(1H1,5X,'MOMENTS OF THE SCATTERING SPECTRUM'//36X,'LINEAR PO
     1LARIZATION',23X,'CIRCULAR POLARIZATION'/5X,'NORMALIZED TO BORN'4X,
     2'VERTICAL',6X,'HORIZONTAL',5X,'ORTHOGONAL',11X,'PRINCIPAL',5X,
     3'ORTHOGONAL'//)
 2000 FORMAT(6X,'ZEROTH',9X,1P3E15.4,5X,1P2E15.4/6X,'FIRST',10X,
     11P3E15.4,5X,1P2E15.4/6X,'SECOND',9X,1P3E15.4,5X,1P2E15.4/
     26X,'FIRST SQUARED',2X,1P3E15.4,5X,1P2E15.4///)
 3000 FORMAT(5X'NORMALIZED TO BORN AT CRITICAL DENSITY FOR REFRACTION'//
     16X,'ZEROTH',9X,1P3E15.4,5X,1P2E15.4/6X,'FIRST',10X,
     21P3E15.4,5X,1P2E15.4/6X,'SECOND',9X,1P3E15.4,5X,1P2E15.4/
     36X,'FIRST SQUARED',2X,1P3E15.4,5X,1P2E15.4///)
      END
```

85

```
*      M)  CONVOLUTION FOR PULSE SHAPES
      SUBROUTINE ZINT(NZ,V)
      COMMON/RMW/DSDZ(5,20),DTDZ(5,20),DUDZ(5,20),RESM,ZM(20)
      DIMENSION P(19),S(5),T(5),U(5)
      DATA BBT/-300./,THRESH/1.E-30/
      DATA ISTAT/20/
      AA=.5
      BB=.5
      K=1
      KM=1
      IF(ABS(V).GT.1.E-5)GO TO 1
*SPECIAL REQUIREMENTS FOR NORMAL INCIDENCE
      IP=2
      Z=0.
      DZ=0.
      DELX=1.
      NPTS=1
      M=MAX0(1,NZ-1)
      P(1)=1.
```

```
      GO TO 8
    1 NPTS=ISTAT-1
      IF(NPTS.LT.19)NPTS=19
      FNPTS=NPTS+1
*COMPARE THE PULSE WIDTH WITH THE SCATTERING FUNCTION
      A=RESM/V
      B=ZM(1)
      C=ZM(NZ)
      IP=1
      IF(NZ.LT.2)GO TO 5
      TA=A+A
      D=C-B
      DZ=(D+TA)/FNPTS
      IF(D.GE.TA)GO TO 2
*PULSE WIDTH DOMINATES
      IP=0
      M=NPTS+1
      DELX=D/FLOAT(NPTS)
      XPO=B-DELX
      GO TO 7
*SCATTERING FUNCTION DOMINATES
    2 M=2*IFIX(.5*FLOAT(IFIX(TA*FNPTS/D)-1))+1
      REMP=1./FLOAT(M+1)
      DELX=TA*REMP
      XPO=-A
      IF(M.EQ.1)GO TO 6
      POM=3.1415927*REMP
      N=(M-1)/2
      DO 3 I=1,N
    3 P(I)=SIN(FLOAT(I)*POM)**2
      N=M+1
      P(N)=1.
      N=M+1
      DO 4 I=N,M
    4 P(I)=P(M+1-I)
      GO TO 7
    5 NPTS=1
      DELX=A
      DZ=A
      M=1
      XPO=B-A
    6 P(1)=1.
*CONVOLUTION INTEGRALS
    7 Z=B-A
      DD=.5*DELX
    8 WRITE (6,1000)
      LNS=1
      DO 30 I=1,NPTS
      Z=Z+DZ
      DO 9 J=1,5
      S(J)=0.
```

```
      T(J)=0.
    9 U(J)=0.
      XP=XP0
      DO 22 J=1,M
      IF(IP.LT.2.OR.NZ.LT.2)GO TO 10
      K=J+1
      KM=J
      PP=ZM(K)-ZM(KM)
      GO TO 15
   10 XP=XP+DELX
      XM=Z-XP
      IF(IP.EQ.0)GO TO 11
      PP=P(J)
      IF(NZ.LT.2)GO TO 15
      X=XM
      GO TO 12
   11 IF(ABS(XM).GE.A)GO TO 22
      PP=COS(3.1415927*XM/TA)**2
      X=XP
   12 IF(X.LT.B.OR.X.GT.C)GO TO 22
      K=2
   13 IF(X.LE.ZM(K).OR.K.EQ.NZ)GO TO 14
      K=K+1
      GO TO 13
   14 KM=K-1
      BB=(ZM(K)-X)/(ZM(K)-ZM(KM))
      AA=1.-BB
      XX=X-BB
      IF(XX.LT.B)PP=PP*(X+BB)/DELX
      XX=X+BB
      IF(XX.GT.C)PP=PP*(C-X+BB)/DELX
   15 DO 21 L=1,5
      II=0
      E=BSDZ(L,K)
      F=BSDZ(L,KM)
   16 II=II+1
      IF(E.LE.0..OR.F.LE.0.)GO TO 17
      G=E/F
      IF(G.GT..1.AND.G.LT.10.)GO TO 17
      G=PP*E**AA*F**BB
      GO TO 18
   17 G=PP*(E**AA*F**BB)
   18 GO TO(19,20,21),II
   19 S(L)=S(L)+G
      E=BTDZ(L,K)
      F=BTDZ(L,KM)
      GO TO 16
   20 T(L)=T(L)+G
      E=BUDZ(L,K)
      F=BUDZ(L,KM)
      GO TO 16
```

```
      21 U(L)=U(L)+G
      22 CONTINUE
         DO 25 L=1,5
         SL=98T
         TL=0.
         UL=0.
         S(L)=DELX*S(L)
         IF(S(L).LT.THRESH)GO TO 23
         SL=10.*ALOG10(S(L))
         TL=DELX*T(L)/S(L)
         R=DELX*U(L)/S(L)-TL*TL
         IF(R.GT.0.)UL=SQRT(R)
      23 S(L)=SL
         T(L)=TL
      25 U(L)=UL
         IF(LNS.LT.14)GO TO 28
         LNS=0
         WRITE(6,3000)
      28 LNS=LNS+1
      30 WRITE(6,2000)Z,S,T,U
         RETURN
    1000 FORMAT(1H1,5X,'SCATTERED PULSE SHAPE FUNCTIONS'//56X,'LINEAR POLAR
        1IZATION',23X,'CIRCULAR POLARIZATION'/5X,'AXIAL STATION (M)',25X,
        2'VERTICAL',6X,'HORIZONTAL',5X,'ORTHOGONAL',11X,'PRINCIPAL',5X,
        3'ORTHOGONAL')
    2000 FORMAT(/5X,F10.2,11X,'DBSM',9X,3F15.3,5X,2F15.3/12X,
        1'MEAN DOPPLER/BODY VELOCITY',3X,1P3E15.4,5X,1P2E15.4/11X,
        2'DOPPLER SPREAD/BODY VELOCITY',2X,1P3E15.4,5X,1P2E15.4)
    3000 FORMAT(1H1)
         END
```

APPENDIX B

EXAMPLE OF OUTPUT

CASE 1 THE CHARACTERS APPEARING ON THE INPUT TITLE CARD ARE WRITTEN WITHIN THESE SPACES

```
 NAMELIST   INPUT
 ASPECD=   0.30000000E 02,
 CPRO  (I)=
      1   0.10000000E 01,   0.10000000E 01,   0.,   0.,   0.,   0.,
      7   0.,   0.,   0.,   0.,   0.,   0.,
     13   0.,   0.,   0.,   0.,   0.,   0.,
     19   0.,   0.,   0.,   0.,   0.,   0.,
     25   0.,   0.,   0.,   0.,   0.,   0.,
     31   0.,   0.,   0.,   0.,   0.,   0.,
     37   0.,   0.,   0.,   0.,   0.,   0.,
     43   0.,   0.,   0.,   0.,   0.,   0.,
     49   0.,   0.,   0.,   0.,   0.,   0.,
     55   0.,   0.,   0.,   0.,   0.,   0.,
     61   0.,   0.,   0.,   0.,   0.,   0.,
     67   0.,   0.,   0.,   0.,   0.,   0.,
     73   0.,   0.,   0.,   0.,   0.,   0.,
     79   0.,   0.,   0.,   0.,   0.,   0.,
     85   0.,   0.,   0.,   0.,   0.,   0.,
     91   0.,   0.,   0.,   0.,   0.,   0.,
     97   0.,   0.,   0.,   0.,   0.,   0.,
    103   0.,   0.,   0.,   0.,   0.,   0.,
    109   0.,   0.,   0.,   0.,   0.,   0.,
    115   0.,   0.,   0.,   0.,   0.,   0.,
    121   0.,   0.,   0.,   0.,   0.,   0.,
    127   0.,   0.,   0.,   0.,   0.,   0.,
    133   0.,   0.,   0.,   0.,   0.,   0.,
    139   0.,   0.,   0.,   0.,   0.,   0.,
    145   0.,   0.,   0.,   0.,   0.,   0.,
    151   0.,   0.,   0.,   0.,   0.,   0.,
    157   0.,   0.,   0.,   0.,   0.,   0.,
    163   0.,   0.,   0.,   0.,   0.,   0.,
    169   0.,   0.,   0.,   0.,   0.,   0.,
    175   0.,   0.,   0.,   0.,   0.,   0.,
    181   0.,   0.,   0.,   0.,   0.,   0.,
    187   0.,   0.,   0.,   0.,   0.,   0.,
    193   0.,   0.,   0.,   0.,   0.,   0.,
    199   0.,   0.,   0.,   0.,   0.,   0.,
    205   0.,   0.,   0.,   0.,   0.,   0.,
    211   0.,   0.,   0.,   0.,   0.,   0.,
    217   0.,   0.,   0.,   0.,   0.,   0.,
    223   0.,   0.,   0.,   0.,   0.,   0.,
    229   0.,   0.,   0.,   0.,   0.,   0.,
    235   0.,   0.,   0.,   0.,   0.,   0.,
 CZPSEC(I)=
      1   0.10000000E 07,   0.10000000E 09,   0.10000000E 11,   0.,   0.,   0.,
      7   0.,   0.,   0.,   0.,   0.,   0.,
     13   0.,   0.,   0.,   0.,   0.,   0.,
     19   0.,   0.,
 EMPRO (I)=
      1   0.11000000E 02,   0.10000000E 01,   0.95100000E 00,   0.81900000E 00,   0.63800000E 00,   0.44900000E 00,
      7   0.28700000E 00,   0.16500000E 00,   0.86300000E-01,   0.40800000E-01,   0.17400000E-01,   0.67400000E-02,
     13   0.,   0.,   0.,   0.,   0.,   0.,
     19   0.,   0.,   0.,   0.,   0.,   0.,
     25   0.,   0.,   0.,   0.,   0.,   0.,
     31   0.,   0.,   0.,   0.,   0.,   0.,
     37   0.,   0.,   0.,   0.,   0.,   0.,
```

```
      43  0.          ,  0.          ,  0.          ,  0.          ,  0.          ,  0.          ,
      49  0.          ,  0.          ,  0.          ,  0.          ,  0.          ,  0.          ,
      55  0.          ,  0.          ,  0.          ,  0.          ,  0.          ,  0.          ,
      61  0.          ,  0.          ,  0.          ,  0.          ,  0.          ,  0.          ,
      67  0.          ,  0.          ,  0.          ,  0.          ,  0.          ,  0.          ,
      73  0.          ,  0.          ,  0.          ,  0.          ,  0.          ,  0.          ,
      79  0.          ,  0.          ,  0.          ,  0.          ,  0.          ,  0.          ,
      85  0.          ,  0.          ,  0.          ,  0.          ,  0.          ,  0.          ,
      91  0.          ,  0.          ,  0.          ,  0.          ,  0.          ,  0.          ,
      97  0.          ,  0.          ,  0.          ,  0.          ,  0.          ,  0.          ,
     103  0.          ,  0.          ,  0.          ,  0.          ,  0.          ,  0.          ,
     109  0.          ,  0.          ,  0.          ,  0.          ,  0.          ,  0.          ,
     115  0.          ,  0.          ,  0.          ,  0.          ,  0.          ,  0.          ,
     121  0.          ,  0.          ,  0.          ,  0.          ,  0.          ,  0.          ,
     127  0.          ,  0.          ,  0.          ,  0.          ,  0.          ,  0.          ,
     133  0.          ,  0.          ,  0.          ,  0.          ,  0.          ,  0.          ,
     139  0.          ,  0.          ,  0.          ,  0.          ,  0.          ,  0.          ,
     145  0.          ,  0.          ,  0.          ,  0.          ,  0.          ,  0.          ,
     151  0.          ,  0.          ,  0.          ,  0.          ,  0.          ,  0.          ,
     157  0.          ,  0.          ,  0.          ,  0.          ,  0.          ,  0.          ,
     163  0.          ,  0.          ,  0.          ,  0.          ,  0.          ,  0.          ,
     169  0.          ,  0.          ,  0.          ,  0.          ,  0.          ,  0.          ,
     175  0.          ,  0.          ,  0.          ,  0.          ,  0.          ,  0.          ,
     181  0.          ,  0.          ,  0.          ,  0.          ,  0.          ,  0.          ,
     187  0.          ,  0.          ,  0.          ,  0.          ,  0.          ,  0.          ,
     193  0.          ,  0.          ,  0.          ,  0.          ,  0.          ,  0.          ,
     199  0.          ,  0.          ,  0.          ,  0.          ,  0.          ,  0.          ,
     205  0.          ,  0.          ,  0.          ,  0.          ,  0.          ,  0.          ,
     211  0.          ,  0.          ,  0.          ,  0.          ,  0.          ,  0.          ,
     217  0.          ,  0.          ,  0.          ,  0.          ,  0.          ,  0.          ,
     223  0.          ,  0.          ,  0.          ,  0.          ,  0.          ,  0.          ,
     229  0.          ,  0.          ,  0.          ,  0.          ,  0.          ,  0.          ,
     235  0.          ,  0.          ,  0.          ,  0.          ,  0.          ,  0.          ,
EMZPCC(I)=
       1  0.10000000E 12,  0.10000000E 08,  0.10000000E 04,  0.          ,  0.          ,  0.          ,
       7  0.          ,  0.          ,  0.          ,  0.          ,  0.          ,  0.          ,
      13  0.          ,  0.          ,  0.          ,  0.          ,  0.          ,  0.          ,
      19  0.          ,  0.          ,
EPPRO (I)=
       1 -0.30000000E 01,  0.10000000E 01,  0.50000000E 00,  0.          , -0.50000000E 01,  0.80000000E 00,
       7  0.20000000E 00,  0.12000000E 01,  0.40000000E 00,  0.30000000E 00,  0.11000000E 02,  0.10000000E 01,
      13  0.98000000E 00,  0.92300000E 00,  0.83500000E 00,  0.72600000E 00,  0.60700000E 00,  0.48700000E 00,
      19  0.37500000E 00,  0.27800000E 00,  0.19800000E 00,  0.13500000E 00,  0.          ,  0.          ,
      25  0.          ,  0.          ,  0.          ,  0.          ,  0.          ,  0.          ,
      31  0.          ,  0.          ,  0.          ,  0.          ,  0.          ,  0.          ,
      37  0.          ,  0.          ,  0.          ,  0.          ,  0.          ,  0.          ,
      43  0.          ,  0.          ,  0.          ,  0.          ,  0.          ,  0.          ,
      49  0.          ,  0.          ,  0.          ,  0.          ,  0.          ,  0.          ,
      55  0.          ,  0.          ,  0.          ,  0.          ,  0.          ,  0.          ,
      61  0.          ,  0.          ,  0.          ,  0.          ,  0.          ,  0.          ,
      67  0.          ,  0.          ,  0.          ,  0.          ,  0.          ,  0.          ,
      73  0.          ,  0.          ,  0.          ,  0.          ,  0.          ,  0.          ,
      79  0.          ,  0.          ,  0.          ,  0.          ,  0.          ,  0.          ,
      85  0.          ,  0.          ,  0.          ,  0.          ,  0.          ,  0.          ,
      91  0.          ,  0.          ,  0.          ,  0.          ,  0.          ,  0.          ,
      97  0.          ,  0.          ,  0.          ,  0.          ,  0.          ,  0.          ,
     103  0.          ,  0.          ,  0.          ,  0.          ,  0.          ,  0.          ,
     109  0.          ,  0.          ,  0.          ,  0.          ,  0.          ,  0.          ,
     115  0.          ,  0.          ,  0.          ,  0.          ,  0.          ,  0.          ,
     121  0.          ,  0.          ,  0.          ,  0.          ,  0.          ,  0.          ,
     127  0.          ,  0.          ,  0.          ,  0.          ,  0.          ,  0.          ,
```

```
      133  0.          ,  0.          ,  0.          ,  0.          ,  0.          ,  0.          ,
      139  0.          ,  0.          ,  0.          ,  0.          ,  0.          ,  0.          ,
      145  0.          ,  0.          ,  0.          ,  0.          ,  0.          ,  0.          ,
      151  0.          ,  0.          ,  0.          ,  0.          ,  0.          ,  0.          ,
      157  0.          ,  0.          ,  0.          ,  0.          ,  0.          ,  0.          ,
      163  0.          ,  0.          ,  0.          ,  0.          ,  0.          ,  0.          ,
      169  0.          ,  0.          ,  0.          ,  0.          ,  0.          ,  0.          ,
      175  0.          ,  0.          ,  0.          ,  0.          ,  0.          ,  0.          ,
      181  0.          ,  0.          ,  0.          ,  0.          ,  0.          ,  0.          ,
      187  0.          ,  0.          ,  0.          ,  0.          ,  0.          ,  0.          ,
      193  0.          ,  0.          ,  0.          ,  0.          ,  0.          ,  0.          ,
      199  0.          ,  0.          ,  0.          ,  0.          ,  0.          ,  0.          ,
      205  0.          ,  0.          ,  0.          ,  0.          ,  0.          ,  0.          ,
      211  0.          ,  0.          ,  0.          ,  0.          ,  0.          ,  0.          ,
      217  0.          ,  0.          ,  0.          ,  0.          ,  0.          ,  0.          ,
      223  0.          ,  0.          ,  0.          ,  0.          ,  0.          ,  0.          ,
      229  0.          ,  0.          ,  0.          ,  0.          ,  0.          ,  0.          ,
      235  0.          ,  0.          ,  0.          ,  0.          ,  0.          ,  0.          ,
 FMHZ  =  0.10000000E 04,
 KASES =          1,
 MUTZ  (I)=
        1          2,          2,          2,          2,          2,          2,          2,          2,
        9          2,          2,          2,          2,          2,          2,          2,          2,
       17          2,          2,          2,          2,
 NZ    =          3,
 POLAD =  0.90000000E 02,     RESM  =  0.10000000E 02,
 RZM   (I)=
        1  0.50000000E-01,  0.50000000E-01,  0.50000000E-01,  0.          ,  0.          ,  0.          ,
        7  0.          ,  0.          ,  0.          ,  0.          ,  0.          ,  0.          ,
       13  0.          ,  0.          ,  0.          ,  0.          ,  0.          ,  0.          ,
       19  0.          ,  0.          ,
 SIZM  (I)=
        1  0.10000000E-03,  0.10000000E-03,  0.10000000E-03,  0.          ,  0.          ,  0.          ,
        7  0.          ,  0.          ,  0.          ,  0.          ,  0.          ,  0.          ,
       13  0.          ,  0.          ,  0.          ,  0.          ,  0.          ,  0.          ,
       19  0.          ,  0.          ,
 SOZM  (I)=
        1  0.10000000E-01,  0.10000000E-01,  0.10000000E-01,  0.          ,  0.          ,  0.          ,
        7  0.          ,  0.          ,  0.          ,  0.          ,  0.          ,  0.          ,
       13  0.          ,  0.          ,  0.          ,  0.          ,  0.          ,  0.          ,
       19  0.          ,  0.          ,
 VMPRO (I)=
        1  0.20000000E 01,  0.10000000E 01,  0.10000000E 00,  0.          ,  0.11000000E 02,  0.10000000E 01,
        7  0.98000000E 00,  0.92300000E 00,  0.83500000E 00,  0.72600000E 00,  0.60700000E 00,  0.48700000E 00,
       13  0.37500000E 00,  0.27800000E 00,  0.19800000E 00,  0.13500000E 00,  0.          ,  0.          ,
       19  0.          ,  0.          ,  0.          ,  0.          ,  0.          ,  0.          ,
       25  0.          ,  0.          ,  0.          ,  0.          ,  0.          ,  0.          ,
       31  0.          ,  0.          ,  0.          ,  0.          ,  0.          ,  0.          ,
       37  0.          ,  0.          ,  0.          ,  0.          ,  0.          ,  0.          ,
       43  0.          ,  0.          ,  0.          ,  0.          ,  0.          ,  0.          ,
       49  0.          ,  0.          ,  0.          ,  0.          ,  0.          ,  0.          ,
       55  0.          ,  0.          ,  0.          ,  0.          ,  0.          ,  0.          ,
       61  0.          ,  0.          ,  0.          ,  0.          ,  0.          ,  0.          ,
       67  0.          ,  0.          ,  0.          ,  0.          ,  0.          ,  0.          ,
       73  0.          ,  0.          ,  0.          ,  0.          ,  0.          ,  0.          ,
       79  0.          ,  0.          ,  0.          ,  0.          ,  0.          ,  0.          ,
       85  0.          ,  0.          ,  0.          ,  0.          ,  0.          ,  0.          ,
       91  0.          ,  0.          ,  0.          ,  0.          ,  0.          ,  0.          ,
       97  0.          ,  0.          ,  0.          ,  0.          ,  0.          ,  0.          ,
      103  0.          ,  0.          ,  0.          ,  0.          ,  0.          ,  0.          ,
      109  0.          ,  0.          ,  0.          ,  0.          ,  0.          ,  0.          ,
```

115	0.,	0.,	0.,	0.,	0.,	0.,
121	0.,	0.,	0.,	0.,	0.,	0.,
127	0.,	0.,	0.,	0.,	0.,	0.,
133	0.,	0.,	0.,	0.,	0.,	0.,
139	0.,	0.,	0.,	0.,	0.,	0.,
145	0.,	0.,	0.,	0.,	0.,	0.,
151	0.,	0.,	0.,	0.,	0.,	0.,
157	0.,	0.,	0.,	0.,	0.,	0.,
163	0.,	0.,	0.,	0.,	0.,	0.,
169	0.,	0.,	0.,	0.,	0.,	0.,
175	0.,	0.,	0.,	0.,	0.,	0.,
181	0.,	0.,	0.,	0.,	0.,	0.,
187	0.,	0.,	0.,	0.,	0.,	0.,
193	0.,	0.,	0.,	0.,	0.,	0.,
199	0.,	0.,	0.,	0.,	0.,	0.,
205	0.,	0.,	0.,	0.,	0.,	0.,
211	0.,	0.,	0.,	0.,	0.,	0.,
217	0.,	0.,	0.,	0.,	0.,	0.,
223	0.,	0.,	0.,	0.,	0.,	0.,
229	0.,	0.,	0.,	0.,	0.,	0.,
235	0.,	0.,	0.,	0.,	0.,	0.,

VPPRO (I)=

1	0.20000000E 01,	0.10000000E 00,	0.10000000E-01,	0.,	0.11000000E 02,	0.10000000E 00,
7	0.98500000E-01,	0.94200000E-01,	0.87400000E-01,	0.78700000E-01,	0.68700000E-01,	0.58300000E-01,
13	0.48000000E-01,	0.38300000E-01,	0.29700000E-01,	0.22300000E-01,	0.,	0.,
19	0.,	0.,	0.,	0.,	0.,	0.,
25	0.,	0.,	0.,	0.,	0.,	0.,
31	0.,	0.,	0.,	0.,	0.,	0.,
37	0.,	0.,	0.,	0.,	0.,	0.,
43	0.,	0.,	0.,	0.,	0.,	0.,
49	0.,	0.,	0.,	0.,	0.,	0.,
55	0.,	0.,	0.,	0.,	0.,	0.,
61	0.,	0.,	0.,	0.,	0.,	0.,
67	0.,	0.,	0.,	0.,	0.,	0.,
73	0.,	0.,	0.,	0.,	0.,	0.,
79	0.,	0.,	0.,	0.,	0.,	0.,
85	0.,	0.,	0.,	0.,	0.,	0.,
91	0.,	0.,	0.,	0.,	0.,	0.,
97	0.,	0.,	0.,	0.,	0.,	0.,
103	0.,	0.,	0.,	0.,	0.,	0.,
109	0.,	0.,	0.,	0.,	0.,	0.,
115	0.,	0.,	0.,	0.,	0.,	0.,
121	0.,	0.,	0.,	0.,	0.,	0.,
127	0.,	0.,	0.,	0.,	0.,	0.,
133	0.,	0.,	0.,	0.,	0.,	0.,
139	0.,	0.,	0.,	0.,	0.,	0.,
145	0.,	0.,	0.,	0.,	0.,	0.,
151	0.,	0.,	0.,	0.,	0.,	0.,
157	0.,	0.,	0.,	0.,	0.,	0.,
163	0.,	0.,	0.,	0.,	0.,	0.,
169	0.,	0.,	0.,	0.,	0.,	0.,
175	0.,	0.,	0.,	0.,	0.,	0.,
181	0.,	0.,	0.,	0.,	0.,	0.,
187	0.,	0.,	0.,	0.,	0.,	0.,
193	0.,	0.,	0.,	0.,	0.,	0.,
199	0.,	0.,	0.,	0.,	0.,	0.,
205	0.,	0.,	0.,	0.,	0.,	0.,
211	0.,	0.,	0.,	0.,	0.,	0.,
217	0.,	0.,	0.,	0.,	0.,	0.,
223	0.,	0.,	0.,	0.,	0.,	0.,
229	0.,	0.,	0.,	0.,	0.,	0.,

```
      235   0.          ,  0.          ,  0.          ,  0.          ,  0.          ,  0.          ,
 VVBZ  (I)=
        1   0.10000000E 00,  0.10000000E 00,  0.10000000E 00,  0.          ,  0.          ,  0.          ,
        7   0.          ,  0.          ,  0.          ,  0.          ,  0.          ,  0.          ,
       13   0.          ,  0.          ,  0.          ,  0.          ,  0.          ,  0.          ,
       19   0.          ,  0.          ,
 ZM    (I)=
        1   0.          ,  0.10000000E 03,  0.20000000E 03,  0.          ,  0.          ,  0.          ,
        7   0.          ,  0.          ,  0.          ,  0.          ,  0.          ,  0.          ,
       13   0.          ,  0.          ,  0.          ,  0.          ,  0.          ,  0.          ,
       19   0.          ,  0.          ,
 $ END
```

AXIAL STATION (M) = 0. MEAN ELECTRON DENSITY/CRITICAL = 8.06115E 00 CHANGED TO 7.89034E 00 KRW = 1.048E 00

(SIN ALPHA)**2 = 2.50000E-01 CHANGED TO 2.42739E-01 NU/OMEGA = 1.59155E-04 MEAN VELOCITY/BODY VELOCITY = 1.000E-01

PROFILE FUNCTIONS**

	RELATIVE RADIUS	ELECTRON DENSITY MEAN (LAYER)	ELECTRON DENSITY MEAN (MESH PT.)	ELECTRON DENSITY RMS FLUCTUATION	COLLISION FREQUENCY LAYER	COLLISION FREQUENCY MESH PT.	ALLOWANCE FOR ATTENUATION SCATTERING ELECTRONS	ALLOWANCE FOR ATTENUATION COLLISIONS	VELOCITY MEAN	VELOCITY RMS FLUCTUATION
1	0.0210	1.0047E 00	1.0045E 00	1.0000E 00	1.0000E 00	1.0000E 00	3.1664E-02	1.0287E 03	9.8106E-01	9.8106E-02
2	0.0271	1.0041E 00	1.0035E 00	1.0000E 00	1.0000E 00	1.0000E 00	3.1654E-02	1.0283E 03	9.7565E-01	9.7565E-02
3	0.0348	1.0023E 00	1.0010E 00	1.0000E 00	1.0000E 00	1.0000E 00	3.1640E-02	1.0278E 03	9.6871E-01	9.6871E-02
4	0.0447	9.9872E-01	9.9634E-01	1.0000E 00	1.0000E 00	1.0000E 00	3.1623E-02	1.0271E 03	9.5978E-01	9.5978E-02
5	0.0574	9.9233E-01	9.8834E-01	1.0000E 00	1.0000E 00	1.0000E 00	3.1600E-02	1.0262E 03	9.4831E-01	9.4831E-02
6	0.0738	9.8187E-01	9.7561E-01	1.0000E 00	1.0000E 00	1.0000E 00	3.1571E-02	1.0251E 03	9.3357E-01	9.3357E-02
7	0.0949	9.6567E-01	9.5619E-01	1.0000E 00	1.0000E 00	1.0000E 00	3.1533E-02	1.0236E 03	9.1463E-01	9.1463E-02
8	0.1159	9.4485E-01	9.3395E-01	1.0000E 00	1.0000E 00	1.0000E 00	3.1495E-02	1.0221E 03	8.9568E-01	8.9568E-02
9	0.1370	9.2133E-01	9.0909E-01	1.0000E 00	1.0000E 00	1.0000E 00	3.1457E-02	1.0205E 03	8.7674E-01	8.7674E-02
10	0.1580	8.9520E-01	8.8162E-01	1.0000E 00	1.0000E 00	1.0000E 00	3.1417E-02	1.0190E 03	8.5779E-01	8.5779E-02
11	0.1791	8.6642E-01	8.5150E-01	1.0000E 00	1.0000E 00	1.0000E 00	3.1376E-02	1.0174E 03	8.3885E-01	8.3885E-02
12	0.2001	8.3502E-01	8.1883E-01	1.0000E 00	1.0000E 00	1.0000E 00	3.1338E-02	1.0159E 03	8.1990E-01	8.1990E-02
13	0.2212	8.0115E-01	7.8379E-01	1.0000E 00	1.0000E 00	1.0000E 00	3.1298E-02	1.0143E 03	8.0096E-01	8.0096E-02
14	0.2422	7.6506E-01	7.4672E-01	1.0000E 00	1.0000E 00	1.0000E 00	3.1257E-02	1.0127E 03	7.8201E-01	7.8201E-02
15	0.2633	7.2714E-01	7.0802E-01	1.0000E 00	1.0000E 00	1.0000E 00	3.1215E-02	1.0110E 03	7.6307E-01	7.6307E-02
16	0.2843	6.8782E-01	6.6817E-01	1.0000E 00	1.0000E 00	1.0000E 00	3.1174E-02	1.0094E 03	7.4412E-01	7.4412E-02
17	0.3054	6.4760E-01	6.2766E-01	1.0000E 00	1.0000E 00	1.0000E 00	3.1131E-02	1.0077E 03	7.2518E-01	7.2518E-02
18	0.3264	6.0697E-01	5.8697E-01	1.0000E 00	1.0000E 00	1.0000E 00	3.1089E-02	1.0060E 03	7.0624E-01	7.0624E-02
19	0.3475	5.6638E-01	5.4653E-01	1.0000E 00	1.0000E 00	1.0000E 00	3.1045E-02	1.0043E 03	6.8729E-01	6.8729E-02
20	0.3685	5.2623E-01	5.0672E-01	1.0000E 00	1.0000E 00	1.0000E 00	3.1001E-02	1.0026E 03	6.6835E-01	6.6835E-02
21	0.3896	4.8688E-01	4.6786E-01	1.0000E 00	1.0000E 00	1.0000E 00	3.0957E-02	1.0009E 03	6.4940E-01	6.4940E-02
22	0.4106	4.4861E-01	4.3018E-01	1.0000E 00	1.0000E 00	1.0000E 00	3.0912E-02	9.9913E 02	6.3046E-01	6.3046E-02
23	0.4317	4.1162E-01	3.9388E-01	1.0000E 00	1.0000E 00	1.0000E 00	3.0867E-02	9.9735E 02	6.1151E-01	6.1151E-02
24	0.4527	3.7609E-01	3.5910E-01	1.0000E 00	1.0000E 00	1.0000E 00	3.0821E-02	9.9555E 02	5.9257E-01	5.9257E-02
25	0.4738	3.4213E-01	3.2594E-01	1.0000E 00	1.0000E 00	1.0000E 00	3.0775E-02	9.9373E 02	5.7362E-01	5.7362E-02
26	0.4948	3.0983E-01	2.9449E-01	1.0000E 00	1.0000E 00	1.0000E 00	3.0727E-02	9.9189E 02	5.5468E-01	5.5468E-02
27	0.5159	2.7927E-01	2.6482E-01	0.	1.0000E 00	1.0000E 00	0.	0.	5.3573E-01	5.3573E-02
28	0.5369	2.5052E-01	2.3697E-01	0.	1.0000E 00	1.0000E 00	0.	0.	5.1679E-01	5.1679E-02
29	0.5580	2.2363E-01	2.1102E-01	0.	1.0000E 00	1.0000E 00	0.	0.	4.9784E-01	4.9784E-02
30	0.5790	1.9866E-01	1.8700E-01	0.	1.0000E 00	1.0000E 00	0.	0.	4.7890E-01	4.7890E-02
31	0.6001	1.7563E-01	1.6495E-01	0.	1.0000E 00	1.0000E 00	0.	0.	4.5995E-01	4.5995E-02
32	0.6211	1.5457E-01	1.4487E-01	0.	1.0000E 00	1.0000E 00	0.	0.	4.4101E-01	4.4101E-02
33	0.6422	1.3549E-01	1.2674E-01	0.	1.0000E 00	1.0000E 00	0.	0.	4.2206E-01	4.2206E-02
34	0.6632	1.1832E-01	1.1050E-01	0.	1.0000E 00	1.0000E 00	0.	0.	4.0312E-01	4.0312E-02
35	0.6843	1.0300E-01	9.6038E-02	0.	1.0000E 00	1.0000E 00	0.	0.	3.8417E-01	3.8417E-02
36	0.7053	8.9384E-02	8.3214E-02	0.	1.0000E 00	1.0000E 00	0.	0.	3.6523E-01	3.6523E-02
37	0.7264	7.7319E-02	7.1845E-02	0.	1.0000E 00	1.0000E 00	0.	0.	3.4628E-01	3.4628E-02
38	0.7474	6.6608E-02	6.1732E-02	0.	1.0000E 00	1.0000E 00	0.	0.	3.2734E-01	3.2734E-02
39	0.7685	5.7054E-02	5.2683E-02	0.	1.0000E 00	1.0000E 00	0.	0.	3.0839E-01	3.0839E-02
40	0.7895	4.8481E-02	4.4547E-02	0.	1.0000E 00	1.0000E 00	0.	0.	2.8945E-01	2.8945E-02
41	0.8106	4.0767E-02	3.7237E-02	0.	1.0000E 00	1.0000E 00	0.	0.	2.7050E-01	2.7050E-02
42	0.8316	3.3871E-02	3.0764E-02	0.	1.0000E 00	1.0000E 00	0.	0.	2.5156E-01	2.5156E-02
43	0.8527	2.7856E-02	2.5243E-02	0.	1.0000E 00	1.0000E 00	0.	0.	2.3261E-01	2.3261E-02
44	0.8737	2.2889E-02	2.0881E-02	0.	1.0000E 00	1.0000E 00	0.	0.	2.1367E-01	2.1367E-02
45	0.8948	1.9199E-02	1.7906E-02	0.	1.0000E 00	1.0000E 00	0.	0.	1.9472E-01	1.9472E-02
46	0.9158	1.6983E-02	1.6439E-02	0.	1.0000E 00	1.0000E 00	0.	0.	1.7578E-01	1.7578E-02
47	0.9369	1.6222E-02	1.6252E-02	0.	1.0000E 00	1.0000E 00	0.	0.	1.5683E-01	1.5683E-02
48	0.9579	1.6385E-02	1.6398E-02	0.	1.0000E 00	1.0000E 00	0.	0.	1.3789E-01	1.3789E-02
49	0.9790	1.5968E-02	1.4656E-02	0.	1.0000E 00	1.0000E 00	0.	0.	1.1894E-01	1.1894E-02
50	1.0000	1.1826E-02	6.7400E-03	0.	1.0000E 00	1.0000E 00	0.	0.	1.0000E-01	1.0000E-02

MEAN WAKE FIELD

SCATTERING COEFFICIENTS

MODE	PARALLEL POLARIZATION ELECTRIC		PARALLEL POLARIZATION MAGNETIC		TRANSVERSE POLARIZATION ELECTRIC		TRANSVERSE POLARIZATION MAGNETIC		LAYERS USED
0	-2.3822E-01	-8.3637E-01	0.	0.	0.	0.	-3.1254E-03	-5.7538E-02	50
1	-3.0094E 00	7.3143E-02	1.2205E-01	3.6154E 00	-1.2205E-01	-3.6154E 00	-4.3457E 00	1.4063E-01	50
2	-2.6323E-02	1.0621E-01	1.2419E-01	3.0608E-02	-1.2419E-01	-3.0608E-02	-3.5596E-02	1.4492E-01	50
3	-8.2374E-05	4.2141E-04	4.8959E-04	9.5181E-05	-4.8959E-04	-9.5181E-05	-1.0999E-04	5.6768E-04	50
4	-1.8580E-07	6.3819E-07	7.4258E-07	2.1423E-07	-7.4258E-07	-2.1423E-07	-2.4701E-07	8.6102E-07	50
5	-2.5414E-10	-5.2728E-10	-5.9468E-10	2.9271E-10	5.9470E-10	-2.9271E-10	-3.3713E-10	-6.7601E-10	50

SCATTERING FROM MEAN WAKE PLASMA

AZIMUTHAL ANGLE		2*PI*(R*SCATTERED POWER (DB)				
		LINEAR POLARIZATION			CIRCULAR POLARIZATION	
NUMBER	DEGREES	PARALLEL	TRANSVERSE	ORTHOGONAL	PRINCIPAL	ORTHOGONAL
0	0.	10.473	12.850	-300.000	11.676	-2.974
1	11.250	10.324	12.677	-2.845	11.667	-3.117
2	22.500	9.870	12.143	2.995	11.642	-3.549
3	33.750	9.088	11.203	6.215	11.601	-4.272
4	45.000	7.934	9.760	8.285	11.547	-5.277
5	56.250	6.345	7.619	9.663	11.485	-6.498
6	67.500	4.251	4.320	10.547	11.416	-7.717
7	78.750	1.728	-1.573	11.033	11.346	-8.446
8	90.000	-0.299	-13.763	11.168	11.278	-8.185
9	101.250	0.166	-0.874	10.967	11.215	-7.059
10	112.500	2.431	4.601	10.419	11.159	-5.631
11	123.750	4.662	. 20	9.478	11.111	-4.287
12	135.000	6.394	9 '53	8.049	11.073	-3.172
13	146.250	7.645	11.123	5.938	11.045	-2.316
14	157.500	8.485	12.014	2.687	11.025	-1.717
15	168.750	8.970	12.520	-3.172	11.013	-1.363
16	180.000	9.128	12.684	-300.000	11.009	-1.246

SQUARE ROOT OF (2*PI*KR) TIMES THE COMPLEX FORWARD SCATTERED FIELD

PARALLEL -2.7794E 00 , 1.8508E 00

TRANSVERSE -2.9387E 00 , 3.2620E 00

PROFILES OF WEIGHTED AVERAGES OF SQUARES OF SCALAR PRODUCTS OF ELECTRIC FIELDS

	LINEAR POLARIZATION			CIRCULAR POLARIZATION		DEPOLARIZATION FACTORS				
	VERTICAL	HORIZONTAL	ORTHOGONAL	PRINCIPAL	ORTHOGONAL					
1	2.7816E-02	2.6604E-03	1.1156E-05	1.4057E-02	1.0160E-03	2.8E-03	2.6E-04	1.1E-06	1.4E-03	1.0E-04
2	2.7922E-02	2.7442E-03	1.8441E-05	1.4128E-02	1.0202E-03	2.8E-03	2.8E-04	1.9E-06	1.4E-03	1.0E-04
3	2.8142E-02	2.8937E-03	2.9647E-05	1.4274E-02	1.0327E-03	2.9E-03	3.0E-04	3.2E-06	1.5E-03	1.1E-04
4	2.8550E-02	3.1502E-03	4.8542E-05	1.4544E-02	1.0665E-03	3.0E-03	3.4E-04	5.3E-06	1.5E-03	1.1E-04
5	2.9260E-02	3.5772E-03	8.0613E-05	1.5012E-02	1.1347E-03	3.1E-03	4.0E-04	8.9E-06	1.6E-03	1.2E-04
6	3.0454E-02	4.2729E-03	1.3542E-04	1.5801E-02	1.2590E-03	3.3E-03	5.1E-04	1.5E-05	1.8E-03	1.3E-04
7	3.2455E-02	5.3991E-03	2.3018E-04	1.7127E-02	1.4793E-03	3.6E-03	6.7E-04	2.6E-05	2.0E-03	1.5E-04
8	3.5033E-02	6.8087E-03	3.5361E-04	1.8852E-02	1.7750E-03	4.0E-03	8.7E-04	4.0E-05	2.2E-03	1.7E-04
9	3.8318E-02	8.5630E-03	5.0780E-04	2.1070E-02	2.1639E-03	4.5E-03	1.2E-03	5.9E-05	2.6E-03	2.0E-04
10	4.2510E-02	1.0773E-02	6.9435E-04	2.3924E-02	2.6595E-03	5.1E-03	1.5E-03	8.0E-05	3.1E-03	2.5E-04
11	4.7897E-02	1.3604E-02	9.1417E-04	2.7619E-02	3.3180E-03	5.7E-03	1.9E-03	1.0E-04	3.6E-03	3.0E-04
12	5.4889E-02	1.7286E-02	1.1669E-03	3.2443E-02	4.1304E-03	6.6E-03	2.5E-03	1.3E-04	4.3E-03	3.6E-04
13	6.4062E-02	2.2095E-02	1.4500E-03	3.8798E-02	5.1113E-03	8.1E-03	3.4E-03	1.7E-04	5.4E-03	4.4E-04
14	7.6248E-02	2.8351E-02	1.7586E-03	4.7257E-02	6.2414E-03	9.8E-03	4.5E-03	2.1E-04	6.8E-03	5.3E-04
15	9.2661E-02	3.6481E-02	2.0874E-03	5.8651E-02	7.4675E-03	1.2E-02	5.7E-03	2.6E-04	8.4E-03	6.4E-04
16	1.1511E-01	4.7199E-02	2.4449E-03	7.4201E-02	8.7158E-03	1.5E-02	7.5E-03	3.2E-04	1.1E-02	7.4E-04
17	1.4632E-01	6.1731E-02	2.9052E-03	9.5743E-02	9.9497E-03	1.9E-02	1.0E-02	4.3E-04	1.4E-02	8.7E-04
18	1.9055E-01	8.2044E-02	3.7073E-03	1.2608E-01	1.1244E-02	2.6E-02	1.4E-02	6.0E-04	1.9E-02	1.1E-03
19	2.5449E-01	1.1115E-01	5.2936E-03	1.6960E-01	1.2927E-02	3.5E-02	1.9E-02	9.3E-04	2.6E-02	1.4E-03
20	3.4903E-01	1.5369E-01	8.2778E-03	2.3326E-01	1.5790E-02	4.8E-02	2.7E-02	1.5E-03	3.6E-02	1.9E-03
21	4.9223E-01	2.1725E-01	1.3664E-02	3.2842E-01	2.1477E-02	6.7E-02	3.8E-02	2.6E-03	5.0E-02	2.8E-03
22	7.1487E-01	3.1466E-01	2.3368E-02	4.7405E-01	3.3271E-02	9.7E-02	5.4E-02	4.3E-03	7.1E-02	4.8E-03
23	1.0708E 00	4.6856E-01	4.1254E-02	7.0256E-01	5.7560E-02	1.4E-01	8.1E-02	7.4E-03	1.0E-01	8.1E-03
24	1.6561E 00	7.2046E-01	7.6179E-02	1.0705E 00	1.0758E-01	2.2E-01	1.3E-01	1.5E-02	1.6E-01	1.5E-02
25	2.6438E 00	1.1490E 00	1.5143E-01	1.6772E 00	2.1328E-01	3.3E-01	2.0E-01	2.6E-02	2.4E-01	2.8E-02
26	1.5188E-01	8.2889E-02	3.9280E-04	2.4026E-02	9.9796E-04	2.4E-02	1.1E-02	6.9E-05	4.0E-03	1.4E-04
27	4.9159E 00	1.8485E 00	8.3032E-01	2.3933E 00	9.4198E-01	5.9E-01	3.3E-01	1.2E-01	3.4E-01	1.4E-01
28	4.1833E 01	1.7890E 01	5.0935E 00	2.3110E 01	6.8094E 00	4.2E 00	2.8E 00	6.9E-01	2.8E 00	6.9E-01
29	1.1548E 02	4.9253E 01	1.6785E 01	6.1464E 01	2.1852E 01	9.1E 00	7.6E 00	2.0E 00	6.6E 00	1.9E 00
30	4.1214E 02	1.7523E 02	6.8733E 01	2.1172E 02	8.9036E 01	2.5E 01	2.7E 01	8.1E 00	2.0E 01	6.6E 00
31	2.3301E 03	9.9057E 02	4.2628E 02	1.1676E 03	5.5736E 02	1.2E 02	1.4E 02	4.7E 01	1.0E 02	3.9E 01
32	1.3697E 00	0.	5.8785E-16	0.	0.	2.7E-01	0.	7.9E-17	0.	0.
33	0.	0.	0.	0.	0.	0.	0.	0.	0.	0.
34	1.0233E 00	0.	1.7592E-07	1.6789E-04	9.5986E-19	2.0E-01	0.	0.	1.1E-06	0.
35	3.3813E 03	1.4275E 03	6.7043E 02	1.6355E 03	9.7735E 02	1.0E 02	2.1E 02	6.5E 01	1.2E 02	5.8E 01
36	7.0333E 02	2.9821E 02	1.3477E 02	3.4476E 02	2.0548E 02	1.7E 01	4.1E 01	1.2E 01	2.2E 01	1.1E 01
37	2.3153E 02	9.8125E 01	4.3231E 01	1.1445E 02	6.7998E 01	6.2E 00	1.4E 01	4.3E 00	8.1E 00	3.9E 00
38	9.7639E 01	4.1290E 01	1.7889E 01	4.8494E 01	2.8946E 01	2.3E 00	5.9E 00	1.6E 00	3.2E 00	1.6E 00
39	4.7975E 01	2.0224E 01	8.6769E 00	2.3868E 01	1.4419E 01	8.6E-01	3.1E 00	8.1E-01	1.6E 00	7.7E-01
40	2.6136E 01	1.0977E 01	4.6931E 00	1.2992E 01	7.9931E 00	4.1E-01	1.8E 00	4.4E-01	8.6E-01	4.4E-01
41	1.5366E 01	6.4294E 00	2.7577E 00	7.6156E 00	4.7984E 00	1.9E-01	9.6E-01	2.2E-01	4.3E-01	2.3E-01
42	9.6210E 00	4.0129E 00	1.7400E 00	4.7446E 00	3.0822E 00	1.3E-01	6.6E-01	1.6E-01	3.0E-01	1.7E-01
43	6.3951E 00	2.6654E 00	1.1761E 00	3.1312E 00	2.1115E 00	6.8E-02	4.3E-01	9.1E-02	1.8E-01	1.1E-01
44	4.5288E 00	1.8983E 00	8.5358E-01	2.1965E 00	1.5447E 00	5.4E-02	3.3E-01	7.4E-02	1.4E-01	8.7E-02
45	3.4381E 00	1.4602E 00	6.6722E-01	1.6485E 00	1.2114E 00	3.1E-02	2.7E-01	5.5E-02	1.1E-01	6.8E-02
46	2.8029E 00	1.2093E 00	5.6045E-01	1.3278E 00	1.0194E 00	2.3E-02	2.0E-01	4.0E-02	7.6E-02	5.2E-02
47	2.4213E 00	1.0604E 00	4.9752E-01	1.1353E 00	9.0913E-01	2.1E-02	1.8E-01	3.7E-02	6.9E-02	4.9E-02
48	2.1174E 00	9.4194E-01	4.4537E-01	9.8695E-01	8.2398E-01	7.2E-03	1.5E-01	2.3E-02	5.1E-02	3.7E-02
49	1.6757E 00	7.7890E-01	3.6525E-01	7.8874E-01	6.8996E-01	6.3E-03	1.3E-01	2.1E-02	4.5E-02	3.3E-02
50	9.6795E-01	5.2971E-01	2.4208E-01	4.8034E-01	4.5133E-01	4.5E-03	9.7E-02	1.5E-02	3.3E-02	2.5E-02

MOMENTS OF THE SCATTERING SPECTRUM

NORMALIZED TO BORN	LINEAR POLARIZATION VERTICAL	LINEAR POLARIZATION HORIZONTAL	LINEAR POLARIZATION ORTHOGONAL	CIRCULAR POLARIZATION PRINCIPAL	CIRCULAR POLARIZATION ORTHOGONAL
ZEROTH	5.7874E-01	2.5411E-01	8.4015E-02	3.6994E-01	9.0151E-02
FIRST	5.0703E-01	2.2179E-01	7.3093E-02	3.2459E-01	7.8869E-02
SECOND	4.3723E-01	1.9030E-01	6.2506E-02	2.8021E-01	6.7893E-02
FIRST SQUARED	4.3723E-01	1.9030E-01	6.2506E-02	2.8021E-01	6.7893E-02

NORMALIZED TO BORN AT CRITICAL DENSITY FOR REFRACTION

ZEROTH	6.1149E 02	2.6850E 02	8.8771E 01	3.9089E 02	9.5254E 01
FIRST	5.3573E 02	2.3434E 02	7.7230E 01	3.4296E 02	8.3333E 01
SECOND	4.6198E 02	2.0108E 02	6.6044E 01	2.9607E 02	7.1736E 01
FIRST SQUARED	4.6198E 02	2.0108E 02	6.6044E 01	2.9607E 02	7.1736E 01

ABSOLUTE

ZEROTH	1.3457E-02	5.9087E-03	1.9536E-03	8.6022E-03	2.0962E-03
FIRST	7.1166E-04	3.1122E-04	1.0256E-04	4.5546E-04	1.1067E-04
SECOND	3.8403E-05	1.6715E-05	5.4901E-06	2.4612E-05	5.9632E-06

DOPPLER/BODY VELOCITY

MEAN	5.2869E-02	5.2670E-02	5.2501E-02	5.2947E-02	5.2796E-02
SPREAD	7.6528E-03	7.3932E-03	7.3407E-03	7.5931E-03	7.5787E-03

AXIAL STATION (M) = 100.00 MEAN ELECTRON DENSITY/CRITICAL = 8.06115E-04 CHANGED TO 8.06115E-04 KRW = 1.048E 00

(SIN ALPHA)**2 = 2.50000E-01 CHANGED TO 2.50000E-01 NU/OMEGA = 1.59155E-02 MEAN VELOCITY/BODY VELOCITY = 1.000E-01

PROFILE FUNCTIONS**

	RELATIVE RADIUS	ELECTRON DENSITY MEAN (LAYER)	ELECTRON DENSITY MEAN (MESH PT.)	ELECTRON DENSITY RMS FLUCTUATION	COLLISION FREQUENCY LAYER	COLLISION FREQUENCY MESH PT.	ALLOWANCE FOR SCATTERING ATTENUATION ELECTRONS	ALLOWANCE FOR SCATTERING ATTENUATION COLLISIONS	VELOCITY MEAN	VELOCITY RMS FLUCTUATION
1	0.0210	1.0047E 00	1.0045E 00	8.0000E-01	1.0000E 00	1.0000E 00	2.8804E-02	7.2946E-04	9.8106E-01	9.8106E-02
2	0.0271	1.0041E 00	1.0035E 00	8.0000E-01	1.0000E 00	1.0000E 00	2.8788E-02	7.2905E-04	9.7565E-01	9.7565E-02
3	0.0348	1.0023E 00	1.0010E 00	8.0000E-01	1.0000E 00	1.0000E 00	2.8763E-02	7.2841E-04	9.6871E-01	9.6871E-02
4	0.0447	9.9872E-01	9.9634E-01	8.0000E-01	1.0000E 00	1.0000E 00	2.8741E-02	7.2786E-04	9.5978E-01	9.5978E-02
5	0.0574	9.9233E-01	9.8834E-01	8.0000E-01	1.0000E 00	1.0000E 00	2.8709E-02	7.2705E-04	9.4831E-01	9.4831E-02
6	0.0738	9.8187E-01	9.7561E-01	8.0000E-01	1.0000E 00	1.0000E 00	2.8663E-02	7.2588E-04	9.3357E-01	9.3357E-02
7	0.0949	9.6567E-01	9.5619E-01	8.0000E-01	1.0000E 00	1.0000E 00	2.8605E-02	7.2441E-04	9.1463E-01	9.1463E-02
8	0.1159	9.4485E-01	9.3395E-01	8.0000E-01	1.0000E 00	1.0000E 00	2.8548E-02	7.2297E-04	8.9568E-01	8.9568E-02
9	0.1370	9.2133E-01	9.0909E-01	8.0000E-01	1.0000E 00	1.0000E 00	2.8484E-02	7.2137E-04	8.7674E-01	8.7674E-02
10	0.1580	8.9520E-01	8.8162E-01	8.0000E-01	1.0000E 00	1.0000E 00	2.8429E-02	7.1996E-04	8.5779E-01	8.5779E-02
11	0.1791	8.6642E-01	8.5150E-01	8.0000E-01	1.0000E 00	1.0000E 00	2.8362E-02	7.1827E-04	8.3885E-01	8.3885E-02
12	0.2001	8.3502E-01	8.1883E-01	1.2000E 00	1.0000E 00	1.0000E 00	4.2461E-02	1.0753E-03	8.1990E-01	8.1990E-02
13	0.2212	8.0115E-01	7.8379E-01	1.2000E 00	1.0000E 00	1.0000E 00	4.2362E-02	1.0728E-03	8.0096E-01	8.0096E-02
14	0.2422	7.6506E-01	7.4672E-01	1.2000E 00	1.0000E 00	1.0000E 00	4.2268E-02	1.0704E-03	7.8201E-01	7.8201E-02
15	0.2633	7.2714E-01	7.0802E-01	1.2000E 00	1.0000E 00	1.0000E 00	4.2164E-02	1.0678E-03	7.6307E-01	7.6307E-02
16	0.2843	6.8782E-01	6.6817E-01	1.2000E 00	1.0000E 00	1.0000E 00	4.2065E-02	1.0653E-03	7.4412E-01	7.4412E-02
17	0.3054	6.4760E-01	6.2766E-01	1.2000E 00	1.0000E 00	1.0000E 00	4.1970E-02	1.0629E-03	7.2518E-01	7.2518E-02
18	0.3264	6.0697E-01	5.8697E-01	1.2000E 00	1.0000E 00	1.0000E 00	4.1867E-02	1.0603E-03	7.0624E-01	7.0624E-02
19	0.3475	5.6638E-01	5.4653E-01	1.2000E 00	1.0000E 00	1.0000E 00	4.1763E-02	1.0576E-03	6.8729E-01	6.8729E-02
20	0.3685	5.2623E-01	5.0672E-01	1.2000E 00	1.0000E 00	1.0000E 00	4.1653E-02	1.0549E-03	6.6835E-01	6.6835E-02
21	0.3896	4.8688E-01	4.6786E-01	1.2000E 00	1.0000E 00	1.0000E 00	4.1553E-02	1.0523E-03	6.4940E-01	6.4940E-02
22	0.4106	4.4861E-01	4.3018E-01	3.0000E-01	1.0000E 00	1.0000E 00	1.0359E-02	2.6234E-04	6.3046E-01	6.3046E-02
23	0.4317	4.1162E-01	3.9388E-01	3.0000E-01	1.0000E 00	1.0000E 00	1.0333E-02	2.6167E-04	6.1151E-01	6.1151E-02
24	0.4527	3.7609E-01	3.5910E-01	3.0000E-01	1.0000E 00	1.0000E 00	1.0303E-02	2.6092E-04	5.9257E-01	5.9257E-02
25	0.4738	3.4213E-01	3.2594E-01	3.0000E-01	1.0000E 00	1.0000E 00	1.0275E-02	2.6020E-04	5.7362E-01	5.7362E-02
26	0.4948	3.0983E-01	2.9449E-01	3.0000E-01	1.0000E 00	1.0000E 00	1.0247E-02	2.5949E-04	5.5468E-01	5.5468E-02
27	0.5159	2.7927E-01	2.6482E-01	3.0000E-01	1.0000E 00	1.0000E 00	1.0215E-02	2.5870E-04	5.3573E-01	5.3573E-02
28	0.5369	2.5052E-01	2.3697E-01	3.0000E-01	1.0000E 00	1.0000E 00	1.0185E-02	2.5792E-04	5.1679E-01	5.1679E-02
29	0.5580	2.2363E-01	2.1102E-01	3.0000E-01	1.0000E 00	1.0000E 00	1.0154E-02	2.5714E-04	4.9784E-01	4.9784E-02
30	0.5790	1.9866E-01	1.8700E-01	3.0000E-01	1.0000E 00	1.0000E 00	1.0121E-02	2.5631E-04	4.7890E-01	4.7890E-02
31	0.6001	1.7563E-01	1.6495E-01	3.0000E-01	1.0000E 00	1.0000E 00	1.0089E-02	2.5550E-04	4.5995E-01	4.5995E-02
32	0.6211	1.5457E-01	1.4487E-01	3.0000E-01	1.0000E 00	1.0000E 00	1.0057E-02	2.5470E-04	4.4101E-01	4.4101E-02
33	0.6422	1.3549E-01	1.2674E-01	3.0000E-01	1.0000E 00	1.0000E 00	1.0021E-02	2.5379E-04	4.2206E-01	4.2206E-02
34	0.6632	1.1832E-01	1.1050E-01	3.0000E-01	1.0000E 00	1.0000E 00	9.9857E-03	2.5289E-04	4.0312E-01	4.0312E-02
35	0.6843	1.0300E-01	9.6038E-02	3.0000E-01	1.0000E 00	1.0000E 00	9.9538E-03	2.5208E-04	3.8417E-01	3.8417E-02
36	0.7053	8.9384E-02	8.3214E-02	3.0000E-01	1.0000E 00	1.0000E 00	9.9144E-03	2.5108E-04	3.6523E-01	3.6523E-02
37	0.7264	7.7318E-02	7.1845E-02	3.0000E-01	1.0000E 00	1.0000E 00	9.8762E-03	2.5011E-04	3.4628E-01	3.4628E-02
38	0.7474	6.6608E-02	6.1732E-02	3.0000E-01	1.0000E 00	1.0000E 00	9.8397E-03	2.4919E-04	3.2734E-01	3.2734E-02
39	0.7685	5.7054E-02	5.2683E-02	3.0000E-01	1.0000E 00	1.0000E 00	9.8028E-03	2.4826E-04	3.0839E-01	3.0839E-02
40	0.7895	4.8481E-02	4.4547E-02	3.0000E-01	1.0000E 00	1.0000E 00	9.7635E-03	2.4726E-04	2.8945E-01	2.8945E-02
41	0.8106	4.0767E-02	3.7237E-02	3.0000E-01	1.0000E 00	1.0000E 00	9.7216E-03	2.4620E-04	2.7050E-01	2.7050E-02
42	0.8316	3.3871E-02	3.0764E-02	3.0000E-01	1.0000E 00	1.0000E 00	9.6777E-03	2.4509E-04	2.5156E-01	2.5156E-02
43	0.8527	2.7856E-02	2.5243E-02	3.0000E-01	1.0000E 00	1.0000E 00	9.6371E-03	2.4406E-04	2.3261E-01	2.3261E-02
44	0.8737	2.2889E-02	2.0881E-02	3.0000E-01	1.0000E 00	1.0000E 00	9.5932E-03	2.4295E-04	2.1367E-01	2.1367E-02
45	0.8948	1.9199E-02	1.7906E-02	3.0000E-01	1.0000E 00	1.0000E 00	9.5482E-03	2.4181E-04	1.9472E-01	1.9472E-02
46	0.9158	1.6983E-02	1.6439E-02	3.0000E-01	1.0000E 00	1.0000E 00	9.5012E-03	2.4062E-04	1.7578E-01	1.7578E-02
47	0.9369	1.6222E-02	1.6252E-02	3.0000E-01	1.0000E 00	1.0000E 00	9.4535E-03	2.3941E-04	1.5683E-01	1.5683E-02
48	0.9579	1.6385E-02	1.6398E-02	3.0000E-01	1.0000E 00	1.0000E 00	9.4039E-03	2.3815E-04	1.3789E-01	1.3789E-02
49	0.9790	1.5968E-02	1.4656E-02	3.0000E-01	1.0000E 00	1.0000E 00	9.3555E-03	2.3693E-04	1.1894E-01	1.1894E-02
50	1.0000	1.1826E-02	6.7400E-03	3.0000E-01	1.0000E 00	1.0000E 00	9.3003E-03	2.3553E-04	1.0000E-01	1.0000E-02

MEAN WAKE FIELD

SCATTERING COEFFICIENTS

MODE	PARALLEL POLARIZATION ELECTRIC		MAGNETIC		TRANSVERSE POLARIZATION ELECTRIC		MAGNETIC		LAYERS USED
0	-2.2828E-06	-1.5110E-04	0.	0.	0.	0.	-1.1661E-07	-8.3129E-06	50
1	-7.0455E-06	-4.3904E-04	-5.0206E-04	8.0560E-06	5.0201E-04	-8.0589E-06	-9.3104E-06	-5.7989E-04	50
2	-9.9772E-08	-6.2653E-06	-7.2020E-06	1.1468E-07	7.2030E-06	-1.1469E-07	-1.3240E-07	-8.3137E-06	50
3	-6.9954E-10	-4.3879E-08	-5.0636E-08	8.0541E-10	5.0557E-08	-8.0541E-10	-9.3003E-10	-5.8408E-08	50
4	-3.0398E-12	-1.9116E-10	-2.2007E-10	3.5032E-12	2.2002E-10	-3.5032E-12	-4.0452E-12	-2.5409E-10	50
5	-8.9037E-15	-5.5990E-13	-6.4514E-13	1.0267E-14	6.4496E-13	-1.0267E-14	-1.1855E-14	-7.4489E-13	50

SCATTERING FROM MEAN WAKE PLASMA

AZIMUTHAL ANGLE NUMBER	AZIMUTHAL ANGLE DEGREES	2*PI*KR*SCATTERED POWER (DB) LINEAR POLARIZATION PARALLEL	LINEAR POLARIZATION TRANSVERSE	LINEAR POLARIZATION ORTHOGONAL	CIRCULAR POLARIZATION PRINCIPAL	CIRCULAR POLARIZATION ORTHOGONAL
0	0.	-64.487	-64.486	-300.000	-64.486	-140.844
1	11.250	-64.618	-64.659	-79.936	-64.512	-117.262
2	22.500	-65.017	-65.192	-74.098	-64.589	-105.032
3	33.750	-65.703	-66.131	-70.883	-64.713	-98.098
4	45.000	-66.715	-67.569	-68.819	-64.884	-93.310
5	56.250	-68.120	-69.701	-67.450	-65.094	-89.717
6	67.500	-70.043	-72.983	-66.577	-65.338	-86.901
7	78.750	-72.729	-78.881	-66.105	-65.608	-84.640
8	90.000	-76.781	-156.027	-65.985	-65.896	-82.802
9	101.250	-84.481	-78.978	-66.202	-66.190	-81.301
10	112.500	-93.431	-73.173	-66.768	-66.479	-80.081
11	123.750	-80.429	-69.978	-67.727	-66.752	-79.100
12	135.000	-75.954	-67.921	-69.172	-66.996	-78.330
13	146.250	-73.491	-66.545	-71.298	-67.200	-77.750
14	157.500	-72.037	-65.652	-74.559	-67.354	-77.345
15	168.750	-71.252	-65.147	-80.425	-67.449	-77.106
16	180.000	-71.003	-64.984	-300.000	-67.482	-77.027

SQUARE ROOT OF (2*PI*KR) TIMES THE COMPLEX FORWARD SCATTERED FIELD

PARALLEL -4.2842E-04 , -4.1509E-04

TRANSVERSE -4.2860E-04 , -4.1508E-04

PROFILES OF WEIGHTED AVERAGES OF SQUARES OF SCALAR PRODUCTS OF ELECTRIC FIELDS

	LINEAR POLARIZATION			CIRCULAR POLARIZATION		DEPOLARIZATION FACTORS				
	VERTICAL	HORIZONTAL	ORTHOGONAL	PRINCIPAL	ORTHOGONAL					
1	1.0015E 00	1.0012E 00	1.3634E-12	1.0013E 00	7.3929E-09	8.7E-10	8.7E-10	1.2E-21	8.7E-10	6.4E-18
2	1.0015E 00	1.0012E 00	4.9786E-13	1.0013E 00	7.7929E-09	8.8E-10	8.8E-10	4.5E-22	8.8E-10	6.8E-18
3	1.0015E 00	1.0012E 00	3.3397E-13	1.0013E 00	8.2226E-09	8.9E-10	8.9E-10	3.0E-22	8.9E-10	7.3E-18
4	1.0015E 00	1.0012E 00	5.8719E-13	1.0013E 00	8.4541E-09	9.0E-10	9.0E-10	5.3E-22	9.0E-10	7.6E-18
5	1.0015E 00	1.0012E 00	2.5637E-12	1.0013E 00	8.4332E-09	9.1E-10	9.1E-10	2.3E-21	9.1E-10	7.7E-18
6	1.0015E 00	1.0012E 00	1.5847E-11	1.0013E 00	8.1543E-09	9.2E-10	9.2E-10	1.4E-20	9.2E-10	7.5E-18
7	1.0014E 00	1.0011E 00	7.6480E-11	1.0013E 00	7.6475E-09	9.4E-10	9.4E-10	6.8E-20	9.4E-10	7.1E-18
8	1.0014E 00	1.0011E 00	2.0885E-10	1.0013E 00	7.0521E-09	9.4E-10	9.4E-10	1.9E-19	9.4E-10	6.5E-18
9	1.0014E 00	1.0011E 00	4.3421E-10	1.0012E 00	6.4318E-09	9.7E-10	9.7E-10	4.0E-19	9.7E-10	6.1E-18
10	1.0013E 00	1.0011E 00	7.7769E-10	1.0012E 00	5.8828E-09	9.8E-10	9.8E-10	7.4E-19	9.8E-10	5.5E-18
11	1.0013E 00	1.0010E 00	1.3352E-09	1.0012E 00	6.5536E-09	9.9E-10	9.8E-10	1.3E-18	9.9E-10	6.2E-18
12	1.0013E 00	1.0010E 00	1.5819E-09	1.0011E 00	6.5582E-09	1.0E-09	1.0E-09	1.5E-18	1.0E-09	6.2E-18
13	1.0012E 00	1.0010E 00	2.2550E-09	1.0011E 00	5.3500E-09	1.0E-09	1.0E-09	2.2E-18	1.0E-09	5.0E-18
14	1.0012E 00	1.0009E 00	3.4015E-09	1.0011E 00	5.7049E-09	1.1E-09	1.1E-09	3.4E-18	1.1E-09	5.4E-18
15	1.0011E 00	1.0009E 00	4.7571E-09	1.0010E 00	6.2252E-09	1.1E-09	1.1E-09	4.9E-18	1.1E-09	5.9E-18
16	1.0011E 00	1.0009E 00	6.3000E-09	1.0010E 00	6.8737E-09	1.0E-09	1.0E-09	6.2E-18	1.0E-09	6.4E-18
17	1.0010E 00	1.0008E 00	7.9952E-09	1.0009E 00	7.6287E-09	1.0E-09	1.0E-09	8.2E-18	1.0E-09	7.2E-18
18	1.0010E 00	1.0008E 00	9.8091E-09	1.0009E 00	8.4787E-09	1.1E-09	1.1E-09	1.0E-17	1.1E-09	8.1E-18
19	1.0009E 00	1.0007E 00	1.1687E-08	1.0008E 00	9.4042E-09	1.0E-09	1.0E-09	1.2E-17	1.0E-09	9.3E-18
20	1.0009E 00	1.0007E 00	1.3585E-08	1.0008E 00	1.0394E-08	1.0E-09	1.0E-09	1.4E-17	1.0E-09	1.0E-17
21	1.0008E 00	1.0007E 00	1.5214E-08	1.0007E 00	1.0595E-08	9.5E-10	9.5E-10	1.5E-17	9.5E-10	1.0E-17
22	1.0007E 00	1.0006E 00	2.1039E-08	1.0007E 00	1.3650E-08	9.0E-10	9.0E-10	2.0E-17	9.0E-10	1.3E-17
23	1.0007E 00	1.0006E 00	2.2433E-08	1.0006E 00	1.5252E-08	7.9E-10	7.9E-10	1.9E-17	7.9E-10	1.4E-17
24	1.0006E 00	1.0005E 00	2.3775E-08	1.0006E 00	1.6274E-08	7.7E-10	7.7E-10	2.1E-17	7.7E-10	1.6E-17
25	1.0006E 00	1.0005E 00	2.4976E-08	1.0006E 00	1.7266E-08	6.6E-10	6.6E-10	1.8E-17	6.6E-10	1.5E-17
26	1.0006E 00	1.0005E 00	2.6029E-08	1.0005E 00	1.8214E-08	6.6E-10	6.5E-10	1.8E-17	6.6E-10	1.6E-17
27	1.0005E 00	1.0005E 00	2.6918E-08	1.0005E 00	1.9099E-08	6.6E-10	6.6E-10	1.9E-17	6.6E-10	1.7E-17
28	1.0005E 00	1.0004E 00	2.7620E-08	1.0005E 00	1.9886E-08	6.1E-10	6.1E-10	1.7E-17	6.1E-10	1.6E-17
29	1.0005E 00	1.0004E 00	2.8133E-08	1.0005E 00	2.0544E-08	5.7E-10	5.7E-10	1.5E-17	5.7E-10	1.6E-17
30	1.0005E 00	1.0004E 00	2.8445E-08	1.0004E 00	2.1106E-08	5.9E-10	5.9E-10	1.6E-17	5.9E-10	1.7E-17
31	1.0005E 00	1.0004E 00	2.8552E-08	1.0004E 00	2.1498E-08	5.6E-10	5.6E-10	1.5E-17	5.6E-10	1.6E-17
32	1.0004E 00	1.0004E 00	2.8455E-08	1.0004E 00	2.1725E-08	5.1E-10	5.1E-10	1.2E-17	5.1E-10	1.5E-17
33	1.0004E 00	1.0004E 00	2.8172E-08	1.0004E 00	2.1786E-08	5.0E-10	5.0E-10	1.2E-17	5.0E-10	1.4E-17
34	1.0004E 00	1.0004E 00	2.7710E-08	1.0004E 00	2.1683E-08	5.0E-10	5.0E-10	1.1E-17	5.0E-10	1.4E-17
35	1.0004E 00	1.0004E 00	2.7102E-08	1.0004E 00	2.1429E-08	4.9E-10	4.9E-10	1.0E-17	4.9E-10	1.4E-17
36	1.0004E 00	1.0004E 00	2.6377E-08	1.0004E 00	2.1048E-08	4.5E-10	4.5E-10	8.9E-18	4.5E-10	1.2E-17
37	1.0004E 00	1.0004E 00	2.5564E-08	1.0004E 00	2.0562E-08	4.7E-10	4.7E-10	9.0E-18	4.7E-10	1.2E-17
38	1.0004E 00	1.0004E 00	2.4701E-08	1.0004E 00	2.0001E-08	4.4E-10	4.4E-10	8.1E-18	4.4E-10	1.1E-17
39	1.0004E 00	1.0004E 00	2.3812E-08	1.0004E 00	1.9389E-08	4.6E-10	4.6E-10	8.0E-18	4.6E-10	1.1E-17
40	1.0004E 00	1.0004E 00	2.2918E-08	1.0004E 00	1.8748E-08	4.5E-10	4.5E-10	6.7E-18	4.5E-10	1.1E-17
41	1.0005E 00	1.0004E 00	2.2027E-08	1.0004E 00	1.8085E-08	3.9E-10	3.9E-10	5.5E-18	3.9E-10	9.0E-18
42	1.0005E 00	1.0004E 00	2.1124E-08	1.0005E 00	1.7386E-08	4.0E-10	4.0E-10	5.4E-18	4.0E-10	8.9E-18
43	1.0005E 00	1.0005E 00	2.0193E-08	1.0005E 00	1.6635E-08	3.8E-10	3.8E-10	4.6E-18	3.8E-10	8.0E-18
44	1.0005E 00	1.0005E 00	1.9204E-08	1.0005E 00	1.5802E-08	3.9E-10	3.9E-10	4.5E-18	3.9E-10	7.8E-18
45	1.0005E 00	1.0005E 00	1.8126E-08	1.0005E 00	1.4855E-08	4.1E-10	4.1E-10	4.5E-18	4.1E-10	7.8E-18
46	1.0005E 00	1.0005E 00	1.6969E-08	1.0005E 00	1.3807E-08	3.6E-10	3.6E-10	3.6E-18	3.6E-10	6.4E-18
47	1.0006E 00	1.0005E 00	1.5791E-08	1.0005E 00	1.2729E-08	3.7E-10	3.7E-10	3.4E-18	3.7E-10	6.0E-18
48	1.0006E 00	1.0005E 00	1.4757E-08	1.0006E 00	1.1823E-08	3.5E-10	3.5E-10	2.9E-18	3.5E-10	5.3E-18
49	1.0006E 00	1.0006E 00	1.4134E-08	1.0006E 00	1.1397E-08	3.6E-10	3.6E-10	2.7E-18	3.6E-10	5.1E-18
50	1.0006E 00	1.0006E 00	1.4217E-08	1.0006E 00	1.1639E-08	3.8E-10	3.8E-10	2.8E-18	3.8E-10	5.4E-18

MOMENTS OF THE SCATTERING SPECTRUM

NORMALIZED TO BORN	LINEAR POLARIZATION VERTICAL	HORIZONTAL	ORTHOGONAL	CIRCULAR POLARIZATION PRINCIPAL	ORTHOGONAL
ZEROTH	1.0009E 00	1.0007E 00	1.2570E-08	1.0008E 00	1.1405E-08
FIRST	1.0010E 00	1.0008E 00	1.0588E-08	1.0009E 00	1.0275E-08
SECOND	1.0010E 00	1.0008E 00	9.2163E-09	1.0009E 00	9.5666E-09
FIRST SQUARED	1.0010E 00	1.0008E 00	9.2163E-09	1.0009E 00	9.5666E-09
NORMALIZED TO BORN AT CRITICAL DENSITY FOR REFRACTION					
ZEROTH	1.0407E-05	1.0405E-05	1.3069E-13	1.0406E-05	1.1858E-13
FIRST	1.0407E-05	1.0405E-05	1.1009E-13	1.0406E-05	1.0683E-13
SECOND	1.0408E-05	1.0406E-05	9.5824E-14	1.0407E-05	9.9465E-14
FIRST SQUARED	1.0408E-05	1.0406E-05	9.5824E-14	1.0407E-05	9.9465E-14
ABSOLUTE					
ZEROTH	2.5276E-10	2.5271E-10	3.1743E-18	2.5274E-10	2.8800E-18
FIRST	1.3792E-11	1.3789E-11	1.4589E-19	1.3791E-11	1.4157E-19
SECOND	8.4633E-13	8.4616E-13	7.7919E-21	8.4624E-13	8.0880E-21
DOPPLER/BODY VELOCITY					
MEAN	5.4567E-02	5.4565E-02	4.5960E-02	5.4566E-02	4.9155E-02
SPREAD	1.9259E-02	1.9259E-02	1.8503E-02	1.9259E-02	1.9800E-02

AXIAL STATION (M) = 200.00 MEAN ELECTRON DENSITY/CRITICAL = 8.06115E-08 CHANGED TO 8.06115E-08 KRW = 1.048E 00

(SIN ALPHA)**2 = 2.50000E-01 CHANGED TO 2.50000E-01 MU/OMEGA = 1.59155E 00 MEAN VELOCITY/BODY VELOCITY = 1.000E-01

PROFILE FUNCTIONS**

	RELATIVE RADIUS	ELECTRON DENSITY MEAN (LAYER)	ELECTRON DENSITY MEAN (MESH PT.)	ELECTRON DENSITY RMS FLUCTUATION	COLLISION FREQUENCY LAYER	COLLISION FREQUENCY MESH PT.	ALLOWANCE FOR SCATTERING ELECTRONS	ALLOWANCE FOR ATTENUATION COLLISIONS	VELOCITY MEAN	VELOCITY RMS FLUCTUATION
1	0.0210	1.0047E 00	1.0045E 00	9.9995E-01	1.0000E 00	1.0000E 00	9155E-02	4.8509E-10	9.9995E-01	9.9588E-02
2	0.0271	1.0041E 00	1.0035E 00	9.9940E-01	1.0000E 00	1.0000E 00	9132E-02	4.8452E-10	9.9940E-01	9.9521E-02
3	0.0348	1.0023E 00	1.0010E 00	9.9842E-01	1.0000E 00	1.0000E 00	9099E-02	4.8369E-10	9.9842E-01	9.9449E-02
4	0.0447	9.9872E-01	9.9634E-01	9.9672E-01	1.0000E 00	1.0000E 00	9050E-02	4.8243E-10	9.9672E-01	9.9365E-02
5	0.0574	9.9233E-01	9.8834E-01	9.9396E-01	1.0000E 00	1.0000E 00	8975E-02	4.8055E-10	9.9390E-01	9.9244E-02
6	0.0738	9.8187E-01	9.7561E-01	9.8932E-01	1.0000E 00	1.0000E 00	1.8857E-02	4.7755E-10	9.8932E-01	9.9033E-02
7	0.0949	9.6567E-01	9.5619E-01	9.8202E-01	1.0000E 00	1.0000E 00	1.8681E-02	4.7310E-10	9.8202E-01	9.8626E-02
8	0.1159	9.4485E-01	9.3395E-01	9.7319E-01	1.0000E 00	1.0000E 00	1.8476E-02	4.6790E-10	9.7319E-01	9.8045E-02
9	0.1370	9.2133E-01	9.0909E-01	9.6286E-01	1.0000E 00	1.0000E 00	1.8243E-02	4.6199E-10	9.6286E-01	9.7294E-02
10	0.1580	8.9520E-01	8.8162E-01	9.5103E-01	1.0000E 00	1.0000E 00	1.7979E-02	4.5532E-10	9.5103E-01	9.6389E-02
11	0.1791	8.6642E-01	8.5150E-01	9.3771E-01	1.0000E 00	1.0000E 00	1.7688E-02	4.4795E-10	9.3771E-01	9.5350E-02
12	0.2001	8.3502E-01	8.1883E-01	9.2292E-01	1.0000E 00	1.0000E 00	1.7373E-02	4.3998E-10	9.2292E-01	9.4194E-02
13	0.2212	8.0115E-01	7.8379E-01	9.0673E-01	1.0000E 00	1.0000E 00	1.7030E-02	4.3129E-10	9.0673E-01	9.2934E-02
14	0.2422	7.6506E-01	7.4672E-01	8.8919E-01	1.0000E 00	1.0000E 00	1.6666E-02	4.2207E-10	8.8919E-01	9.1579E-02
15	0.2633	7.2714E-01	7.0802E-01	8.7042E-01	1.0000E 00	1.0000E 00	1.6275E-02	4.1216E-10	8.7042E-01	9.0133E-02
16	0.2843	6.8782E-01	6.6817E-01	8.5051E-01	1.0000E 00	1.0000E 00	1.5854E-02	4.0175E-10	8.5051E-01	8.8600E-02
17	0.3054	6.4760E-01	6.2766E-01	8.2959E-01	1.0000E 00	1.0000E 00	1.5437E-02	3.9095E-10	8.2959E-01	8.6980E-02
18	0.3264	6.0697E-01	5.8697E-01	8.0776E-01	1.0000E 00	1.0000E 00	1.4996E-02	3.7978E-10	8.0776E-01	8.5275E-02
19	0.3475	5.6638E-01	5.4653E-01	7.8516E-01	1.0000E 00	1.0000E 00	1.4539E-02	3.6821E-10	7.8516E-01	8.3487E-02
20	0.3685	5.2623E-01	5.0672E-01	7.6187E-01	1.0000E 00	1.0000E 00	1.4072E-02	3.5637E-10	7.6187E-01	8.1622E-02
21	0.3896	4.8688E-01	4.6786E-01	7.3802E-01	1.0000E 00	1.0000E 00	1.3597E-02	3.4433E-10	7.3802E-01	7.9685E-02
22	0.4106	4.4861E-01	4.3018E-01	7.1369E-01	1.0000E 00	1.0000E 00	1.3114E-02	3.3210E-10	7.1369E-01	7.7685E-02
23	0.4317	4.1162E-01	3.9388E-01	6.8897E-01	1.0000E 00	1.0000E 00	1.2625E-02	3.1973E-10	6.8897E-01	7.5630E-02
24	0.4527	3.7609E-01	3.5910E-01	6.6394E-01	1.0000E 00	1.0000E 00	1.2134E-02	3.0728E-10	6.6394E-01	7.3530E-02
25	0.4738	3.4213E-01	3.2594E-01	6.3868E-01	1.0000E 00	1.0000E 00	1.1640E-02	2.9477E-10	6.3868E-01	7.1396E-02
26	0.4948	3.0983E-01	2.9449E-01	6.1328E-01	1.0000E 00	1.0000E 00	1.1144E-02	2.8223E-10	6.1328E-01	6.9236E-02
27	0.5159	2.7927E-01	2.6482E-01	5.8781E-01	1.0000E 00	1.0000E 00	1.0649E-02	2.6969E-10	5.8781E-01	6.7059E-02
28	0.5369	2.5052E-01	2.3697E-01	5.6236E-01	1.0000E 00	1.0000E 00	1.0158E-02	2.5725E-10	5.6236E-01	6.4872E-02
29	0.5580	2.2363E-01	2.1102E-01	5.3700E-01	1.0000E 00	1.0000E 00	9.6706E-03	2.4491E-10	5.3700E-01	6.2680E-02
30	0.5790	1.9866E-01	1.8700E-01	5.1183E-01	1.0000E 00	1.0000E 00	9.1876E-03	2.3268E-10	5.1183E-01	6.0486E-02
31	0.6001	1.7563E-01	1.6495E-01	4.8694E-01	1.0000E 00	1.0000E 00	8.7132E-03	2.2066E-10	4.8694E-01	5.8294E-02
32	0.6211	1.5457E-01	1.4487E-01	4.6240E-01	1.0000E 00	1.0000E 00	8.2469E-03	2.0885E-10	4.6240E-01	5.6107E-02
33	0.6422	1.3549E-01	1.2674E-01	4.3831E-01	1.0000E 00	1.0000E 00	7.7915E-03	1.9732E-10	4.3831E-01	5.3927E-02
34	0.6632	1.1832E-01	1.1050E-01	4.1474E-01	1.0000E 00	1.0000E 00	7.3470E-03	1.8606E-10	4.1474E-01	5.1756E-02
35	0.6843	1.0300E-01	9.6038E-02	3.9176E-01	1.0000E 00	1.0000E 00	6.9149E-03	1.7512E-10	3.9176E-01	4.9600E-02
36	0.7053	8.9384E-02	8.3214E-02	3.6944E-01	1.0000E 00	1.0000E 00	6.4973E-03	1.6454E-10	3.6944E-01	4.7464E-02
37	0.7264	7.7318E-02	7.1845E-02	3.4781E-01	1.0000E 00	1.0000E 00	6.0942E-03	1.5433E-10	3.4781E-01	4.5355E-02
38	0.7474	6.6608E-02	6.1732E-02	3.2692E-01	1.0000E 00	1.0000E 00	5.7062E-03	1.4451E-10	3.2692E-01	4.3281E-02
39	0.7685	5.7054E-02	5.2683E-02	3.0677E-01	1.0000E 00	1.0000E 00	5.3336E-03	1.3507E-10	3.0677E-01	4.1250E-02
40	0.7895	4.8481E-02	4.4547E-02	2.8739E-01	1.0000E 00	1.0000E 00	4.9763E-03	1.2602E-10	2.8739E-01	3.9268E-02
41	0.8106	4.0767E-02	3.7237E-02	2.6876E-01	1.0000E 00	1.0000E 00	4.6340E-03	1.1736E-10	2.6876E-01	3.7341E-02
42	0.8316	3.3871E-02	3.0764E-02	2.5088E-01	1.0000E 00	1.0000E 00	4.3074E-03	1.0908E-10	2.5088E-01	3.5469E-02
43	0.8527	2.7856E-02	2.5243E-02	2.3376E-01	1.0000E 00	1.0000E 00	3.9955E-03	1.0118E-10	2.3376E-01	3.3649E-02
44	0.8737	2.2889E-02	2.0881E-02	2.1739E-01	1.0000E 00	1.0000E 00	3.6987E-03	9.3670E-11	2.1739E-01	3.1873E-02
45	0.8948	1.9199E-02	1.7906E-02	2.0177E-01	1.0000E 00	1.0000E 00	3.4168E-03	8.6531E-11	2.0177E-01	3.0130E-02
46	0.9158	1.6983E-02	1.6439E-02	1.8693E-01	1.0000E 00	1.0000E 00	3.1504E-03	7.9783E-11	1.8693E-01	2.8413E-02
47	0.9369	1.6222E-02	1.6252E-02	1.7287E-01	1.0000E 00	1.0000E 00	2.8989E-03	7.3414E-11	1.7287E-01	2.6722E-02
48	0.9579	1.6385E-02	1.6398E-02	1.5959E-01	1.0000E 00	1.0000E 00	2.6619E-03	6.7412E-11	1.5959E-01	2.5082E-02
49	0.9790	1.5968E-02	1.4656E-02	1.4702E-01	1.0000E 00	1.0000E 00	2.4394E-03	6.1777E-11	1.4702E-01	2.3560E-02
50	1.0000	1.1826E-02	6.7400E-03	1.3500E-01	1.0000E 00	1.0000E 00	2.2273E-03	5.6405E-11	1.3500E-01	2.2300E-02

MEAN WAKE FIELD

SCATTERING COEFFICIENTS

MODE	PARALLEL POLARIZATION ELECTRIC		PARALLEL POLARIZATION MAGNETIC		TRANSVERSE POLARIZATION ELECTRIC		TRANSVERSE POLARIZATION MAGNETIC		LAYERS USED
0	9.3180E-08	6.1308E-09	0.	0.	0.	0.	6.5880E-08	-4.4668E-09	50
1	-2.0447E-08	-3.8489E-08	5.0249E-08	8.4704E-09	-7.0214E-08	-5.9514E-09	-2.7932E-08	-3.7149E-08	50
2	-2.6589E-10	-2.9856E-09	3.9870E-10	2.8875E-10	-4.9212E-10	-2.9851E-10	-3.5502E-10	-7.4445E-10	50
3	-1.7463E-12	-3.1751E-11	1.1908E-12	2.0080E-12	4.3656E-12	-2.0091E-12	-2.3207E-12	-1.9050E-11	50
4	-7.1391E-15	3.3314E-21	5.6997E-14	8.2282E-15	2.1922E-15	-8.2282E-15	-9.5012E-15	-1.0523E-13	50
5	-1.9855E-17	-8.6649E-16	-2.7078E-17	2.2896E-17	9.8382E-16	-2.2896E-17	-2.6438E-17	1.4441E-16	50

SCATTERING FROM MEAN WAKE PLASMA

AZIMUTHAL ANGLE NUMBER	DEGREES	2*PI*KR*SCATTERED POWER (DB) LINEAR POLARIZATION PARALLEL	TRANSVERSE	ORTHOGONAL	CIRCULAR POLARIZATION PRINCIPAL	ORTHOGONAL
0	0.	-141.869	-144.936	-300.000	-143.630	-154.999
1	11.250	-141.874	-144.966	-158.288	-143.306	-154.971
2	22.500	-141.880	-145.062	-152.443	-142.963	-154.896
3	33.750	-141.859	-145.117	-149.218	-142.469	-154.791
4	45.000	-141.778	-145.126	-147.139	-141.905	-154.684
5	56.250	-141.605	-144.996	-145.752	-141.337	-154.606
6	67.500	-141.331	-144.681	-144.860	-140.809	-154.589
7	78.750	-140.969	-144.187	-144.366	-140.350	-154.661
8	90.000	-140.548	-143.564	-144.224	-139.973	-154.847
9	101.250	-140.107	-142.885	-144.419	-139.681	-155.161
10	112.500	-139.679	-142.214	-144.963	-139.469	-155.614
11	123.750	-139.293	-141.600	-145.902	-139.328	-156.200
12	135.000	-138.963	-141.075	-147.330	-139.246	-156.898
13	146.250	-138.701	-140.656	-149.442	-139.206	-157.655
14	157.500	-138.512	-140.352	-152.693	-139.192	-158.375
15	168.750	-138.398	-140.169	-158.553	-139.190	-158.913
16	180.000	-138.360	-140.107	-300.000	-139.190	-159.115

SQUARE ROOT OF (2*PI*KR) TIMES THE COMPLEX FORWARD SCATTERED FIELD

PARALLEL 2.6227E-08 , -7.6255E-08

TRANSVERSE -3.3860E-09 , -5.6547E-08

PROFILES OF WEIGHTED AVERAGES OF SQUARES OF SCALAR PRODUCTS OF ELECTRIC FIELDS

	LINEAR POLARIZATION			CIRCULAR POLARIZATION		DEPOLARIZATION FACTORS				
	VERTICAL	HORIZONTAL	ORTHOGONAL	PRINCIPAL	ORTHOGONAL					
1	1.0004E 00	1.0004E 00	3.4243E-18	1.0004E 00	1.2860E-18	2.1E-18	2.1E-18	7.4E-36	2.1E-18	2.8E-36
2	1.0004E 00	1.0004E 00	1.2342E-18	1.0004E 00	6.3111E-19	2.2E-18	2.2E-18	2.7E-36	2.2E-18	1.4E-36
3	1.0004E 00	1.0004E 00	1.7829E-18	1.0004E 00	5.8663E-18	2.2E-18	2.2E-18	3.8E-36	2.2E-18	8.2E-36
4	1.0004E 00	1.0004E 00	5.8670E-18	1.0004E 00	2.0057E-17	2.3E-18	2.3E-18	1.2E-35	2.3E-18	4.6E-35
5	1.0004E 00	1.0004E 00	9.4706E-18	1.0004E 00	2.3088E-17	2.3E-18	2.3E-18	2.1E-35	2.3E-18	5.1E-35
6	1.0004E 00	1.0004E 00	2.2488E-18	1.0004E 00	7.4396E-17	2.4E-18	2.4E-18	4.4E-36	2.4E-18	1.7E-34
7	1.0004E 00	1.0004E 00	5.4694E-18	1.0004E 00	1.7233E-17	2.4E-18	2.4E-18	1.3E-35	2.4E-18	3.7E-35
8	1.0004E 00	1.0004E 00	1.3402E-17	1.0004E 00	3.5583E-17	2.4E-18	2.4E-18	2.9E-35	2.4E-18	7.8E-35
9	1.0004E 00	1.0004E 00	2.2346E-18	1.0004E 00	3.5006E-17	2.4E-18	2.4E-18	3.9E-36	2.4E-18	9.1E-35
10	1.0005E 00	1.0005E 00	3.1751E-18	1.0005E 00	3.7190E-17	2.4E-18	2.4E-18	8.9E-36	2.4E-18	1.1E-34
11	1.0005E 00	1.0005E 00	3.1417E-19	1.0005E 00	1.6060E-17	2.4E-18	2.4E-18	5.6E-37	2.4E-18	3.1E-35
12	1.0005E 00	1.0005E 00	4.8464E-18	1.0005E 00	7.0279E-18	2.3E-18	2.3E-18	7.4E-36	2.3E-18	1.8E-35
13	1.0005E 00	1.0005E 00	4.7095E-18	1.0005E 00	1.9873E-17	2.4E-18	2.4E-18	1.3E-35	2.4E-18	4.9E-35
14	1.0005E 00	1.0005E 00	5.6809E-18	1.0005E 00	7.5862E-17	2.4E-18	2.4E-18	1.4E-35	2.4E-18	1.7E-34
15	1.0005E 00	1.0005E 00	4.6492E-18	1.0005E 00	3.4628E-18	2.3E-18	2.3E-18	6.3E-36	2.3E-18	6.3E-36
16	1.0005E 00	1.0005E 00	7.8575E-18	1.0005E 00	3.6195E-17	2.2E-18	2.2E-18	2.0E-35	2.2E-18	8.5E-35
17	1.0005E 00	1.0005E 00	1.0313E-17	1.0005E 00	8.3031E-18	2.2E-18	2.2E-18	1.6E-35	2.2E-18	1.1E-35
18	1.0005E 00	1.0005E 00	5.5157E-18	1.0005E 00	1.7218E-17	2.2E-18	2.2E-18	1.6E-35	2.2E-18	2.2E-35
19	1.0005E 00	1.0005E 00	1.0932E-17	1.0005E 00	1.3334E-17	2.1E-18	2.1E-18	2.2E-35	2.1E-18	3.2E-35
20	1.0005E 00	1.0005E 00	2.4324E-17	1.0005E 00	5.8511E-17	2.1E-18	2.1E-18	6.6E-35	2.1E-18	1.3E-34
21	1.0005E 00	1.0005E 00	1.2611E-17	1.0005E 00	1.8024E-16	2.0E-18	2.0E-18	3.0E-35	2.0E-18	3.6E-34
22	1.0005E 00	1.0005E 00	2.5186E-17	1.0005E 00	1.8235E-16	1.9E-18	1.9E-18	6.7E-35	1.9E-18	4.5E-34
23	1.0005E 00	1.0005E 00	4.4070E-17	1.0005E 00	2.7451E-16	1.9E-18	1.9E-18	9.4E-35	1.9E-18	4.6E-34
24	1.0005E 00	1.0005E 00	3.2739E-17	1.0005E 00	8.1768E-16	1.9E-18	1.9E-18	7.4E-35	1.9E-18	1.5E-33
25	1.0005E 00	1.0005E 00	3.4849E-17	1.0005E 00	9.3303E-16	1.8E-18	1.8E-18	8.2E-35	1.8E-18	1.6E-33
26	1.0005E 00	1.0005E 00	4.0622E-17	1.0005E 00	2.0009E-15	1.7E-18	1.7E-18	7.0E-35	1.7E-18	3.7E-33
27	1.0005E 00	1.0005E 00	5.9070E-17	1.0005E 00	2.6408E-15	1.7E-18	1.7E-18	9.5E-35	1.7E-18	4.6E-33
28	1.0005E 00	1.0005E 00	6.8921E-17	1.0005E 00	5.2545E-15	1.6E-18	1.6E-18	1.5E-34	1.6E-18	8.6E-33
29	1.0006E 00	1.0006E 00	3.2655E-17	1.0006E 00	8.5260E-15	1.6E-18	1.6E-18	5.8E-35	1.6E-18	1.2E-32
30	1.0006E 00	1.0006E 00	8.2848E-17	1.0006E 00	1.2508E-14	1.5E-18	1.5E-18	1.8E-34	1.5E-18	1.9E-32
31	1.0006E 00	1.0006E 00	1.8356E-17	1.0006E 00	1.8873E-14	1.4E-18	1.4E-18	1.7E-35	1.4E-18	2.5E-32
32	1.0006E 00	1.0006E 00	1.8381E-17	1.0006E 00	2.3591E-14	1.4E-18	1.4E-18	2.3E-35	1.4E-18	2.8E-32
33	1.0006E 00	1.0006E 00	6.4063E-17	1.0006E 00	3.8857E-14	1.3E-18	1.3E-18	1.2E-34	1.3E-18	4.9E-32
34	1.0006E 00	1.0006E 00	1.5939E-16	1.0006E 00	5.3685E-14	1.4E-18	1.4E-18	2.8E-34	1.4E-18	6.9E-32
35	1.0006E 00	1.0006E 00	1.0991E-16	1.0006E 00	7.6659E-14	1.3E-18	1.3E-18	1.3E-34	1.3E-18	9.8E-32
36	1.0006E 00	1.0006E 00	7.6037E-17	1.0006E 00	9.9875E-14	1.2E-18	1.2E-18	9.2E-35	1.2E-18	1.2E-31
37	1.0006E 00	1.0006E 00	1.1666E-16	1.0006E 00	1.3685E-13	1.2E-18	1.2E-18	1.3E-34	1.2E-18	1.6E-31
38	1.0006E 00	1.0006E 00	1.3935E-16	1.0006E 00	1.8315E-13	1.1E-18	1.1E-18	1.7E-34	1.1E-18	2.0E-31
39	1.0007E 00	1.0007E 00	1.9919E-16	1.0007E 00	2.4212E-13	1.1E-18	1.1E-18	2.4E-34	1.1E-18	2.8E-31
40	1.0007E 00	1.0007E 00	1.3589E-16	1.0007E 00	3.2017E-13	1.1E-18	1.1E-18	1.1E-34	1.1E-18	3.4E-31
41	1.0007E 00	1.0007E 00	1.1966E-16	1.0007E 00	4.1090E-13	1.0E-18	1.0E-18	1.4E-34	1.0E-18	3.9E-31
42	1.0007E 00	1.0007E 00	1.4007E-16	1.0007E 00	5.3695E-13	1.0E-18	1.0E-18	1.2E-34	1.0E-18	5.2E-31
43	1.0007E 00	1.0007E 00	1.0377E-16	1.0007E 00	6.9835E-13	9.3E-19	9.3E-19	1.1E-34	9.3E-19	6.3E-31
44	1.0007E 00	1.0007E 00	1.3580E-16	1.0007E 00	8.8924E-13	9.4E-19	9.4E-19	1.1E-34	9.4E-19	8.2E-31
45	1.0007E 00	1.0007E 00	7.1398E-17	1.0007E 00	1.1198E-12	9.6E-19	9.6E-19	8.7E-35	9.6E-19	1.0E-30
46	1.0007E 00	1.0007E 00	6.8360E-17	1.0007E 00	1.4052E-12	8.6E-19	8.6E-19	3.4E-35	8.6E-19	1.2E-30
47	1.0008E 00	1.0008E 00	9.8500E-17	1.0008E 00	1.7900E-12	8.5E-19	8.5E-19	3.8E-35	8.5E-19	1.5E-30
48	1.0008E 00	1.0008E 00	1.0342E-16	1.0008E 00	2.2231E-12	8.1E-19	8.1E-19	6.7E-35	8.1E-19	1.7E-30
49	1.0008E 00	1.0008E 00	1.2754E-16	1.0008E 00	2.7636E-12	8.2E-19	8.2E-19	5.4E-35	8.2E-19	2.2E-30
50	1.0008E 00	1.0008E 00	9.2008E-17	1.0008E 00	3.4195E-12	8.2E-19	8.2E-19	2.0E-35	8.2E-19	2.6E-30

MOMENTS OF THE SCATTERING SPECTRUM

	LINEAR POLARIZATION			CIRCULAR POLARIZATION	
NORMALIZED TO BORN	VERTICAL	HORIZONTAL	ORTHOGONAL	PRINCIPAL	ORTHOGONAL
ZEROTH	1.0005E 00	1.0005E 00	4.1434E-17	1.0005E 00	8.6857E-14
FIRST	1.0005E 00	1.0005E 00	2.9149E-17	1.0005E 00	2.8732E-14
SECOND	1.0005E 00	1.0005E 00	2.4970E-17	1.0005E 00	1.6594E-14
FIRST SQUARED	1.0005E 00	1.0005E 00	2.1736E-17	1.0005E 00	9.7559E-15
NORMALIZED TO BORN AT CRITICAL DENSITY FOR REFRACTION					
ZEROTH	1.0403E-13	1.0403E-13	4.3080E-30	1.0403E-13	9.0307E-27
FIRST	1.0402E-13	1.0402E-13	3.0306E-30	1.0402E-13	2.9873E-27
SECOND	1.0402E-13	1.0402E-13	2.5962E-30	1.0402E-13	1.7253E-27
FIRST SQUARED	1.0402E-13	1.0402E-13	2.2599E-30	1.0402E-13	1.0143E-27
ABSOLUTE					
ZEROTH	6.3293E-19	6.3293E-19	2.6211E-35	6.3293E-19	5.4946E-32
FIRST	3.7125E-20	3.7125E-20	1.0816E-36	3.7125E-20	1.0661E-33
SECOND	2.4526E-21	2.4526E-21	5.3402E-38	2.4526E-21	2.4167E-35
DOPPLER/BODY VELOCITY					
MEAN	5.8655E-02	5.8655E-02	0.	5.8655E-02	0.
SPREAD	2.0848E-02	2.0848E-02	0.	2.0848E-02	0.

SCATTERED PULSE SHAPE FUNCTIONS

AXIAL STATION (M)		LINEAR POLARIZATION VERTICAL	LINEAR POLARIZATION HORIZONTAL	LINEAR POLARIZATION ORTHOGONAL	CIRCULAR POLARIZATION PRINCIPAL	CIRCULAR POLARIZATION ORTHOGONAL
-0.39	DBSM	-300.000	-300.000	-300.000	-300.000	-300.000
MEAN DOPPLER/BODY VELOCITY		0.	0.	0.	0.	0.
DOPPLER SPREAD/BODY VELOCITY		0.	0.	0.	0.	0.
10.76	DBSM	-16.401	-19.591	-32.384	-18.135	-32.156
MEAN DOPPLER/BODY VELOCITY		5.3049E-02	5.287[illegible]E-02	5.1755E-02	5.3119E-02	5.2390E-02
DOPPLER SPREAD/BODY VELOCITY		9.4346E-03	9.234[illegible]E-03	9.5444E-03	9.3949E-03	9.7989E-03
21.92	DBSM	-25.019	-27.811	-48.881	-26.537	-48.734
MEAN DOPPLER/BODY VELOCITY		5.3237E-02	5.3080E-02	5.0992E-02	5.3298E-02	5.1974E-02
DOPPLER SPREAD/BODY VELOCITY		1.1015E-02	1.0855E-02	1.1312E-02	1.0988E-02	1.1633E-02
33.07	DBSM	-33.638	-36.031	-65.378	-34.939	-65.312
MEAN DOPPLER/BODY VELOCITY		5.3425E-02	5.3290E-02	5.0241E-02	5.3477E-02	5.1562E-02
DOPPLER SPREAD/BODY VELOCITY		1.2428E-02	1.2298E-02	1.2773E-02	1.2410E-02	1.3189E-02
44.23	DBSM	-42.256	-44.250	-81.874	-43.340	-81.891
MEAN DOPPLER/BODY VELOCITY		5.3613E-02	5.3508E-02	4.9501E-02	5.3657E-02	5.1153E-02
DOPPLER SPREAD/BODY VELOCITY		1.3726E-02	1.362[illegible]E-02	1.4027E-02	1.3714E-02	1.4557E-02
55.38	DBSM	-50.875	-52.470	-98.371	-51.742	-98.469
MEAN DOPPLER/BODY VELOCITY		5.3803E-02	5.371[illegible]E-02	4.8772E-02	5.3838E-02	5.0747E-02
DOPPLER SPREAD/BODY VELOCITY		1.4939E-02	1.485[illegible]E-02	1.5125E-02	1.4931E-02	1.5787E-02
66.54	DBSM	-59.493	-60.690	-114.868	-60.144	-115.047
MEAN DOPPLER/BODY VELOCITY		5.3993E-02	5.392[illegible]E-02	4.8053E-02	5.4019E-02	5.0344E-02
DOPPLER SPREAD/BODY VELOCITY		1.6087E-02	1.602[illegible]E-02	1.6103E-02	1.6083E-02	1.6908E-02
77.69	DBSM	-68.111	-68.910	-131.365	-68.545	-131.625
MEAN DOPPLER/BODY VELOCITY		5.4183E-02	5.4137E-02	4.7345E-02	5.4201E-02	4.9945E-02
DOPPLER SPREAD/BODY VELOCITY		1.7183E-02	1.714[illegible]E-02	1.6982E-02	1.7181E-02	1.7941E-02
88.85	DBSM	-76.730	-77.[illegible]29	-147.862	-76.947	-148.203.
MEAN DOPPLER/BODY VELOCITY		5.4375E-02	5.4350E-02	4.6648E-02	5.4383E-02	4.9549E-02
DOPPLER SPREAD/BODY VELOCITY		1.8238E-02	1.821[illegible]E-02	1.7778E-02	1.8238E-02	1.8902E-02
100.00	DBSM	-85.348	-85.349	-164.359	-85.349	-164.781
MEAN DOPPLER/BODY VELOCITY		5.4567E-02	5.456[illegible]E-02	4.5960E-02	5.4566E-02	4.9155E-02
DOPPLER SPREAD/BODY VELOCITY		1.9259E-02	1.925[illegible]E-02	1.8503E-02	1.9259E-02	1.9800E-02
111.15	DBSM	-94.943	-94.943	-183.415	-94.943	-180.085
MEAN DOPPLER/BODY VELOCITY		5.5008E-02	5.500[illegible]E-02	4.5411E-02	5.5007E-02	4.4314E-02
DOPPLER SPREAD/BODY VELOCITY		1.9430E-02	1.943[illegible]E-02	1.8495E-02	1.9430E-02	1.7887E-02
122.31	DBSM	-104.537	-104.538	-202.470	-104.538	-195.389
MEAN DOPPLER/BODY VELOCITY		5.5453E-02	5.545[illegible]E-02	4.4868E-02	5.5453E-02	3.9949E-02
DOPPLER SPREAD/BODY VELOCITY		1.9603E-02	1.960[illegible]E-02	1.8482E-02	1.9603E-02	1.6158E-02
133.46	DBSM	-114.132	-114.132	-221.526	-114.132	-210.692
MEAN DOPPLER/BODY VELOCITY		5.5902E-02	5.590[illegible]E-02	4.4332E-02	5.5901E-02	3.6015E-02
DOPPLER SPREAD/BODY VELOCITY		1.9777E-02	1.977[illegible]E-02	1.8466E-02	1.9777E-02	1.4597E-02

144.62	RCSM	-123.726	-123.727	-240.582	-123.727	-225.996
	MEAN DOPPLER/BODY VELOCITY	5.6354E-02	5.6355E-02	4.3802E-02	5.6354E-02	3.2467E-02
	DOPPLER SPREAD/BODY VELOCITY	1.9952E-02	1.9955E-02	1.8446E-02	1.9953E-02	1.3186E-02
155.77	RCSM	-133.321	-133.321	-259.638	-133.321	-241.300
	MEAN DOPPLER/BODY VELOCITY	5.6810E-02	5.6810E-02	4.3279E-02	5.6810E-02	2.9270E-02
	DOPPLER SPREAD/BODY VELOCITY	2.0130E-02	2.0130E-02	1.8421E-02	2.0130E-02	1.1911E-02
166.93	RCSM	-142.916	-142.916	-278.693	-142.916	-256.603
	MEAN DOPPLER/BODY VELOCITY	5.7270E-02	5.7269E-02	4.2762E-02	5.7270E-02	2.6387E-02
	DOPPLER SPREAD/BODY VELOCITY	2.0309E-02	2.0309E-02	1.8394E-02	2.0309E-02	1.0760E-02
178.08	RCSM	-152.510	-152.510	-297.749	-152.510	-271.907
	MEAN DOPPLER/BODY VELOCITY	5.7733E-02	5.7733E-02	4.2251E-02	5.7733E-02	2.3788E-02
	DOPPLER SPREAD/BODY VELOCITY	2.0489E-02	2.0489E-02	1.8363E-02	2.0489E-02	9.7196E-03
189.24	RCSM	-162.105	-162.105	-300.000	-162.105	-287.211
	MEAN DOPPLER/BODY VELOCITY	5.8200E-02	5.8200E-02	0.	5.8200E-02	2.1465E-02
	DOPPLER SPREAD/BODY VELOCITY	2.0671E-02	2.0671E-02	0.	2.0671E-02	8.7799E-03
200.39	RCSM	-300.000	-300.000	-300.000	-300.000	-300.000
	MEAN DOPPLER/BODY VELOCITY	0.	0.	0.	0.	0.
	DOPPLER SPREAD/BODY VELOCITY	0.	0.	0.	0.	0.